

# ERRATA

NATIONAL ADVISORY COMMITTEE FOR AERONAUTICS

## TECHNICAL REPORT NO. 696

### TENSILE ELASTIC PROPERTIES OF TYPICAL STAINLESS STEELS AND NONFERROUS METALS AS AFFECTED BY PLASTIC DEFORMATION AND BY HEAT TREATMENT

By D. J. McADAM, JR., and R. W. MEBS

During tests subsequent to those from which this report was prepared, it was found that a constant percentage error had been introduced into strain readings made with the particular Tuckerman extensometer used, because its collimator had been equipped with an objective lens of focal length differing from the standard value for this instrument. An investigation has disclosed that this collimator was a very early type. At the time of its manufacture (1923), the objective lens was not ground to a fixed focal length, but the collimator had been equipped with an auxiliary "focal adjuster" lens, in order to make the instrument direct reading. This auxiliary lens had long since been discarded from the collimator, due to certain difficulties in its adjustment. This fact was not known to the authors until after the report was in print.

The following corrections in values given in the diagrams and tables are therefore necessary.

(1) All values of the modulus of elasticity should be multiplied by the factor 1.075, *with the following exceptions:*

(a) Inconel L, cold drawn, as received (figs. 11 and 15 and the value of 70° F. in the right hand side of fig. 21); (b) aluminum-monel metal H, quenched and cold-drawn (figs. 7 and 19); (c) 13:2 chromium nickel steel E, as received (figs. 37 and 38 and the value at 1240° F. in fig. 34); (d) the modulus values (obtained from Rep. No. 670) plotted as squares in figure 30; (e) modulus values for 18:8 chromium-nickel steel 2A-1 and 13:2 chromium-nickel steel E in table IV. No correction should be made to these excepted values, since they were calculated from readings obtained with the Ewing extensometer with 5:1 ratio.

(2) Values of the stress coefficients of the modulus,  $C_0$  and  $C'$ , will not be changed.

These corrections will not affect the conclusions reached in this report, since these conclusions are based upon a comparison of values obtained with the different metals and upon the characteristics of the various curves. The corrections, moreover, will not affect the usefulness of the illustrations showing the influence of the various factors on the elastic properties of metals.

## REPORT No. 696

# TENSILE ELASTIC PROPERTIES OF TYPICAL STAINLESS STEELS AND NONFERROUS METALS AS AFFECTED BY PLASTIC DEFORMATION AND BY HEAT TREATMENT

By D. J. McADAM, JR., and R. W. MEBS

### SUMMARY

A general discussion is given of the relationships between stress, strain, and permanent set. From stress-set curves are derived proof stresses based on five different percentages of permanent set. The influence of prior plastic extension on these values is illustrated and discussed. A discussion is given of the influence of work-hardening, rest interval, and internal stress on the form of the proof stress-extension curve.

From corrected stress-strain curves are derived curves of variation of the secant modulus with stress. For fully annealed single-phase metals, the stress-modulus line is curved. After more or less work-hardening (unless the metal is relatively soft), the stress-modulus line becomes straight. Hardening by the addition of a second micro-constituent also tends to straighten the stress-modulus line.

A straight stress-modulus line means that the stress-strain curve is a quadratic parabola; the linear stress coefficient of the modulus of elasticity may then be represented by a constant ( $C_0$ ). When the stress-modulus line is curved, a second constant ( $C'$ ) is needed to represent the curvature; this constant is a quadratic stress coefficient of the modulus. The stress-strain curve may therefore be approximated either by superposition of a cubic parabola on a quadratic parabola or by a single parabola whose exponent ranges between 2 and 3. The relations are represented by a set of simple equations.

The variations of  $E_0$  (the modulus of elasticity at zero stress) and  $C_0$  with prior plastic extension are illustrated and discussed. The variations of  $E_0$ ,  $C_0$ , and the proof stresses consist in a wavelike basic curve with superposed oscillations due to varying duration of the rest interval and to the extension spacing.

The elastic properties of monel metal, Inconel, and aluminum-monel metal are considered. Comparison is made between diagrams of various types, for work-hardened metal and for metal that has been annealed either for complete softening or for relief of internal stress. A study is made of the effect of annealing temperature on the proof stresses and on  $E_0$  and  $C_0$ . The proof stresses of cold-worked metal may be greatly increased by suitable annealing without important loss of yield strength.

The effect of annealing on the elastic properties of 18:8 chromium-nickel steel and also the influence of plastic extension on the proof stresses and on  $E_0$  and  $C_0$  are discussed. The influence of heat treatment and of plastic extension on the elastic properties of 13:2 chromium-nickel steel is considered. The proof stresses for these alloys may be greatly increased by suitable annealing or other heat treatment.

Comparison of the elastic properties of copper with those of the other metals throws much light on the interrelationship between various factors affecting these properties.

The directional variation of the modulus of elasticity of metal crystals and the variation of crystal orientation with plastic deformation is discussed. These data are then applied to a discussion of the influence of plastic extension on the form and the initial slope of the stress-strain curve. It is shown that the forms of the curves of variation of  $E_0$  and  $C_0$  with prior plastic extension are affected by three factors: the work-hardening factor, the internal stress, and the change of crystal orientation. These factors also affect the inclination of the entire stress-strain curve up to the yield point.

### INTRODUCTION

An investigation of the tensile elastic properties of high-strength aircraft metals sponsored by the National Advisory Committee for Aeronautics is being conducted at the National Bureau of Standards. In a previous report (reference 1) has been described the results obtained with five steels whose compositions were within the ordinary range of 18:8 chromium-nickel steel. In the annealed condition, this alloy is relatively soft. It can be strengthened by cold work but not (to an important extent) by heat treatment. Four of the compositions were in three degrees of hardness (designated fully annealed, half-hard, and hard), and one was in two degrees of hardness.

The elastic properties considered were the modulus of elasticity and the elastic strength. The elastic strength was expressed in terms of five indices, each representing the stress that resulted in a chosen amount of permanent extension (permanent set) after removal of the

tensile load. The five percentages of permanent set were: 0.001, 0.003, 0.01, 0.03, and 0.1. The stresses that cause these permanent extensions were termed "proof" stresses. The proof stresses were obtained by interpolation from curves of variation of permanent set with previously applied stress.

From corresponding curves of variation of the total extension (both elastic and permanent) with stress, corrected graphs were obtained, representing the variation of elastic strain with stress. From these graphs (for 18 : 8 chromium-nickel steel), which were found to be curved from the origin, were derived the variations of the secant modulus with stress. Stress-modulus lines thus obtained were found to be curved for fully annealed metal. After a small amount of prior plastic extension, however, the stress-modulus lines became straight. The half-hard and the hard 18 : 8 alloys generally gave straight stress-modulus lines.

Equations were derived to represent these stress-modulus lines. One of the constants in the equation is Young's modulus and the other is the stress coefficient of the secant modulus. By use of these constants obtained from the stress-strain curve and by use of the proof stresses obtained from the stress-set curve, a fairly good picture of the elastic properties of a metal may be obtained.

A study was made of the influence of prior plastic extension on the elastic properties of 18 : 8 chromium-nickel steel. The information was presented by curves of variation with prior plastic extension of the modulus at zero stress, of its stress coefficient, and of the five proof stresses.

Consideration was also given to the influence of positive and negative creep on the stress-strain and the stress-set curves and on seven derived indices. The observed variation of these indices with plastic extension was found to be greatly affected by the duration of the interval between plastic extension and the beginning of the next determination of a stress-strain or a stress-set curve, and also by the "extension spacing" (amount and distribution of the intervals of plastic extension between two determinations of stress-strain or stress-set curves).

The present report includes the results of a continued investigation of the elastic properties of 18 : 8 chromium-nickel steel. It also includes the results of investigation of a heat-treatable stainless steel and of four nonferrous metals. The heat-treatable steel contained about 13 percent chromium and 2 percent nickel. Three of the nonferrous metals were high-strength alloys: monel metal, aluminum-monel metal (K-monel metal), and Inconel (an alloy containing about 13 percent chromium, 82 percent nickel, and 5 percent iron). The other nonferrous metal was copper. Three specimens of oxygen-free copper, which is being used in an investigation of creep of metals, were used for

this investigation of elastic properties. The information thus obtained, which is included in this report, makes it possible to compare the elastic properties of a pure, relatively soft metal with the elastic properties of metals that have been hardened by alloying and by cold work, and thus to evaluate the separate and the combined influences of important factors affecting the elastic properties of metals.

The monel metal used in this investigation is also being used in an investigation of creep of metals at elevated temperatures. In that investigation as well as in an investigation of elastic properties, it is necessary to separate (as far as possible) the total strain into its two components—plastic strain and elastic strain.

In addition to continued study of the influence of plastic extension on elastic properties, this report includes the results of investigation of the influence of annealing, especially annealing for relief of internal stress without important decrease of strength. The report also considers the influence of heat treatment on the elastic properties of 13 : 2 chromium-nickel steel.

The metals used in this investigation and the methods of experiment are described in section I. A brief outline of the relationship between stress, strain, and permanent set, and of the methods of obtaining stress-deviation and stress-set curves, is given in section II. Sections III to VIII, inclusive, consider the tensile elastic properties of the six previously mentioned metals, as affected by plastic extension and by annealing or other heat treatment. Section IX gives a general discussion of the influence of crystal orientation on the elastic properties of metals and of the variation of crystal orientation with plastic extension of a polycrystalline aggregate. The information thus assembled is applied in section X to a discussion of the influence of three important factors on the variation of the secant modulus, the variation of the modulus of elasticity, and the variation of its stress coefficient, with prior plastic extensions. Section X considers the form of the stress-strain (or stress-deviation line) as affected by the three factors associated with plastic extension. The conclusions reached in this discussion are chiefly based on a comparison of diagrams obtained with the six metals considered in this report.

## I. MATERIALS, APPARATUS, AND METHODS

### MATERIALS AND SPECIMENS

The 18 : 8 chromium-nickel steel used in this investigation was supplied by the Allegheny Ludlum Steel Corporation through the cooperation of Dr. V. N. Krivobok, associate director of research. The monel metal, the aluminum-monel metal, and the Inconel were supplied by the International Nickel Co. through the cooperation of Mr. A. J. Wadhams, director of research. The 13 : 2 chromium-nickel steel was supplied

by the Carpenter Steel Co. through the cooperation of Mr. G. V. Luerssen. The oxygen-free copper was supplied by the Scomet Engineering Co. through the cooperation of Mr. Sidney Rolle, assistant manager. Acknowledgment is made to all these companies and to their representatives for their generous cooperation.

All six metals were supplied in the form of round rods. The 13:2 chromium-nickel steel was supplied in the annealed condition (heated to 1,240° F and slowly cooled in the furnace). The copper was cold-rolled. The other four metals were cold-drawn. The compositions of the metals are given in table I. The tensile properties of the rods as received are given in table II. In each serial designation, the composition is indicated by the first letter (in reference 1 the composition is indicated by a number). The 18:8 chromium-nickel steel used in the investigation of the effect of relief of internal stress was supplied in half-hard and hard condition. The degree of hardness is indicated by the letters M or H, respectively, following the letter representing the composition. In order to indicate any annealing or tempering treatment given to the metal, the serial designation includes also a number representing the temperature of the treatment (the number of Fahrenheit degrees in hundreds). Details of thermal treatment are given in table III.

Only tension-test specimens were used in this investigation. The diameters of these specimens over their gage length and the corresponding bar diameters are given in table II. As the error (in pounds) in estimation of the load is practically independent of the load, the percentage error decreases with increase in load; hence, the percentage error in estimation of both load and stress decreases with increase in the cross section of the specimen. For this reason, the gage diameters were made as large as possible. In other respects, the specimens were according to the standard of the American Society for Testing Materials for threaded specimens with 2-inch gage length. The ratio of gage length to diameter was unimportant in this investigation because the investigation of elastic properties never required extension beyond the point of beginning local contraction.

#### APPARATUS

A pendulum hydraulic testing machine of 50,000-pound capacity was used. The specimens were held in grips with spherical seats. In some of the earlier experiments, a Ewing extensometer with ratio 5:1 was used. The smallest scale division on this instrument corresponds to a change of length of 0.00008 inch, and readings could be estimated to about  $\pm 0.000008$  inch; this sensitivity corresponds to a strain sensitivity of  $\pm 4.0 \times 10^{-4}$  percent for the 2-inch gage length used. The Ewing extensometer measures the average of the extensions on two opposite sides of the specimen. In the later experiments, a pair of Tuckerman optical

strain gages were used; these gages were attached to the opposite sides of the specimens. The smallest scale division on this extensometer corresponds to a change in length of 0.00004 inch. By means of a vernier on this instrument, it is possible to estimate changes of length to within about 0.000002 inch; this sensitivity corresponds to a strain sensitivity of  $1.0 \times 10^{-4}$  percent for the 2-inch gage length used.

#### METHOD OF INVESTIGATION

The experiments consisted in determining the total strains at various stresses, and the corresponding permanent extensions after release of load. The results thus obtained were used in plotting correlated stress-strain and stress-set curves. From the stress-set curves, proof stresses were obtained corresponding to permanent sets of 0.001, 0.003, 0.01, 0.03, and 0.1 percent. From the stress-strain curves, values were obtained for the modulus of elasticity.

As one object of the investigation was to determine the variation of elastic properties with plastic deformation, the previously mentioned correlated information was obtained with specimens that had received various degrees of cold-work. In order to investigate the effects of numerous small variations in prior plastic deformation, specimens were extended by numerous short stages; and stress-strain and stress-set curves were obtained after each of these stages. With the same specimen, it was thus possible to obtain a sequence of curves representing the variation of elastic properties with plastic deformation.

#### ACCURACY OF DETERMINATION OF STRESS-SET CURVES

Permanent set was not measured at zero load but at a load of 200 pounds. In order to determine the error in setting at this load, a series of extensometer readings was taken (with the same specimen) involving repeated increase of the load to a maximum (the selected value of this maximum being low enough to avoid permanent set) and reduction again to the minimum. The maximum difference between two successive readings at the minimum was equivalent to a load change of 6 pounds. This value corresponds to a stress error of 30 to 120 pounds per square inch, depending on the gage diameter of the specimen used. This stress error corresponds to a strain error of 0.0001 to 0.0004 percent, assuming a modulus of 30 million pounds per square inch. The effect of this error would be most important in determination of the lower part of a stress-set curve. As proof stresses in this report are based on permanent sets of 0.001, 0.003, 0.01, 0.03, and 0.1 percent, the corresponding maximum errors in these proof stresses probably would not exceed 10 to 40 percent, 3 to 12 percent, 1 to 4 percent, 0.3 to 1.2 percent, and 0.1 to 0.4 percent, respectively.

When a stress-set curve was plotted however, a number of determinations of permanent set were made and the curve was faired through all these points. The probable error involved in determining proof stresses, therefore, would be somewhat less than those for single measurements. The percentage error in determining values for the proof stress corresponding to a permanent set of 0.001 percent, however, is rather large. The error, nevertheless, is insufficient to invalidate the results; as shown in a number of figures to be discussed, variations of the 0.001-percent proof stress (with the various factors) are qualitatively similar to variations of the proof stresses corresponding to higher values of permanent set.

## II. THE RELATIONSHIP BETWEEN STRESS, STRAIN, AND PERMANENT SET

### RELATIONSHIP BETWEEN STRESS-STRAIN AND STRESS-SET CURVES

Investigation of the elastic properties of metals involves investigation of the relationship between stress, strain, and permanent set. A stress-strain curve alone gives incomplete information about elastic properties. This information needs to be supplemented by information about the relation between stress and the slight plastic extension (permanent set) remaining after removal of the stress. For the study of elastic properties, consequently, use should be made of both stress-strain and stress-set curves. The stress-set relationship was studied by means of a series of gradually increasing cycles of application and removal of stress, and by observation of the permanent set at the end of each cycle. The maximum stress was small in the first cycle but was increased from one cycle to the next until the total permanent set amounted to 0.1 percent or more. A stress-set curve is obtained by plotting the stress at the top of the cycle against the total permanent set at the bottom.

Each cycle of application and removal of stress may be represented by a continuous stress-strain curve. The ascending and descending portions of this curve generally do not coincide but form a loop, known as a hysteresis loop. The greatest width of the loop and the opening at the bottom depend on the stress range and on the number and the size of any previous cycles. Unless the loop is closed at the bottom, the width of the loop depends also on the duration of the cycle. The width of the opening at the bottom of the loop is a measure of the net permanent set due to the cycle. The net permanent set is the difference between the positive and the negative creep occurring during the cycle. (Positive creep tends to occur chiefly near the top and negative creep near the bottom of the loop.) The interrelationship between stress, strain, and permanent set, therefore, cannot be studied successfully without considering the influence of hysteresis and of

positive, and negative creep. In the previous report (reference 1), considerable attention was given to hysteresis, as affected by cyclic repetition and cycle frequency.

The stress-strain relationship may be studied conveniently with the help of a stress-deviation curve. Such a curve is obtained by plotting, instead of total strains, the differences between the total strains and the strains estimated by use of an assumed constant value of the modulus of elasticity. These differences represent deviations from an assumed straight stress-strain line, whose slope represents the assumed value of the modulus. By a suitable choice of the assumed value of the modulus, the stress-deviation curve gives a very sensitive representation of the variation of strain with stress.

A series of gradually increasing cycles of application and removal of stress, in determining a stress-set curve, may be represented by a continuous, complex stress-deviation curve, in which each cycle of stress is represented by a hysteresis loop. The entire series of cycles is thus represented by a series of gradually increasing hysteresis loops, as illustrated in figure 3 of reference 1. From the origin of such a series of loops may be drawn a continuously rising curve, starting at the origin of the series and passing through the tops of all the hysteresis loops. By this method were obtained the numerous stress-deviation curves shown in the previous report and in the present report. A curve thus obtained is practically identical with a curve obtained by uninterrupted increase of stress. A stress-set curve may be obtained from the same series of hysteresis loops by plotting the stress at the top of each loop against the total permanent set at the bottom.

### THE INFLUENCE OF CREEP, AND OF OTHER CHANGES DEPENDENT ON TIME, ON THE FORM OF THE STRESS DEVIATION AND THE STRESS-SET CURVES

The observed net permanent set, due to a stress cycle, depends not only on the positive and negative creep during the cycle but also on the negative creep during the interval between the removal of the stress and the observation of the permanent set. The observed permanent set therefore depends considerably on the duration of the cycle and on the time interval at the end of the cycle. A stress-set curve being based on a series of cycles, the course of such a curve is affected by the duration of the individual cycles and by the time intervals between the cycles. The course of the ascending part of a hysteresis loop, especially near the beginning of the ascent, may be affected by negative creep if time is not given for the most rapid part of the negative creep at the end of the preceding cycle. The courses of a stress-deviation curve and a stress-set curve are also influenced by the "rest interval" between any prior plastic deformation and the beginning of the determination of the

correlated curves. The type of curve, therefore, is affected more or less by the entire time schedule.

In the investigation described in the previous report, a definite time schedule was followed during each cycle. After loading, the strain was measured immediately. An interval of 1 minute, however, was provided between the end of each cycle and the instant of observation of the permanent set (at the beginning of the next cycle). This interval was found sufficient to permit practically all the thermal creep and the most rapid portion of the inelastic creep.<sup>1</sup> In the experiments described in the present report, a 2-minute rest interval was provided before strain measurement after both application and removal of load.

In the previous report, much attention was given to the effect of the rest interval between plastic extension and the beginning of determination of the next pair of correlated curves. This rest interval was intentionally varied between about 2 minutes and several days; occasionally the interval was considerably longer. In some experiments, provision was made for a rest interval of 30 minutes with the specimen in boiling water. The short rest interval at this temperature was found to have as much effect on the elastic properties of 18:8 chromium-nickel steel as a rest interval of a day or more at room temperature. Continued attention was given to the influence of the rest interval during the experiments described in the present report.

#### CORRELATED STRESS-DEVIATION AND STRESS-SET CURVES

By correlating stress-deviation and stress-modulus curves, information may be obtained about the elastic strength and the modulus of elasticity. In this report, as in the previous report, such correlated curves and diagrams derived from them are used in studying the influence of plastic deformation and of heat treatment on elastic properties of typical metals.

Correlated stress-deviation and stress-set curves are shown in figure 1 and in a number of other figures of the same type. The stress-set curves are in the lower row of each figure; directly above the origin of each stress-set curve is the origin of a corresponding pair of stress-deviation curves. The broken curve of each pair of stress-deviation curves is based on the observed total deviations at the indicated stresses. (The experimentally determined points upon which this curve is based, are differentiated by keyed symbols.) Each broken curve represents the influence of stress on total deviation. The continuous curve of each pair of stress-deviation curves is derived from the broken curve by deducting from the total deviations the deviations equivalent to the corresponding stress-set curve. Each continuous stress-deviation curve, therefore,

presumably represents the influence of stress on elastic deviation.

### III. THE TENSILE ELASTIC PROPERTIES OF MONEL METAL AS AFFECTED BY PLASTIC DEFORMATION AND BY ANNEALING

#### DESCRIPTION OF THE MONEL METAL

In the study of the elastic properties of high-strength nonferrous metals, it appears desirable to begin with a single-phase alloy, that is, an alloy whose elastic strength depends chiefly on plastic deformation. The alloy chosen for this purpose was monel metal.

The monel metal (designated G) had been obtained primarily for use in an investigation of creep of metals at elevated temperatures. For this purpose, it was desired that the alloy contain, as nearly as possible, only one metallographic constituent. The composition (given in table I), therefore, is adapted for this purpose and not primarily for giving the highest obtainable strength. In order to secure a fine-grained material, cold-worked uniformly throughout the cross section, the cross section had been reduced by cold drawing somewhat more than usual for ordinary commercial cold-drawn rod of this size.

The recrystallization range for cold-worked monel metal is about 1,100° to 1,200° F but depends considerably on the degree of cold work. For investigation of the elastic properties, one specimen was tested as received. Another specimen was tested after annealing at 800° F. Annealing at this temperature generally removes a large proportion of the internal stress without an important loss of tensile strength and hardness and with an improvement in elastic strength. Two specimens also were tested after annealing for recrystallization. One of these specimens was annealed at a temperature (1,200° F) just above the recrystallization range; the other specimen was annealed at 1,400° F. In the discussion of the results obtained with monel metal, attention will first be directed to the metal in a relatively soft condition, after annealing at 1,200° and 1,400° F.

#### THE INFLUENCE OF PRIOR PLASTIC EXTENSION ON THE STRESS-SET CURVE AND ON THE DERIVED PROOF STRESSES FOR FULLY ANNEALED MONEL METAL

Correlated stress-deviation and stress-set curves obtained with annealed monel metal are shown in figure 1 and in the diagram at the left of figure 3. The stress-set curves in each figure are in the lower section. The origin of each curve is shifted to the right a constant distance from the origin of the preceding curve. Each curve thus has its own scale of abscissas. Distances between the origins have no relation to the scale of abscissas.

All the curves of figure 1 were obtained with a specimen that had been annealed at 1,400° F. All the

<sup>1</sup> A general discussion of thermal creep and inelastic creep is given in reference 1.

curves of the diagram at the left of figure 3 were obtained with a specimen that had been annealed at 1,200° F. The curves were obtained consecutively from left to right, by methods described in sections I and II, and with intervening (varying) amounts of prior plastic extension. Neither the intervening percentages nor the total percentages of prior plastic extension are indicated in figures 1 and 3. The curves in each figure are numbered consecutively, however, and the percentages of prior plastic extension may be found by referring to the correspondingly numbered experimental points in figures 2 and 4, which are derived from the stress-set curves in figures 1 and 3, respectively.

From each stress-set curve in figures 1 and 3 are derived five proof-stress values, corresponding to the five previously mentioned percentages of permanent set. In figures 2 and 4, these proof stresses are plotted against the corresponding percentages of prior plastic extension. The five curves thus obtained are separated by using five different indicated scales of ordinates. The ordinates in these figures, as in figures 1 and 3, represent "true stresses," based on the sectional area at the beginning of determination of each stress-set (or stress-deviation) curve. A true-stress value, consequently, is obtained by multiplying the corresponding nominal stress (stress based on the initial sectional area) by 1 plus the fractional extension (1 plus  $\frac{1}{100}$  of the extension in percent).

After the initial stress-set curve had been determined, a second curve was determined with practically no intervening plastic extension. The specimen was then extended by numerous small stages to the beginning of local contraction (maximum load). After each of these stages, the specimen was allowed to rest without stress for an interval of varying duration, and a stress-set curve was then determined. The duration of the prior rest interval is indicated by the symbol placed at an experimentally determined point on each stress-set curve. The duration, as shown in figures 1 and 3, ranged from 3 minutes to 164 hours.

As shown in figures 2 and 4, the experimental points in each curve (with the exception of the last experimental point in each curve of fig. 2) are distributed in pairs, which are separated by relatively long plastic extensions. Each pair of experimental points is derived from a pair of stress-set curves determined with no intervening plastic extension. The difference in prior plastic extension (for the curves of a pair), therefore, is merely the extension made in determining the first curve of the pair. The alternate long and short plastic extensions were made to reveal the influence of one of the variables affecting the form of the stress-set curve and the values of the derived proof stresses. This variable is the distribution of the determinations

of stress-set curves throughout the range of plastic extension; it has been termed "extension spacing."

The stress-set relationship, as affected by plastic extension, rest interval, and extension-spacing, may best be studied by considering both the stress-set curves and the derived curves of variation of proof stresses with prior plastic extension. The steeper the stress-set curve, the higher are the derived proof stresses.

The initial stress-set curves (curves 1 in figs. 1 and 3) show no appreciable permanent set at stresses below about 30,000 pounds per square inch. With increase in stress above about 30,000 pounds per square inch, permanent set increases at an increasing rate, and a yield point is reached at about 40,000 pounds per square inch. In curve 2 of each of these figures, the stress at which permanent set becomes appreciable is lower than in curve 1, and curve 2 remains below curve 1. Curve 3, up to the yield point, is below curve 2. Minimum steepness is found in curve 5 of figure 1 and in curve 3 of figure 3. These and other variations in steepness can best be studied by means of the corresponding variations of proof stresses, as shown in figures 2 and 4.

As indices of elastic strength, the proof stresses based on 0.001 and 0.003 percent permanent set probably should receive more consideration than the three proof stresses based on larger percentages of permanent set. The 0.10 percent proof stress probably should be viewed as an index of resistance to yield rather than as an index of elastic strength. In the discussion of curves of variation of proof stress with prior extension (figs. 2 and 4), therefore, chief attention will be given to the curves representing the 0.001- and the 0.003-percent proof stresses.

Corresponding to the previously described variation in steepness of the stress-set curve, there are variations in height of the derived curves in figures 2 and 4. The curves representing 0.001- and 0.003-percent proof stress descend rapidly from the origin and reach a minimum when the prior plastic extension is about 1 percent. Beyond this minimum, the curves rise rapidly until they reach a maximum, at an extension of a few percent. The extension at the maximum depends considerably on the variations in the rest interval and on the extension spacing of the experimental points. Beyond this maximum, the 0.001-percent curves oscillate through a relatively wide vertical range, without a general upward trend until the prior extension exceeds about 20 percent. The 0.003-percent curves, beyond the first maximum, show a general upward trend, with wide oscillations.

The prior extension at the first minimum is not the same in all the curves of each figure. In figure 2, the minimum is at point 5 in the lower two curves but is at

points 3 and 4 in the upper three curves. In figure 4, the first minimum is at point 3 in the lower three curves but is at point 2 in the upper two curves. The extension at the first minimum evidently decreases with increase in the permanent set on which the proof stress is based. In each figure, however, all five points derived from stress-set curve 2 are below the corresponding points derived from stress-set curve 1. This relationship is in accordance with the fact that stress-set curves 2, throughout the range shown in figures 1 and 3, are below curves 1.

Beyond the first maximum in the curves of figures 2 and 4, the oscillations are due largely to the combined influence of the rest interval and the extension spacing. The prior rest intervals, for the curves in figures 1 and 3, were alternately long and short. A relatively long rest interval preceded the determination of the first experimental point of each pair and thus followed a relatively long plastic extension. Preceding the second experimental point of each pair was a relatively short rest interval. The alterations in the duration of the rest interval, therefore, correspond qualitatively to the alternations in the extension interval. The evidence in figures 1 to 4 indicates that the combined influence of the duration of the rest interval and the extension spacing greatly affects the steepness of the stress-set curve and the form of the proof stress-extension curves for monel metal.

The first stress-set curve of a consecutive pair (figs. 1 and 3) evidently tends to be less steep than the second curve. To this relationship there are few exceptions. Prominent examples of this relationship are: Pairs 13-14 and 19-20 of figure 1, and pairs 3-4, 13-14, and 15-16 of figure 3. Corresponding to these differences in slope are differences in the derived proof stresses; these differences cause the second experimental point of each pair in figures 2 and 4 to be (with few exceptions) higher than the first. The only conspicuous exceptions in figure 2 are pairs 1-2 and 9-10. The only exception in figure 4 is pair 1-2. The important exceptions generally are found within an initial range of relatively small prior plastic extension. This range is the region of the previously described initial descent of the curve, followed by a rise and another descent, all within a relatively small range of prior plastic extension. In this range, the oscillations caused by the extension spacing and the varying duration of the rest interval evidently are superposed on a basic curve consisting of an initial descent followed by a rise and a subsequent irregular course. The course of this basic curve may mask the tendency of the second point of a consecutive pair to be higher than the first. An example of this effect is pair 9-10 of figure 2.

The first experimental point of each pair (figs. 2 and 4) was obtained after a relatively long stage of plastic

extension and after a relatively long rest interval. Because of the combined influence of this variation of the rest interval and this extension spacing, the second experimental point of each pair tends to be higher than the first. With 18 : 8 chromium-nickel steel, as shown in the previous report, each of these factors (separately) tends to cause the second point of a pair (in a diagram such as those in figs. 2 and 4) to be higher than the first. The evidence in figures 2 and 4 thus indicates that the combined influence of both these factors is qualitatively the same for monel metal as for 18 : 8 chromium-nickel steel but does not determine whether the separate influence of each factor is qualitatively the same for both alloys.

The influence of the extension spacing alone on proof stresses of 18 : 8 chromium-nickel steel was established (in reference 1) by curves of the type shown in figures 2 and 4 but with all the rest intervals relatively long, that is, a day or more. In such curves, the second experimental point of a pair, with few exceptions, is higher than the first. The exceptions are pairs of points in regions of prominent rise or descent of the basic curve. In such regions, the influence of the extension spacing may be partly masked by the course of the basic curve.

The separate influence of duration of the rest interval on proof stresses of 18 : 8 chromium-nickel steel was revealed in the previous report by diagrams of the type shown in figures 2 and 4 but with all the extension intervals short. Some entire diagrams were derived from a consecutive series of stress-set curves with practically no intervening extension intervals. The rest intervals, however, varied over a wide range. In the resultant diagrams, therefore, the influence of duration of the rest interval was clearly revealed. The shorter the rest interval, the higher generally are the resultant experimental points in diagrams such as those in figures 2 and 4.

A separate evaluation of the influences of extension spacing and rest interval has not been attempted for the metals discussed in this report. The combined influence of the two factors, however, is clearly shown. For monel metal, the combined influence evidently is qualitatively the same as for 18 : 8 chromium-nickel steel. That the separate influence of each of these variables also is qualitatively the same is indicated by scattered evidence, to be mentioned later.

The initial descent of the curves in figures 2 and 4 is very different from the course of the corresponding curves for 18 : 8 chromium-nickel steel shown in the previous report. In those curves, practically without exception, the initial direction is upward. A second stress-set curve following the initial stress-set curve without intervening plastic extension, was found to be steeper than the initial curve. Proof stresses derived

from the second curve, consequently, were higher (frequently much higher) than those derived from the initial curve. These results were obtained with five compositions of 18:8 chromium-nickel steel, with specimens annealed, half-hard, and hard. The very different results obtained with annealed monel metal, however, are not due to inherent difference (in this respect) between monel metal and 18:8 chromium-nickel steel. Reasons for the initial descent of the curves in figures 2 and 4 are given later.

**THE INFLUENCE OF PRIOR PLASTIC EXTENSION ON THE STRESS-SET CURVE AND ON THE DERIVED PROOF STRESSES FOR WORK-HARDENED MONEL METAL**

Attention will now be given to the same alloy in the work-hardened condition. The alloy to be considered first is monel metal G, which has been cold-drawn and not afterward annealed, even for relief of internal stress. In this condition, as shown in table II, the tensile strength is about one-third greater than that of the annealed alloy.

In the diagram at the left of figure 9 are correlated stress-deviation and stress-set curves for this work-hardened alloy. In the diagram at the left of figure 10 are the derived curves of variation of proof stress with prior plastic extension. The stress-set curves, in the lower section at the left of figure 9, are numbered consecutively; the derived points representing proof stresses are correspondingly numbered in figure 10. Abscissas of these points thus represent the prior plastic extensions for the corresponding stress-set curves in figure 9. In each curve of figure 10, as in figures 2 and 4, the experimental points are distributed in pairs separated by relatively long intervals of plastic extension.

In the study of the stress-set curves for monel metal G (fig. 9), attention should first be given to the initial pair of curves, designated 1 and 2. These curves were obtained with practically no intervening extension. The slight extension made in determining curve 1 has caused curve 2 to be much steeper than curve 1 throughout the entire range used in deriving proof stresses. This slight initial plastic extension, therefore, has increased both the elastic strength and the yield strength. In the derived diagram (fig. 10), consequently, the second experimental point is considerably higher than the first point in each curve except the lowest. In the curve for 0.001-percent proof stress, the second experimental point is no higher than the first. Because of the relatively large error inherent in the estimation of the 0.001-percent proof stress, however, not much weight should be given to this exception. The evidence appears to indicate that all five proof stresses derived from stress-set curve 2 are higher than those derived from stress-set curve 1. In this respect, the work-hardened monel metal G behaves very differently from the same metal in the fully annealed condition (figs. 1 to 4).

The combined influence of the extension spacing and the duration of the rest interval causes the second point of each pair to be higher than the first. This difference in height, in figure 10, as in figures 2 and 4, tends to increase with work-hardening. As shown in the previous report, work-hardening has a similar effect on the range of oscillation in the proof stress-extension curves for 18:8 chromium-nickel steel.

The general trend in the curves for 0.001- and 0.003-percent proof stresses, somewhat obscured by superposed oscillations due to the extension spacing and the variations of the rest interval, is upward between points 1 and 4. Each of these curves then descends abruptly to a minimum at point 5. Point 5 is lower than point 3 in spite of the much longer rest interval prior to determination of point 3 and is even below point 1. From point 5 these two curves rise throughout the rest of their length to the beginning of local contraction. This description of the basic curve applies only to the curves of variation of the 0.001- and the 0.003-percent proof stresses. The curves representing 0.01-, 0.03-, and 0.1-percent proof stresses would probably rise continuously if they were free from the superposed oscillations due to the extension spacing and the variations of the rest interval.

The basic curve for work-hardened monel metal G (for 0.001- and 0.003-percent proof stresses) evidently differs greatly from the basic curve for fully annealed monel metal (figs. 2 and 4). The basic curve for annealed monel metal first descends abruptly to a minimum and then rises rapidly and traverses a maximum, all within a small range of prior plastic extension. The basic curve for work-hardened monel metal G first rises to a maximum, then descends rapidly to a minimum, and again rises. Reasons for this difference are given later.

**THE INFLUENCE OF PRIOR PLASTIC EXTENSION ON THE STRESS-SET CURVE AND ON THE DERIVED PROOF STRESSES FOR MONEL METAL ANNEALED FOR RELIEF OF INTERNAL STRESS**

The great difference between work-hardened metal G and fully annealed metals G-12 and G-14, as regards the form of the basic proof stress-extension curve, suggested the desirability of determining the effect of annealing for relief of internal stress. For this purpose, specimens of the cold-drawn alloy G were annealed at 800° F, as described in table III. Correlated stress-deviation and stress-set curves obtained with this alloy (G-8) are shown in the diagram at the right of figure 9. Proof stresses derived from the stress-set curves are shown in figure 10. In each of these figures, comparison may readily be made between the curves obtained with alloys G and G-8, and information may thus be obtained about the influence of relief of internal stress. Attention will first be given to the diagrams for alloy G-8.

The initial stress-set curve for monel metal G-8 is steeper than curve 2, throughout the range shown in

figure 9. In the derived diagram (fig. 10), point 1 is lower than point 2 in the curve for 0.1-percent proof stress, is at the same height in the curve for 0.03-percent proof stress, but is higher than point 2 in the curves for 0.001-, 0.003-, and 0.01-percent proof stresses. The initial trend of the curve for 0.001- and 0.003-percent proof stresses is downward to point 3. In the absence of superposed oscillations, which are due to the extension spacing and to the variations of the rest interval, the lower three curves possibly would reach a minimum at a prior extension of a little less than 1 per cent and would then rise to a maximum, as do the curves for fully annealed monel metal (figs. 2 and 4). Such a course appears to be suggested by the curve for 0.01-percent proof stress. It is also possible, however, that the relatively high position of point 6 in each of these curves is due entirely to the combined influence of the extension spacing and the variations of the rest interval.

In reference 1 evidence was presented that an exceptionally high point due to these two factors tends to be followed by an exceptionally low point, and vice versa. By adjusting the extension spacing and the rest intervals, the oscillations may be greatly accentuated. Such accentuation possibly exists in the diagram for metal G-8 (fig. 10). The long rest interval prior to point 3 has caused a depression at this point in each of the lower two curves. From point 3, there is a rebound due to the relatively short rest interval prior to point 4. This rebound tends to accentuate the following depression (at only slight additional extension) at point 5; this exceptionally low point tends to accentuate the following rebound and thus tends to cause point 6 to be exceptionally high. Such accentuated oscillations, due largely to variations in the rest interval, probably arise when the experimental points are separated by small intervals of prior plastic extension, as are points 1 to 6 in the diagram for monel metal G-8.

If the relatively high position of point 6 is due entirely to such accentuated oscillation, the basic curves (for 0.001- and 0.003-percent proof stresses) may descend at a decreasing rate throughout the entire extent to the beginning of local contraction. In order to determine whether the basic curve has this form or has an abrupt rise to a maximum following the initial descent, it would be necessary to determine a series of points with long prior rest intervals. The initial descent of the lower three basic curves, however, is well established.

The initial trend of the lower three curves for metal G-8 is opposite to the initial trend of the corresponding curves for metal G. Annealing monel metal for relief of internal stress, like annealing for complete softening, evidently causes the initial trend of the lower proof stress-extension curves to be opposite to the initial trend of the curves for unannealed, work-hardened monel metal.

Comparison of initial proof stresses in the diagrams for metals G and G-8 (fig. 10) shows that annealing for relief of internal stress has increased the initial 0.001-, 0.003-, and 0.01-percent proof stresses but has decreased the 0.03- and the 0.1-percent proof stresses. Annealing for relief of internal stress although it has slightly decreased the yield stress and (tensile strength), therefore, has considerably increased the elastic strength

#### THE FACTORS INVOLVED IN THE FORM OF THE PROOF STRESS-EXTENSION CURVE

The form of the curve of variation of proof stress with prior plastic extension depends largely on two factors, work-hardening and relief of internal stress.<sup>2</sup> Work-hardening is the principal cause of the continuous ascent of the curves for 0.03- and 0.1-percent proof stresses. The wave-like form of the basic curves (especially the curves for 0.001-, 0.003-, and 0.01-proof stresses), the superposed oscillations, and the tendency to recoil and rebound from high and low points may be attributed largely to variations of internal stress. Tensile internal stress tends to lower the proof stresses, especially the proof stresses corresponding to very small amounts of permanent set. Relief of internal stress, either by annealing or by mechanical treatment, tends to elevate the proof stresses. Alternate increase and partial relief of internal stress, during the stages of plastic extension, therefore, would cause oscillations in the proof stress-extension curves. The oscillations in curves such as those in figures 2, 4, and 10, consequently, may be due to the opposite oscillations in the magnitude of the internal stress. At a minimum in such a curve, the internal stress probably reaches a temporary maximum, at which the stress is partly relieved by local flow in regions of highest tensile stress. This relief of internal stress proceeds until a minimum is reached (at a maximum in the proof stress-extension curve) at which the stress again begins to build up.

Such variations of internal stress would be influenced by the spacing of interspersed cycles such as those used in determining stress-set curves. They would also be influenced by variation of the rest interval and consequent variation in the amount of negative creep. The temporary upper limit of stress, at which relief by local flow begins, evidently would increase with the increase in hardness due to plastic extension. Thus, it is possible to account for the general increase of the range of oscillation of the proof-stress-extension curves with increase in the hardness of the metal.

#### REASONS FOR THE DIFFERENCE IN INITIAL TREND OF THE PROOF-STRESS-EXTENSION CURVES FOR WORK-HARDENED AND ANNEALED MONEL METAL

The conclusions as to the influence of internal stress on the form of the proof-stress-extension curve are

<sup>2</sup> The term "internal stress" in this report, as in the previous report, is used in the ordinary technical sense and has no reference to interatomic forces as affected by space-lattice irregularities.

supported by evidence based on the relationship between the diagrams for monel metal G and G-8 (fig. 10). Comparison of these diagrams shows that annealing for relief of internal stress increases the initial proof stresses that may be considered indices of elastic strength and changes the initial trend of the corresponding proof-stress-extension curves from a rise to a descent. This relationship suggests that the initial steep descent of the lower curves for monel metal G-8 is due to restoration of internal stress. With slight plastic extension, the internal stress evidently increases to a temporary maximum and thus causes descent of the curves to a minimum. Similar reasoning suggests that increase of internal stress causes the initial descent of the curves for fully annealed monel metal (figs. 2 and 4). Slight plastic extension of fully annealed metal evidently causes increase of internal stress from zero.

Another factor affecting the initial trend of the proof-stress-extension curve is work hardening. Work hardening tends to increase the proof stresses. When the first slight plastic extension causes increase of internal stress, the initial trend of the proof-stress-extension curve depends on the relative magnitude of the elevating effect of the work hardening and the depressing effect of the increase of internal stress. When the rate of work hardening is high, the elevating effect may predominate and cause the curve to rise. (An example of this effect is given in section VII.) In the initial descent of the curves for annealed monel metal G-14, G-12, and G-8, however, the predominant factor is evidently the increase of internal stress.

The initial rise of the (lower) curves for the unannealed, work-hardened metal G (fig. 10), however, cannot be attributed to predominance of the influence of work hardening. The rate of work hardening of this previously cold-worked metal would be much less than that of the fully annealed metal. The initial rise of the curves for work-hardened monel metal G, therefore, must be due to a decrease of internal stress caused by the plastic extension. The internal stress in the severely cold-drawn metal probably was so high that slight tensile extension caused relief of internal stress and thus caused the initial rise of the proof-stress-extension curves.

The effect of slight tensile extension evidently depends on the magnitude of the initial internal stress. When the internal stress is zero or at a minimum, slight tensile extension causes the internal stress to increase. When the initial internal stress is high, slight plastic extension decreases the internal stress. These changes in internal stress cause opposite changes in the proof stresses based on small values of permanent set.

#### COMPARISON OF STRESS-DEVIATION AND STRESS-SET CURVES FOR MONEL METAL

An incomplete view of the elastic properties of a metal is obtained by considering only the relation between stress and the deformation that remains after the stress has been released. Consideration should be given also to the influence of stress on the accompanying total strain and on the elastic strain. These relations are revealed by the stress-deviation curves for monel metal and by derived curves and indices.

Stress-deviation curves for monel metal are shown in the upper rows of figures 1, 3, and 9. The value  $E_A$ , given in each of these figures, is the assumed modulus used in obtaining the deviations, as described in section II. Each broken curve represents the influence of stress on total deviation. Each solid-line curve (in the upper rows of figs. 1, 3, and 9) has been obtained from the corresponding broken-line curve by deducting values of permanent set obtained from the stress-set curve directly below.

In the study of the influence of the extension spacing and the duration of the rest interval on the stress-deviation curve, it is of interest to observe whether such variations have similar or opposite effects on the slopes of the stress-deviation and stress-set curves. As discussed earlier in this section, the first stress-set curve of a pair, because of the influence of the extension spacing and of the variations of the rest interval, tends to be less steep than the second curve. Illustrations of this tendency are: Pair 19-20 of figure 1; pairs 11-12, 13-14, and 15-16 of figure 3; pairs 3-4, 5-6, and 7-8 in the diagrams at the left of figure 9; and pairs 5-6, and 7-8 in the diagram at the right of figure 9. The corrected stress-deviation curves of the same pairs, however, generally show the opposite relationship. This fact is illustrated by pair 19-20 of figure 1, pairs 13-14 and 15-16 of figure 3, and pairs 3-4 and 5-6 in the diagram at the left of figure 9. In pair 11-12 of figure 3 and in pair 7-8 of figure 9, the first and the second curve are about equally steep. The first curve of pair 5-6 at the right of figure 9 is less steep than the second. Although there is a general tendency for the first corrected stress-deviation curve of a pair to be steeper than the second, there are exceptions, just as there are exceptions to the general tendency for the first stress-set curve of a pair to be less steep than the second. Numerous examples of this opposite relationship between the slopes of the stress-deviation and stress-set curves of a pair will be found in diagrams yet to be considered.

#### THE VARIATION OF THE MODULUS OF ELASTICITY WITH STRESS FOR MONEL METAL

The corrected stress-deviation curves of figures 1, 3, and 9, with few exceptions, show prominent curva-

ture from the origin. The exceptions are curves 1 to 4 in figure 1, curve 1 of figure 3, and curve 1 in the diagram at the right of figure 9. No exceptions are found among the curves for cold-drawn, unannealed monel metal G. With the exceptions mentioned, the slope of each curve decreases continuously from the origin. This result evidently means that the modulus of elasticity decreases continuously with increase in stress.

The secant modulus<sup>3</sup> given by the ratio of stress to elastic strain has been used in this report and in the previous report to study the variation of the modulus with stress and with prior plastic extension.

Graphs of variation of the secant modulus of elasticity with stress have been derived from all the corrected stress-deviation curves in figures 1, 3, and 9 and are shown in figures 5, 7, and 11. The graphs are numbered consecutively in each figure to correspond to the stress-deviation curves from which they are derived. Each stress-modulus line has been shifted to the right from the preceding line and has been given a separate abscissa scale. Abscissas, increasing from left to right, represent values of the secant modulus of elasticity. The scale of abscissas is indicated in each figure. Ordinates represent true stress, that is, stress based on the cross section at the beginning of determination of the curve.

In the derivation of a stress-modulus line from a stress-deviation curve, values of the secant modulus were estimated for various points on the continuous stress-deviation curve. These points in figures 5, 7, and 11, therefore, represent not results of single experiments but selected points on the corresponding stress-deviation curves.

The prior plastic extension corresponding to each stress-modulus line is indicated in the derived diagrams (figs. 6, 8, and 12). In these diagrams, abscissas represent prior plastic extensions and ordinates represent indices derived from the stress-modulus lines. The experimental points in figures 6, 8, and 12 are numbered to correspond to the stress-modulus lines from which they are derived (figs. 5, 7, and 11).

In the diagram for fully annealed monel metal G-14 (fig. 5), stress-modulus lines 1 to 11 are curved from the origin. In the diagram for monel metal G-12 (fig. 7), stress-modulus lines 1 to 10 are curved from the origin. All the other stress-modulus lines in these two figures are straight. The plastic extension at which the stress-modulus line becomes straight is about 10 percent. In the diagrams for work-hardened monel metal G and G-8 (fig. 11), the stress-modulus lines are straight except at high stresses. The stress-modulus line for monel metal evidently tends to be practically straight when the prior plastic extension of the metal

(whether by tensile extension or by cold drawing) is more than about 10 percent.

In this respect, monel metal is similar to the 18:8 chromium-nickel steels discussed in the previous report. The stress-modulus line for annealed 18:8 alloy was found to be straight when the prior plastic extension was more than about 12 percent. Unannealed cold-drawn 18:8 alloys (half-hard and hard) generally gave straight stress-modulus lines.

#### THE INDICES OF VARIATION OF THE MODULUS OF ELASTICITY WITH STRESS FOR MONEL METAL

The Young's modulus, or the modulus at zero stress ( $E_0$ ), was determined by extrapolating the stress-modulus line to zero stress. When the stress-modulus line is straight, the variation of the secant modulus ( $E$ ) with stress ( $S$ ) may be represented, as in reference 1 by

$$E = E_0 - kS \quad (1)$$

The constant  $k$  is the slope of the stress-modulus line. As stated in reference 1, however, it is sometimes more convenient to write equation (1) in the form

$$E = E_0(1 - C_0S), \quad (2)$$

where  $C_0 = k/E_0$  represents the stress coefficient<sup>4</sup> of the secant modulus.

When the stress-modulus line is curved from the origin, as are some lines in figures 5 and 7, the stress coefficient of the modulus is not constant but varies with the stress. The variation of the modulus with stress then cannot be represented by  $C_0$  alone. The curved stress-modulus lines may be represented approximately by adding another term to equation (2) and thus obtaining

$$E = E_0[1 - C_0S(1 + QS)] = E_0(1 - C_0S - C'S^2) \quad (3)$$

where  $C' = QC_0$  is an index of the curvature of the stress-modulus line.

The second constant ( $C'$ ) is needed for use with monel metal that has been fully annealed and afterward not extended more than about 15 or 20 percent. For sufficiently work-hardened monel metal, the stress coefficient of the modulus of elasticity is practically constant and is represented by  $C_0$ .

Values of  $C_0$  are indicated (figs. 5, 7, and 11) by a number adjacent to each stress-modulus line. Values of  $C'$  are also indicated for lines 9 and 10 of figure 5 and for lines 1, 8, 9, and 10 of figure 7. (These values indicate the fractional change of the modulus per pound per square inch.) The value of  $E_0$  for each stress-modulus line is indicated by the intersection of the line with the horizontal axis.

<sup>3</sup> It should be noted that this modulus differs from a frequently used "secant modulus" based on the variation to total strain with stress.

<sup>4</sup> The index  $C_0$  is expressed as fractional change of the modulus per pound per square inch. In reference 1 this index is designated  $C_1$ .

THE INFLUENCE OF PRIOR PLASTIC EXTENSION FOR MONEL METAL ON THE MODULUS OF ELASTICITY AND ON ITS STRESS COEFFICIENTS

The values of  $E_0$  and  $C_0$  given in figures 5, 7, and 11 have been used in deriving diagrams of a different type in figures 6, 8, and 12. These derived diagrams represent the variation of the modulus of elasticity and its linear stress coefficient with prior plastic extension. Abscissas represent percentages of prior plastic extension. Ordinates of two of the curves represent values of the modulus of elasticity; the ordinate scale for these curves is at the left of each figure. Ordinates of the other curve represent values of the stress coefficient of the modulus; the ordinate scale for this curve is at the right of each figure.

The experimentally determined points in figures 6, 8, and 12 have been numbered to correspond to the consecutively numbered stress-modulus lines in figures 5, 7, and 11. Before the general trend of the curves in figures 6, 8, and 12 is considered, attention will be given to the abrupt oscillations (at pairs of experimental points) due to the influence of the extension spacing and of the variation of the rest interval. Except for monel metal G-8 (fig. 12), the oscillations in the curve for  $C_0$  are qualitatively similar to the corresponding oscillations in the curve for  $E_0$ . Each abrupt rise or drop in a curve for  $E_0$  is accompanied by a similar change in direction in the curve for  $C_0$ .

The abrupt oscillations in the curves for  $E_0$  and  $C_0$  (figs. 6, 8, and 12), however, are accompanied by opposite oscillations in the corresponding proof stress-extension curves (figs. 2, 4, and 10). This relationship is in accordance with the fact that the modulus-extension curves are based on stress-deviation curves, whereas the proof-stress-extension curves are based on stress-set curves. It has been shown that a difference in steepness of the stress-deviation curves of a pair (due to the influence of the extension spacing and of the variations of the rest interval) is accompanied by the opposite difference in steepness of the corresponding stress-set curves. Examples of opposite variation of the modulus-extension curves and the proof-stress-extension curves may be found by comparing the pairs of experimental points listed below, with the corresponding pairs in figures 2, 4, and 10; pair 19-20 of figure 6; pairs 9-10, 13-14, and 15-16 of figure 8; pair 5-6 in the diagram for monel metal G in figure 12; and pairs 5-6 and 7-8 in the diagram for monel G-8 in figure 12. Numerous examples of similar relationship may be found by comparing diagrams of the same two types obtained with metals yet to be discussed. A similar relationship was also found for the 18:8 chromium-nickel steels discussed in the previous report.

The magnitude of such oscillations, as shown in the previous report, is affected by the duration of the rest interval. Increase in the rest interval tends to de-

crease the slope of the stress-set curve and to increase the initial slope ( $E_0$ ) and the curvature ( $C_0$ ) of the corrected stress-strain curve. In this respect, the effect of increase of the rest interval is opposite to the effect of decrease of internal stress. Such an effect of the rest interval, therefore, evidently cannot be attributed to negative creep, which generally occurs during rest after plastic extension. The effect of the rest interval apparently is some kind of softening effect. This softening effect, at least for a while, is greater than any beneficial effect of relief of internal stress by negative creep.

The variation of  $E_0$  with prior plastic extension (figs. 6, 8, and 12) is represented by lines connecting the experimental points. These graphs give no distinct impression of a general upward or downward trend; with plastic extension of annealed monel metal to the beginning of local contraction (figs. 6 and 8), the modulus of elasticity remains nearly constant. The basic curves for annealed monel metal, however, probably follow the courses indicated approximately by the dotted lines. The basic curve for monel metal G-14 rises gradually to a maximum, at plastic extension of 10-15 percent, and then descends at a decreasing rate. The basic curve for monel metal G-12 rises rapidly to a maximum, at a plastic extension of 2-5 percent, then descends at a decreasing rate, and finally reascends. The modulus-extension curves for annealed monel metal are very different from the curves for the 18:8 chromium-nickel steels discussed in the previous report and also very different from the curves for other metals discussed in sections IV to VIII. As shown in section X, the course of these basic  $E_0$  curves is due to the combined influence of three factors.

The  $E_0$  curves for work-hardened monel metal (fig. 12) show no distinct evidence of upward or downward trend. Tensile extension of these specimens, which had already been severely cold-worked, would be expected to cause very little change in the modulus of elasticity.

The  $C_0$  curves for annealed monel metal G-14 and G-12 (figs. 6 and 8) are similar in general trend. The trend is better indicated in figure 8 than in figure 6 because of the more numerous experimental points obtained with metal G-12. Each curve starts at a very low value of  $C_0$  and rises, with irregular oscillations, until it reaches a maximum at prior plastic extension of about 10 percent. In the curve for metal G-12, the most rapid rise is within the first 3 percent of prior plastic extension. In the curve for metal G-14, if enough experimental points had been determined, the most rapid rise probably would begin at a prior plastic extension of a little more than 3 percent, as indicated by the curved broken line in figure 6.

The highest point in each curve for  $C_0$  (in figs. 6 and 8) is the point at which the corresponding stress-

modulus line (figs. 5 and 7) changes from a curve to a straight line. The strongly curved stress-modulus lines 10 (figs. 5 and 7) give low points 10 in the modulus-extension curves of figures 6 and 8. The straight stress-modulus lines 12 in figures 5 and 7 give high points in the modulus-extension curves of figures 6 and 8, respectively.

Beyond the highest point in the  $C_0$  curves (figs. 6 and 8), each curve descends at a gradually decreasing rate and is still descending slightly at the beginning of local contraction. With further extension, by drawing or by rolling, the curve would be expected to become practically horizontal. This expectation is confirmed by the horizontal course of the  $C_0$  curve for severely cold-worked monel metal G (fig. 12). As would be expected,  $C_0$  is lower for monel metal G than for annealed monel metal that has been extended to the beginning of local contraction (figs. 6 and 8). The evidence therefore indicates that plastic extension beyond the maximum in the  $C_0$  curves tends to cause continuous descent at a decreasing rate. Reasons for the rise and descent of the  $C_0$  curve are given in section X.

Annealing work-hardened monel metal at 800° F. for relief of internal stress causes the  $C_0$  curve to take a different course from that of the curve for unannealed metal G. The  $C_0$  curve for monel metal G-8 (fig. 12) starts at a very low value of  $C_0$  and rises continuously throughout the extent here shown (to the beginning of local contraction). The influence of internal stress and of other factors on the course of the  $C_0$  curve is discussed in section X.

#### THE INFLUENCE OF PRIOR PLASTIC EXTENSION ON THE CURVATURE OF THE STRESS-MODULUS LINE FOR MONEL METAL

The rise and the descent of the  $C_0$  curves for annealed monel metal (figs. 6 and 8) with plastic extension means that the slope of the stress-modulus line first decreases and then increases. Within the range of plastic extension that causes the slope of the stress-modulus line to decrease, the line is curved. Consideration must now be given to the variation of this curvature with prior plastic extension. An index of the curvature of the stress-modulus line is  $C'$ , the coefficient of the last term in equation (5). The variations of the curvature of the stress-modulus line for annealed monel metal are shown by the values of  $C'$  obtained from the stress-modulus lines for monel metal G-14 and G-12 (figs. 5 and 7) plotted as ordinates in figure 46, with abscissas representing prior plastic extensions.

The quadratic stress coefficient ( $C'$ ) of the modulus was obtained directly from the stress-modulus curves in the following manner: Straight lines were drawn tangent to the curves at the zero values of stress. For some conveniently selected value of stress, which was the same for each curve of the series obtained with a

single specimen, the deviation of this line from the curve was measured. This deviation, divided by the product of  $E_0$  and the stress squared, gave the value of  $C'$ .

The  $C'$  curves in figure 46 start at low values of  $C'$  and rise rapidly to a maximum, which is reached at a plastic extension of about 1 percent. The value of  $C'$  at the maximum is many times the initial value. With further plastic extension, the curves have a general downward trend and disappear at plastic extension of about 10 percent. At this extension, the stress-modulus line becomes straight and  $C_0$  reaches a maximum (figs. 6 and 8). The  $C'$  curves for annealed monel metal (fig. 46) show that plastic extension first increases and then decreases the curvature of the stress-modulus line. The reasons for this variation of  $C_0$  and  $C'$  are given in section X.

#### THE FORM OF THE STRESS-DEVIATION CURVE FOR MONEL METAL

These variations of  $C_0$  and  $C'$  with plastic extension are evidently due to variations in form of the stress-strain and the stress-deviation curves. The general equation for the stress-strain curve is derived from equation (3)

$$\epsilon = S/E = S/E_0(1 - C_0S - C'S^2) \quad (4)$$

where  $\epsilon$  is the total elastic strain. As the linear and quadratic correction terms are generally small compared with 1, equation (4) may be written

$$\epsilon = (1/E_0)(S + C_0S^2 + C'S^3) \quad (5)$$

The strain corresponding to the tangent to the stress-strain line at the origin is  $S/E_0$ . The deviation ( $\epsilon_d$ ) from this tangent is

$$\epsilon_d = \epsilon - S/E_0 = (1/E_0)(C_0S^2 + C'S^3) \quad (6)$$

When the stress-modulus line is straight,  $C'$  is zero and the last term of equation (6) disappears. The stress-deviation relationship corresponding to a straight stress-modulus line, therefore, is represented by

$$\epsilon_d = C_0S^2/E_0 \quad (7)$$

which is the equation for a quadratic parabola. When  $C_0$  is zero,  $C_0S^2$  of equation (6) disappears. The stress-deviation line corresponding to this relationship is represented by

$$\epsilon_d = C'S^3/E_0 \quad (8)$$

which is the equation for a cubic parabola.

The stress-deviation curve for monel metal that has been plastically extended more than about 10 percent, therefore, is a quadratic parabola. The initial stress-modulus line obtained with monel metal G-12 (fig. 7) and stress-modulus lines 2 and 3 obtained with monel metal G-14 (fig. 5) are vertical at the origin, indicating that  $C_0$  is zero. The corresponding stress-deviation curves are cubic parabolas. As  $C_0$  for line 1 obtained

with monel metal G-14 is very small, the corresponding stress-deviation curve evidently approximates a cubic parabola. The other curved stress-modulus lines in figures 5 and 7 evidently are derived from stress-deviation curves that are cubics intermediate between a quadratic and a cubic parabola.

#### THE SECANT MODULUS AT ANY STRESS

The secant modulus at any stress may be calculated from corresponding values of  $E_0$  and  $C_0$  provided that the stress-modulus line is straight. When the stress-modulus line is curved, the modulus at a given stress may be calculated from  $E_0$  by means of equation (5) if the values of both  $C_0$  and  $C'$  are known. The intermediate curves in figures 6, 8, and 12 represent the variations of the secant moduli corresponding to some arbitrarily selected stresses. In figures 6 and 8, curves  $E_{50}$  show the variation of the secant modulus corresponding to a tensile stress of 50,000 pounds per square inch. In figure 12, curve  $E_{100}$  shows the variation of the modulus corresponding to a tensile stress of 100,000 pounds per square inch. These curves have not been extended to the left of the point of change of the stress-modulus line from a curve to a straight line. This point of change is indicated by the change from a broken to a solid line in the curves of variation of  $E_0$  and  $C_0$ . Modulus values corresponding to stresses between zero and either 50,000 or 100,000 pounds per square inch can be estimated from these diagrams by interpolation.

#### THE EFFECT OF ANNEALING ON THE INITIAL PAIR OF STRESS-SET CURVES AND ON THE DERIVED PROOF STRESSES ON COLD-DRAWN MONEL METAL.

The effect of annealing on the initial pair of stress-set curves obtained with cold-drawn monel metal is shown in the diagram at the right of figure 3. The curves there shown are the initial pairs of curves obtained with the metal as received and after annealing at 800, 1,200, and 1,400° F. The stress-set curves are in the lower row.

Annealing at 800° F for relief of internal stress has increased the steepness of both the first and the second curves, throughout the extent here shown. Annealing at either 1,200 or 1,400° F, for complete recrystallization, has greatly depressed both stress-set curves of the initial pair. The softening effect of the annealing at 1,400° F evidently was somewhat greater than the softening effect of the annealing at 1,200° F.

The effects of annealing on the proof stresses obtained by the first and the second loading are shown in the two diagrams for monel metal in figure 20. One of these diagrams, designated "first loading," represents proof stresses obtained from the initial stress-set curve after annealing at various temperatures. The diagram

designated "second loading" represents results obtained from the second stress-set curve of each initial pair. Abscissas in these diagrams represent temperatures in degrees; ordinates represent proof stresses. Results obtained with unannealed, cold-drawn monel metal are plotted at an abscissa representing room temperature (70° F). The broken lines connecting corresponding points at abscissas 70° F and 800° F do not represent the actual variation of proof stresses with temperature. The actual variation is not linear.

As illustrated by the diagram designated "first loading," annealing for relief of internal stress (at 800° F) has caused great improvement in the 0.001-, the 0.003-, and the 0.01-percent proof stresses. This annealing, however, has slightly decreased the 0.03-percent proof stress and has considerably decreased the 0.1-percent proof stress. As illustrated by the diagram designated "second loading," annealing at 800° F has lowered all the proof stresses relative to the proof stresses obtained (by second loading) with the metal as received. The 0.003-percent proof stress and the 0.01-percent proof stress obtained by second loading with the metal annealed at 800° F, however, are greater than the corresponding proof stresses obtained by first loading with the metal as received.

Annealing for the relief of internal stress, therefore, causes much improvement in the initial proof stresses that may be considered indices of elastic strength but causes some decrease in the initial proof stresses that may be considered indices of yield strength. On second loading, however, much of the improvement due to relief of internal stress by annealing evidently is lost. This relationship is in accordance with the previously discussed initial descent of the lower proof-stress-extension curves for monel metal G-8.

#### THE EFFECT OF ANNEALING ON THE MODULUS OF ELASTICITY AND ON ITS STRESS COEFFICIENT FOR COLD-DRAWN MONEL METAL

In the consideration of the effect of annealing on the modulus of elasticity and on its stress coefficient, attention will be confined to results derived from initial stress-modulus curves. Results so obtained are shown in the diagram at the left of figure 21.

The modulus at zero stress ( $E_0$ ) evidently is little affected by annealing. No change has resulted from annealing (at 800° F) for relief of internal stress; a slight decrease has resulted from annealing for recrystallization, at 1,200 and 1,400° F. The linear stress coefficient ( $C_0$ ) of the modulus, however, has been greatly decreased by annealing for relief of internal stress. Not much further change has been caused by annealing for recrystallization. The probable variation of the quadratic stress coefficient  $C'$  with annealing temperature is represented approximately by the broken curve.

#### IV. THE TENSILE ELASTIC PROPERTIES OF INCONEL AS AFFECTED BY PLASTIC DEFORMATION AND BY ANNEALING

##### DESCRIPTION OF THE INCONEL

The composition of the Inconel is given in table I. As the percentage of iron is small, the alloy may be classed as nonferrous. This alloy, which is of the Nichrome type, has good resistance to plastic deformation and to oxidation at elevated temperatures. As it is practically a single-phase alloy, its elastic strength depends chiefly on plastic deformation and only slightly on heat treatment.

The alloy was supplied in the form of cold-drawn round rods, which had not been subsequently annealed. For investigation of the elastic properties, one specimen was tested as received, one specimen was annealed at 850° F for relief of internal stress, and one specimen was annealed at 1,750° F for complete recrystallization. Details of the annealing treatment are given in table III. These specimens were tested by the same methods that were used for monel metal. In discussing the results obtained with Inconel, attention will be directed first to the metal in a relatively soft condition, after annealing at 1,750° F.

##### THE INFLUENCE OF PRIOR PLASTIC EXTENSION ON THE STRESS-SET CURVE AND ON THE DERIVED PROOF STRESSES FOR FULLY ANNEALED INCONEL

Correlated stress-deviation and stress-set curves obtained with fully annealed Inconel are shown in the diagram at the right of figure 13. All the curves in this diagram were obtained with a single specimen of Inconel, which had been annealed at 1,750° F. The curves were obtained consecutively, with intervening stages of prior plastic extension. Proof stresses derived from these curves are plotted in figure 14.

Stress-set curves 1 and 2 (fig. 13) have about the same curvature. A very different relationship, however, exists between the curves of every other pair. The first curve of each of these pairs is less steep than the second. This difference in slope tends to increase with an increase in the prior plastic extension. The difference in slope between the stress-set curves of a pair causes an abrupt rise in the proof stress-extension curves. The influence of the extension spacing and of the variations of the rest interval evidently is qualitatively the same for Inconel as for monel metal.

The oscillations, which are due to the influence of the extension spacing and the variations of the rest interval, are superposed on a basic curve of variation of proof stress with prior plastic extension. The form of this basic curve would be more clearly revealed if all the experimental points had been determined with long prior rest intervals. The superposed oscillations would thus have been minimized. The course of the basic curve in figure 6, however, can be qualitatively deter-

mined by tracing it through the low points of the superposed oscillations. Point 1, based on the initial stress-set curve was obtained after a very long rest interval. The basic curve, therefore, should start from this point and should pass through the other points that have been determined with a long rest interval.

The basic curves for the 0.001-, 0.003-, and 0.01-percent proof stresses evidently descend rapidly and reach a minimum at slight plastic extension. The curves for the 0.03- and 0.1-percent proof stresses have slight initial downward trend. The minimum is at about point 7 in the curves for the 0.001- and 0.003-percent proof stresses, at about point 5 in the curve for the 0.01-percent proof stresses, and at point 2 in the curves for the 0.03- and 0.1-percent proof stresses. The extension at the minimum evidently tends to decrease with an increase in the value of the permanent set on which the proof stress is based. In this respect, the proof stress-extension curves for Inconel resemble the corresponding curves for annealed monel metal (figs. 2 and 4).

With further plastic extension, the curve for the 0.001-percent proof stress has practically no general upward or downward trend. The other curves have a general upward trend. The superposed oscillations in the lower three curves tend to increase in amplitude with prior plastic extension.

##### THE INFLUENCE OF PRIOR PLASTIC EXTENSION ON THE STRESS-SET CURVE AND ON THE DERIVED PROOF STRESSES FOR WORK-HARDENED INCONEL

In the diagram at the left of figure 13 are stress-deviation and stress-set curves obtained with cold-drawn, unannealed Inconel L. The proof stresses derived from these stress-set curves are plotted in a diagram in figure 10, which shows the variation of the proof stresses with prior plastic extension. The stress-set curves in figure 13 and the derived experimental points in figure 10, are correspondingly numbered.

These experiments with unannealed work-hardened Inconel L were made before<sup>5</sup> the testing procedure was as fully developed as in the experiments described in the preceding portion of this report. The experimental points were not distributed in pairs. Moreover, no long rest intervals were provided (except the interval prior to determination of the initial stress-set curve). Most of the experimental points were obtained with a very short prior rest interval.

The initial stress-set curve for Inconel L (fig. 13) is much less steep than curve 2. This relationship is revealed also by the relative heights of the corresponding points in the proof-stress-extension curves. In each of these curves point 2 is higher than point 1. Because of the absence of distinct pairs of experimental

<sup>5</sup> The Inconel L tests were made 40 months before the experiments with annealed Inconel (L-8.5 and L-17.5).

points, the influence of the extension spacing is less conspicuous in this diagram than in the previously considered diagrams of this type. The influence of duration of the rest interval, however, is clearly revealed. The two stress-set curves that were obtained with a relatively long prior rest interval (fig. 13) are much less steep than the other curves, and the corresponding points in each of the lower three proof-stress-extension curves (fig. 10) are at depressions.

The depression in each of these curves, however, is not due entirely to the influence of duration of the rest interval. The oscillations due to variations of the rest interval are superposed on a basic curve of variation of proof stress with prior plastic extension. The exact course of this basic curve could be determined only by experiments with all the rest intervals long. Nevertheless, some conclusions can be drawn as to the probable course of this curve. Although points 2 and 3 were both obtained with short rest intervals, point 3 in each curve is higher than point 2; this difference in height is very great in the curves for 0.001 percent and 0.003 percent proof stresses. This relationship appears to indicate that the initial rise in each of the curves as drawn is due largely to an initial rise in the basic curve. Similar reasoning leads to the conclusion that the second rise in the lower two curves as drawn is due largely to a rise in the basic curve. The basic curves, therefore, probably are qualitatively similar to the curves as drawn. In the curves as drawn, however, the rise, descent, and reascent are accentuated by the differences in duration of the rest interval. The basic curve for cold-drawn unannealed Inconel L, therefore, probably is similar in form to the curve for cold-drawn unannealed monel metal G (fig. 10).

A specimen of work-hardened Inconel was annealed at 850° F for relief of internal stress. The specimen was then extended by small stages, and stress-deviation and stress-set curves were obtained as usual. They are shown in the diagram for Inconel L-8.5 in figure 13. A comparison of the initial stress-set curves for metals L and L-8.5 shows that annealing for relief of internal stress has greatly increased the steepness of the stress-set curve. Proof stresses derived from these curves have been plotted in the diagram at the right of figure 10, in which abscissas represent prior plastic extensions. The experimental points in this diagram are arranged in pairs. The first point of each pair was obtained with a long prior rest interval; the second point was obtained with a relatively short rest interval. As in previously described diagrams, the second point of each pair generally is higher than the first. The influence of duration of the rest interval and of the extension spacing, therefore, is qualitatively the same for this metal as for the metals previously described.

The basic 0.001- and 0.003-percent proof-stress curves, for Inconel that had been annealed for relief of

internal stress, evidently have an initial rise to a maximum, followed by abrupt descent. In this respect, these curves resemble the basic curves for unannealed monel metal G and unannealed Inconel L, rather than the curves for monel metal (G-8), which was annealed for relief of internal stress. This unexpected relationship possibly is due to incomplete relief of internal stress by the annealing at 850° F. Slight internal stress remaining after this treatment would be reduced, rather than increased, by plastic extension, and thus would account for the initial rise of the proof-stress-extension curves.

#### THE VARIATION OF THE MODULUS OF ELASTICITY WITH STRESS FOR INCONEL

The corrected stress-deviation curves for Inconel, in the upper row of figure 13, are curved from the origin. The modulus of elasticity for Inconel as for monel metal, evidently tends to decrease with an increase of stress. From the corrected stress-deviation curves for Inconel have been derived curves of variation of the modulus of elasticity with stress (fig. 15). The curves are numbered consecutively to correspond to the stress-deviation curves from which they are derived. The plastic extension prior to determination of each stress-modulus line may be found by reference to the correspondingly numbered points in the derived diagrams of figures 12 and 16, which will be described later.

In the diagram for fully annealed Inconel, in the lower row of figure 17, stress-modulus line 1 (as drawn) is straight and vertical. Not much importance, however, should be assigned to the straightness of this line, because a slight change in either the uncorrected initial stress-deviation curve or the initial stress-set curve (fig. 13) would change the initial stress-modulus line (fig. 15) to a slightly curved line. Curved lines were obtained with fully annealed monel metal (figs. 5 and 7) and with other annealed single-phase metals to be described later.

Stress-modulus lines 2 to 6, inclusive, obtained with annealed Inconel (fig. 15), are curved from the origin. The curvature decreases from line 2 to line 6. Lines 11 to 16, inclusive, are straight. For lines 7 to 10, inclusive, the course of the ideal line is less clearly indicated. It may be that the curvature of these lines should decrease gradually in passing from curve 7 to curve 10. Not much error probably has been introduced, however, by drawing these lines straight. The evidence, therefore, indicates that prior plastic extension of a few percent causes the stress-modulus line for annealed Inconel to become practically straight. As would be expected, consequently, the stress modulus lines for the more severely cold-worked Inconel L (fig. 15) are practically straight except in the upper part.

The stress-modulus lines for work-hardened Inconel L-8.5 (fig. 15), which had been annealed for relief of

internal stress, are slightly curved. The slope of the initial line is much less than the slope of the initial stress-modulus line for unannealed Inconel L (in the same figure). The annealing, moreover, has decreased the value of  $E_0$ . This relationship will be discussed later in connection with figure 21.

THE INFLUENCE OF PRIOR PLASTIC EXTENSION ON THE MODULUS OF ELASTICITY AND OF ITS STRESS-COEFFICIENTS FOR INCONEL

The values of  $E_0$  and  $C_0$ , given in figure 7, have been used in deriving diagrams to represent the variation of the modulus of elasticity, and of its stress-coefficients, with prior plastic extension. The experimentally determined points in these diagrams (figs. 12, 16, and 46) have been numbered to correspond with the consecutively numbered stress-modulus lines (fig. 7).

Before the general trend of the curves in figures 12 and 16 is considered, attention will be given to the abrupt oscillations due to the influence of the extension spacing and of the variations of the rest interval. In the diagram for annealed Inconel (fig. 16), the abrupt oscillations of the  $C_0$  curve are qualitatively similar to the oscillations of the  $E_0$  curve. Each abrupt rise or drop in the curve for  $E_0$ , at a pair of experimental points, is accompanied by a similar abrupt change in direction in the curve for  $C_0$ . The correspondence in oscillations is less pronounced in the  $E_0$  and  $C_0$  curves for unannealed work-hardened Inconel L (fig. 12). This fact probably is due to the absence of distinct pairs of experimental points, and hence, to the absence of a pronounced influence of extension spacing.

A comparison should also be made between the modulus-extension curves (fig. 16) and the proof stress-extension curves (fig. 14) obtained with annealed Inconel L-17.5. The abrupt oscillations at pairs of experimental points in the curves for  $E_0$  and  $C_0$ , with few exceptions, are accompanied by the opposite oscillations in the proof stress-extension curves. As previously mentioned in the discussion of monel metal, such a relationship is to be expected. No such correspondence in oscillations, however, is found by comparison of the modulus-extension curves with the proof-stress-extension curves for work-hardened Inconel L (figs. 12 and 10, respectively).

Consideration will now be given to the general trend of the  $E_0$  curve for annealed Inconel L-17.5 (fig. 16). The variation of  $E_0$  with prior plastic extension is represented by the lines connecting the experimental points. The basic curve, as indicated by the dotted line representing its course, rises rapidly to a maximum and then descends at a decreasing rate. The maximum in this curve is at the point of change of the stress-modulus line (fig. 15) from a curve to a straight line. The course of the modulus-extension curve depends on the interrelationship between three factors, to be discussed in section X.

The  $E_0$  curve for unannealed work-hardened Inconel L (fig. 12) descends rapidly from the origin. The rate decreases rapidly, however, and the curve becomes practically horizontal at a prior plastic extension of about 2 percent. As the course of the curve beyond the beginning of local contraction is always somewhat erratic, the slight rise of the curve beyond about 2 percent extension may not represent a rise of the basic curve. The  $E_0$  curve for work-hardened Inconel differs greatly in form from the curve for work-hardened monel metal (fig. 12). The  $E_0$  curve for work-hardened Inconel L-8.5 (fig. 12), which was annealed for relief of internal stress, starts much lower than the curve for unannealed, work-hardened Inconel L, and descends much more slowly. The reasons for these forms of the  $E_0$  curve are given in section X.

The  $C_0$  curve for annealed Inconel L-17.5 (fig. 16) starts at a very low value<sup>6</sup> of  $C_0$  and rises rapidly to point 7. Beyond point 7 the curve descends, at first rapidly, but at a gradually decreasing rate, without any indication of a reascent. The highest point in the  $C_0$  curve is the point at which the stress-modulus line (fig. 15) changes from a curve to a straight line. At this point,  $C'$  (the index of curvature of the stress-modulus line) becomes zero. The variation of  $C'$  with plastic extension is shown in figure 46. With increase in the plastic extension from zero,  $C'$  increases rapidly from a low value to a high maximum, then descends less rapidly, and reaches zero at about the same prior plastic extension at which  $C_0$  reaches a maximum (fig. 16). The  $C'$  curve for Inconel (fig. 46), therefore, is similar in this respect to the curves for annealed monel metal (in the same figure).

In the diagram for unannealed work-hardened Inconel L (fig. 12), the basic  $C_0$  curve descends continuously at a decreasing rate. The reascent in the curve as drawn in figure 12, for the reason given above, may not indicate a reascent in the basic curve. The basic  $C_0$  curve probably is similar in form to the basic  $E_0$  curve.

In the diagram for Inconel that has been annealed for relief of internal stress (L-8.5 of fig. 12), the  $C_0$  curve starts at a very low value, and rises slowly. The trend of this curve, therefore, is similar to the trend of the  $C_0$  curve for monel metal G-8. As previously stated, the annealing of Inconel at 850° F may have left considerable internal stress. With plastic extension, the internal stress would at first tend to change very little. It is possible thus to account for the slowness of the ascent of the  $C_0$  curve for metal L-8.5.

As the stress-modulus lines for Inconel L-8.5 (fig. 15) are slightly curved, the stress-coefficient of the modulus is not constant, and only the initial rate of change of

<sup>6</sup> The  $C'$  curve for annealed Inconel (fig. 46) probably should start at a value of  $C'$  greater than zero, comparable with the values of  $C'$  at the origins of the curves for monel metal. This has been discussed previously.

the modulus with stress is represented by  $C_0$ . The average rate of change between zero stress and 100,000 pounds per square inch stress (designated  $C_{100}$ ) has been plotted in figure 12 to show the variation of this index with prior plastic extension. The index evidently differs appreciably from  $C_0$ .

The slight curvature of the stress-modulus lines for Inconel L-8.5 possibly is not unusual for a work-hardened metal that has been annealed for relief of internal stress. The decrease in  $C_0$  caused by annealing for relief of internal stress possibly tends to be accompanied by an appearance of a slight curvature of the stress-modulus line. The stress-modulus lines for annealed, work-hardened monel metal G-8 (fig. 11), however, are practically straight.

The intermediate curves in the diagrams for Inconel (figs. 12 and 16) represent the variations of the secant moduli corresponding to arbitrarily selected stresses. In figure 16, the  $E_{50}$  curve shows the variation of the secant modulus corresponding to tensile stress of 50,000 pounds per square inch. In figure 12 the  $E_{100}$  curve shows the variations of the secant modulus corresponding to a tensile stress of 100,000 pounds per square inch. The curve for annealed Inconel has not been extended to the left of the point of change of the stress-modulus line from a curve to a straight line.

THE EFFECT OF ANNEALING ON THE INITIAL PAIR OF STRESS-SET CURVES AND ON THE DERIVED PROOF STRESSES FOR COLD-DRAWN INCONEL

The effect of annealing on the initial pair of stress-set curves may be observed by comparing the first two curves of each of the three diagrams in figure 13. Annealing at 850° F for relief of internal stress evidently has increased the steepness of both the first and second curves. The second curve obtained with Inconel L-8.5 is only slightly less steep than the first. In this respect this metal differs from monel metal G-8, for which the second curve is considerably less steep than the first. This difference possibly is due to a difference in the degree of relief of internal stress. Annealing monel metal at 800° F is known to eliminate most of the internal stress. It is possible that somewhat more internal stress remains after annealing Inconel at 850° F.

The effect of annealing on the initial proof stresses, and on the proof stresses derived from the second stress-set curve of each initial pair, is shown in the two diagrams for Inconel in figure 20. One of these diagrams, designated "first loading," represents proof stresses obtained from the initial stress-set curve at three temperatures. The other diagram, designated "second loading," represents results obtained from the second stress-set curve of each initial pair. Abscissas in these diagrams represent annealing temperatures; ordinates represent proof stresses. Results obtained with unannealed, cold-drawn Inconel are plotted at an abscissa representing room temperature (70° F). The broken lines

connecting corresponding points at abscissas 70° F and 850° F do not represent the actual variation of proof stresses with temperature. The actual variation is not linear.

As illustrated by the diagram designated "first loading," annealing for the relief of internal stress (at 850° F) has caused great improvement in the 0.001- and 0.003-percent proof stresses, and has caused slight improvement in the 0.01-percent proof stress. This annealing, however, had no effect on the 0.03-percent proof stress and slightly lowered the 0.1-percent proof stress. As represented by the diagram designated "second loading," annealing at 850° F has greatly increased the 0.001- and 0.003-percent proof stresses, has slightly increased the 0.01-percent proof stress, and has slightly lowered the 0.03- and 0.1-percent proof stresses relative to the proof stresses obtained by second loading with the metal as received. Annealing for relief of internal stress, therefore, causes much improvement in the (initial) proof stresses that may be considered indices of elastic strength, but causes some decrease in the proof stress (0.1 percent) that may be considered as an index of yield strength. The effect of annealing for relief of internal stress, on the initial proof stresses, is qualitatively the same for Inconel as for monel metal (fig. 20).

By means of these two diagrams for Inconel, it is possible to compare the results of relief of internal stress due to annealing at 850° F with the results of relief of internal stress due to slight plastic extension. This relationship is revealed by comparing the heights of corresponding curves in the first-loading and second-loading diagrams, at abscissas representing 850° F and 70° F, respectively. This comparison shows that the slight plastic extension during first loading caused about as much improvement in proof stresses as did the annealing at 850° F. The rise of the second-loading curves, between abscissas representing 70° F and 850° F, however, indicates that the slight plastic extension during the first loading did not remove all the internal stress.

THE EFFECT OF ANNEALING ON THE MODULUS OF ELASTICITY AND ON ITS STRESS COEFFICIENT FOR COLD-DRAWN INCONEL

In considering the effect of annealing on the modulus of elasticity, and on its stress coefficient, attention will be confined to results derived from initial stress-modulus lines. Results so obtained are shown in the diagram at the right of figure 21.

The initial modulus at zero stress ( $E_0$ ) evidently is decreased by annealing at 850° F, and it is still further decreased by annealing at 1,750° F. The modulus of severely cold-worked Inconel L, therefore, is lowered by annealing. This evidence alone might appear to imply that the modulus (for Inconel) is always increased by cold work. As shown in figures 12 and 16,

however, cold work under some conditions may decrease the modulus. Fully annealed Inconel (fig. 16) when plastically extended, shows a rapid *increase* of  $E_0$  until the prior plastic extension reaches about 1.9 percent. With further plastic extension,  $E_0$  decreases. Unannealed, cold-drawn Inconel (fig. 12), however, shows a rapid *decrease* of  $E_0$  with prior plastic extension. The complex variation of the modulus of elasticity with plastic deformation and with annealing evidently is due to the operation of more than one factor. These factors are discussed in section X.

The linear stress-coefficient ( $C_0$ ) of the modulus evidently is greatly decreased by annealing for relief of internal stress. Further decrease is caused by annealing for recrystallization. The effects of annealing on  $C_0$  and  $E_0$  therefore, are qualitatively similar. The  $C_0$  curve for Inconel is similar to the  $C_0$  curve for monel metal (fig. 12), but the  $E_0$  curve for Inconel differs greatly from the  $E_0$  curve for monel metal.

## V. THE TENSILE ELASTIC PROPERTIES OF ALUMINUM-MONEL METAL AS AFFECTED BY PLASTIC DEFORMATION AND BY HEAT TREATMENT

### DESCRIPTION OF THE ALUMINUM-MONEL METAL

Aluminum-monel metal, unlike monel metal and Inconel, may have its strength greatly increased by heat treatment. Heating to 1,450° F or higher gives a solid solution consisting of a single phase. Rapid cooling from this temperature preserves this single solid solution practically unchanged. In this condition the metal is relatively soft and is easily workable; it probably differs little in properties from ordinary annealed monel metal. Reheating to 1,000–1,100° F, however, causes a precipitation of a second microconstituent in finely divided form, and thus causes great increase in hardness.

The aluminum-monel metal supplied for this investigation was in two different conditions. Both samples probably had been heated to about 1,450° F and rapidly cooled; both samples had then been cold drawn. One of the samples (J) had then been reheated, probably to 1,000–1,100° F; the other sample (H) had not been reheated. Sample (H), as shown in table II, is somewhat softer than the severely cold-drawn monel metal G; the other sample (J) is much harder. The tensile strengths of metals H, G, and J are 116,960, 125,700, and 164,150 pounds per square inch, respectively.

### THE INFLUENCE OF PRIOR PLASTIC EXTENSION ON THE STRESS-SET CURVE AND ON THE DERIVED PROOF STRESSES FOR WORK-HARDENED ALUMINUM-MONEL METAL H

Stress-deviation and stress-set curves obtained with aluminum-monel metal are shown in figure 17. The proof stresses derived from the stress-set curves are plotted as ordinates in figure 18, with the corresponding prior plastic extensions as abscissas. In the diagram

at the left of each of these figures are curves obtained with work-hardened aluminum-monel metal (H).

The initial stress-set curve for monel metal H is much less steep than the second stress-set curve. This relationship is similar to that found for unannealed, work-hardened monel metal (G) and Inconel (L). As the experiments with aluminum-monel metal were made before the test procedure had been fully developed, all the curves but one were obtained with short prior-rest intervals. The experimental points in each stress-set curve, moreover, are too few to show more than qualitative relationships between the curves of this series. The one curve obtained with a relatively long prior-rest interval, however, is less steep than the following curve. The influence of duration of the rest interval, therefore, is qualitatively the same for aluminum-monel metal as for the ordinary monel metal and Inconel.

The intervals of plastic extension between the determinations of stress-set curves, as shown in the diagram at the left of figure 18, are of approximately the same length, instead of being alternately long and short as they are in all but one of the previously discussed diagrams of this type. The wide oscillations due to the combinations of extension spacing and rest intervals used in the previous tests, therefore, are not found in the curves for this material.

The initial trend of each of the basic curves (fig. 18) evidently is upward. The curves for the 0.001-, 0.003-, and 0.01-percent proof stresses then descend to a minimum at small plastic extension (point 5). The second minimum, at point 8, probably is due to the influence of the relatively long prior-rest interval. The basic curves for the 0.001- and 0.003-percent proof stresses probably consist of an initial rise and descent, followed by a reascent, at least to the beginning of local contraction. This basic curve thus resembles the curve for the work-hardened alloys previously discussed, monel metal G and Inconel L (fig. 10). The initial rise and descent of the curves for the 0.001- and 0.003-percent proof stresses, however, is much less steep for aluminum-monel metal H than for monel metal G or Inconel L. This difference may be due to the fact that the stress-set curves for aluminum-monel metal (as previously stated) are based on too few experimental points.

### THE INFLUENCE OF PRIOR PLASTIC EXTENSION ON THE STRESS-SET CURVE AND ON THE DERIVED PROOF STRESSES FOR HEAT-TREATED ALUMINUM-MONEL METAL J

Stress-set curves for heat-treated aluminum-monel metal J are shown in the diagram at the right of figure 17. (No stress-deviation curves were obtained with this heat-treated alloy.) The proof stresses derived from these stress-set curves are plotted as ordinates in the diagram at the right of figure 18, with prior plastic

extensions as abscissas. This alloy had been heat-treated by the manufacturers. The temperature of reheating, as previously stated, generally ranges from 1,000 to 1,100° F. At this temperature, the strengthening effect of previous cold work is not entirely eliminated, and the alloy is further strengthened by the precipitation of a finely divided microconstituent.

The initial stress-set curve is steeper than the second curve. In this respect, the heat-treated alloy J differs from the work-hardened alloy H; it is similar to fully annealed monel metal (G-12 and G-14), to annealed Inconel (L-17.5), and to work-hardened monel metal and Inconel that have been annealed for the relief of internal stress (G-8 and L-8.5). The reheating treatment of aluminum-monel metal (at 1,000–1,100° F) apparently has removed most of the internal stress due to the previous cold work. A difference in the internal stress would account for the difference between metals H and J with respect to the relative steepness of the stress-set curves of the first pair.

As shown in figure 18, the experimental points and the stress-set curves from which they are derived, are distributed in pairs, separated by relatively long intervals of prior plastic extension. The first stress-set curve of each pair was determined after a relatively long rest interval; the second stress-set curve was determined after a very short rest interval. The influence of the extension spacing and of the duration of the rest interval has caused the first stress-set curve of each pair (fig. 17), with the exception of the first pair, to be much less steep than the second curve. In figure 18, consequently, the second experimental point of each pair except the first pair is higher than the first. This difference in height of the experimental points of a pair increases with the prior plastic extension. The relatively great difference between the rest intervals for the points of each pair has caused the abrupt rises of the curves to be generally greater in figure 18 than in most of the previously discussed diagrams of this type.

In spite of the short rest interval prior to point 2, in the diagram for the metal J in figure 18, the curves for the 0.001- and 0.003-percent proof stresses show an initial rapid descent. This rapid descent doubtless is the initial trend of the basic curve. The qualitative course of the basic curve may be traced through the experimental points representing long rest intervals. The first minimum in this curve is reached at small plastic extension, probably less than 1 percent. The curve then rises, and attains a maximum. The basic curves for the 0.001- and 0.003-percent proof stresses show practically no continued upward trend. The basic curve for the 0.01-percent proof stress also shows an initial descent to a minimum. The 0.03- and 0.1-percent proof stress curves, however, show no initial descent but have a general upward trend at a gradually decreasing rate.

The basic curves for heat treated aluminum-monel metal, therefore, are qualitatively similar to the basic curves obtained with the monel metal and Inconel that have been either fully annealed or annealed for the relief of internal stress.

#### THE VARIATION OF THE MODULUS OF ELASTICITY WITH STRESS FOR ALUMINUM-MONEL METAL

Because no stress-deviation curves were obtained with heat treated aluminum-monel (J), no information has as yet been obtained about the modulus of elasticity of this alloy. Stress-deviation curves, however, were obtained with the work-hardened aluminum-monel metal (H). These curves are shown in the upper row of the diagram at the left of figure 17. From these stress-deviation curves have been derived curves of variation of the modulus of elasticity with stress. These curves are shown in the lower diagram of figure 7.

The vertical direction of the initial stress-modulus line (fig. 7) cannot be accepted without additional evidence. This line is based on only three points in figure 17. All of the other stress-modulus lines for aluminum-monel metal H (fig. 7) are sloping and straight except near the upper end. In this respect they are similar to the stress-modulus lines obtained with the previously described cold-worked metals G and L (figs. 11 and 15). As shown in section III, a straight, sloping stress-modulus line is obtained when the stress-deviation line is a quadratic parabola. This line is the characteristic stress-deviation line for cold-worked monel metal and Inconel. Moreover, the sloping stress-modulus line has been shown (reference 1) to be the characteristic stress-deviation line for cold-worked 18:8 alloy.

#### THE INFLUENCE OF PRIOR PLASTIC EXTENSION ON THE MODULUS OF ELASTICITY AND OF ITS STRESS COEFFICIENTS FOR ALUMINUM-MONEL METAL H

In figure 19, values of  $E_0$  and  $C_0$ , derived from the stress-modulus lines in figure 7, are plotted as ordinates, and the corresponding prior plastic extensions are plotted as abscissas. The experimentally determined points in figure 19 have been numbered to correspond to the consecutively numbered stress-modulus lines in figure 7.

In previously described diagrams of this type (figs. 6, 8, 12, and 16), oscillations in the  $E_0$  curve generally are accompanied by similar oscillations in the  $C_0$  curve. Because of the absence of distinct pairs of experimental points in the curves of figure 19, however, such a relationship does not appear in this figure.

The  $E_0$  curve shows no distinct evidence of either upward or downward trend; the oscillations are within a very narrow range. In this respect, as would be expected, the  $E_0$  curve for cold-worked aluminum-monel metal H resembles the curve for cold-worked monel metal G (fig. 12).

The  $C_0$  curve (fig. 19), as drawn, rises abruptly from zero. As previously shown, however, the initial value of  $C_0$  is based on the probably incorrect vertical direction of the initial stress modulus line (fig. 7); the initial value possibly should be much greater. The  $C_0$  curve, moreover, would be expected to oscillate within a narrow range, as does  $C_0$  curve for cold-worked monel metal G (fig. 12).

## VI. THE TENSILE ELASTIC PROPERTIES OF 18:8 CHROMIUM-NICKEL STEEL AS AFFECTED BY PLASTIC DEFORMATION AND BY ANNEALING

### DESCRIPTION OF THE 18:8 CHROMIUM-NICKEL STEEL

The previous report considered the elastic properties of 18:8 chromium-nickel steel as affected by plastic deformation. Consideration will now be given to the elastic properties of this alloy as affected by annealing, especially annealing for the relief of internal stress. Further consideration will then be given to the influence of plastic deformation.

The 18:8 alloy used in this continued investigation was supplied in two different degrees of hardness, designated "half-hard" and "hard." The different degrees of hardness are due to different amounts of cold drawing. Both the half-hard metal (DM) and the hard metal (DH) are from the same heat. The composition is given in table I.

Specimens of half-hard and hard metal were tested as received. Other specimens, before testing, were "annealed" for complete recrystallization and softening. For complete recrystallization, it is necessary to heat this alloy only to about 1,200° F. For the complete solution of any precipitated carbides, however, it is necessary to heat the alloy to about 1,800° F. Rapid cooling from this temperature prevents reprecipitation of the carbides and the alloy is in its softest condition. The softening treatment actually given consisted in heating to 1,830° F and in quenching in water. Other specimens were annealed at various temperatures to obtain various degrees of relief of internal stress. Details of these treatments are given in table III.

### THE EFFECT OF ANNEALING ON THE INITIAL PAIR OF STRESS-SET CURVES AND ON THE DERIVED PROOF STRESSES FOR 18:8 CHROMIUM-NICKEL STEEL

The specimens as received and after annealing at various temperatures were subjected to tension tests to obtain correlated stress-deviation and stress-set curves. The initial pair of each of these types of curve was obtained with every specimen. A few of the annealed specimens were extended, by numerous small stages, to the beginning of local contraction, and correlated stress-deviation and stress-set curves were determined after each stage of extension. In the study of the influence of annealing on elastic strength, how-

ever, attention will be confined to the initial pair of stress-set curves and to the derived proof stresses.

The stress-set curves (and the stress-deviation curves) of each initial pair have been determined (as usual) with practically no intervening plastic extension. Pairs of stress-set curves obtained with the specimens as received and after annealing at various temperatures are shown in the lower row of figure 22; corresponding pairs of stress-deviation curves are shown in the upper row. In the diagrams at the left and right of figure 22 are results obtained with half-hard metal DM and with hard metal DH, respectively. The duration of the anneal, unless otherwise indicated, was 30 minutes.

Before the influence of annealing temperature on either the first or the second stress-set curve is considered, a comparison will be made between the first and second stress-set curves of each pair. In each diagram of figure 22, the second stress-set curve of each pair is steeper than the first. This difference in steepness is greatest for the initial pair of stress-set curves, for both DM and DH, and tends to decrease with increase in the annealing temperature, at least up to 900° F. These differences in steepness also are greater for the hard metal than for the half-hard metal. The difference in steepness between the first and second stress-set curves is qualitatively the same for this work-hardened 18:8 alloy as received as it is for the work-hardened monel metal G (fig. 9), the work-hardened Inconel L (fig. 13), and the work-hardened aluminum-monel metal H (fig. 17).

The influence of the annealing temperature on either the first or the second stress-set curve may be seen in the lower row of curves in figure 22. The first stress-set curve becomes steeper with an increase in the annealing temperature to 900° F; with a further increase in the annealing temperature to 1,830° F, the curve becomes much less steep. The second stress-set curve becomes steeper with an increase in the annealing temperature to 700° F; with a further increase in the annealing temperature to 900° F the curve becomes slightly less steep throughout the extent here shown. If the curves are compared throughout a wider range of stress, however, very little difference is found between the (second loading) curves obtained after annealing at 700° F and then at 900° F. With a further increase in the annealing temperature to 1,830° F, the curves become much less steep. These variations are qualitatively the same for half-hard and hard metal.

The variations of the proof stresses with annealing temperature are shown in the four diagrams of figure 23. The diagrams designated "first loading" and "second loading" are derived from the first and second curves, respectively, of the pairs of curves in the lower row of figure 22. Ordinates in these diagrams represent proof stresses, and abscissas represent annealing temperatures. An abscissa of 70° F is used to represent results

obtained with specimens as received. All the experimental points at 1,830° F were obtained with a specimen of initially half-hard material DM. Because almost the same proof stresses would be obtained by annealing either initially half-hard or hard material at 1,830° F, the experimental points obtained with the half-hard material DM have been plotted in both the upper and lower diagrams of figure 23.

All the curves in the diagrams representing first loading, and most of the curves in the diagrams representing second loading, rise to a maximum at an annealing temperature of 900°–950° F, and then descend at a decreasing rate. The initial rise is generally greater in a curve representing first loading than in the corresponding curve representing second loading. In the diagram representing first loading of half-hard metal DM, each curve rises (from 70° F) first at an increasing, then at a decreasing rate. In the corresponding diagram for hard metal DH, the curves for the 0.001-, 0.003-, and 0.01-percent proof stresses have a slight initial descent. This initial descent may be due to unavoidable inaccuracies in measurement. These curves possibly should be nearly horizontal up to an annealing temperature of about 500°. Additional experiments would be required to determine whether the steep rise of the curves with an increase in annealing temperature above 500° F is characteristic of a severely work-hardened 18:8 alloy.

In the second-loading diagram for half-hard material, there is no evidence of any important rise of the curves of variation of the 0.001-, 0.003-, and the 0.01-percent proof stresses. Because of the wide scatter of experimental points of the lower two curves, the evidence for the indicated initial descent of these curves must be considered inconclusive. The curves for the 0.03- and the 0.10-percent proof stresses rise considerably throughout this range of temperature. Annealing this half-hard metal for relief of internal stress, therefore, evidently causes no important improvement in the proof stresses that may be viewed as indices of elastic strength (on second loading). Such annealing, however, evidently does cause some improvement in the proof stresses that may be viewed as indices of yield strength.

In the second loading diagram for hard metal DH, the curves for the 0.003- and the 0.01-percent proof stresses rise considerably with an increase in the annealing temperature from 70° F to about 700° F. This rise suggests that there should be a similar important rise in the less accurately determinable curve for the 0.001-percent proof stress. The curve for the 0.03-percent proof stress also rises with an increase in the annealing temperature, probably to 800° or 900° F. No clear evidence of a general upward trend, however, is found in the curve for the 0.1-percent proof stress. Annealing this hard metal for relief of internal stress evidently causes some improvement in the proof stresses that may be viewed as indices of elastic strength

(on second loading) but causes practically no improvement in the proof stress (0.1-percent) that may be viewed as an index of yield strength.

#### RELIEF OF INTERNAL STRESS BY PLASTIC EXTENSION AND BY ANNEALING

The rise in the proof-stress curves with an increase of the annealing temperature from 70° F to 900° F probably is due chiefly to relief of internal stress. This diminution of the internal stress probably is caused by local creep of the metal in the regions where the stress is greatest. Annealing at temperatures as low as 500° F evidently caused important relief of the internal stress in the half-hard metal DM. In the hard metal DH, relief of the internal stress evidently is slight at temperatures below about 750° or 800° F. In both the half-hard and the hard metals, the maximum relief of internal stress probably is caused by annealing at 900° to 950° F.

Some manufacturers of stainless steel have advocated annealing at a temperature of 390° to 570° F for about 36 hours. It has been thought that the long time at this relatively low temperature would have much of the beneficial effects that are caused by annealing at 900° F. In order to investigate the possibilities of this suggested heat treatment, specimens of metals DM and DH were heated at 482° F for 44 hours. The results are represented by the stress-deviation and stress-set curves in figure 22 and by the indicated experimental points in figure 23. The results show that the long time at this temperature has caused little increase of the proof stresses above the values obtained by annealing at the same temperature for 30 minutes.

A comparison of the corresponding second-loading and first-loading diagrams throws some light on the interrelationship between the relief of internal stress by annealing and the relief of internal stress by slight plastic extension. At an abscissa representing 70° F each curve for second loading is much higher than the corresponding curve for first loading. The slight plastic extension in determining the initial stress-set curve has, therefore, greatly increased the proof stresses. Similar elevation of proof stresses by slight plastic extension has been found with work-hardened monel metal and with work-hardened Inconel (fig. 20). The effect of the slight plastic extension of these metals, as shown in figures 20 and 23, is qualitatively similar to the effect of annealing for the relief of internal stress.

A part of the elevation of the proof stresses caused by the slight plastic extension is due to work-hardening; a part is also due to the influence of the duration of the rest interval. The second-loading curves in this figure were obtained after a rest interval of 31 to 37 minutes, whereas the initial curves were obtained long after the cold drawing and generally weeks after the machining. This difference in the duration of the rest interval

is responsible for some of the difference in height between the first-loading and second-loading curves. Nevertheless, much of this difference in height would be found (as shown in the previous report) even if the rest intervals prior to both the first and second loading were long.

The second-loading curves at an abscissa ( $70^{\circ}$  F) representing unannealed material generally differ little in height from the first-loading curves at an abscissa ( $900^{\circ}$  F) representing maximum relief of internal stress by annealing. This relationship (with due allowance for the previously mentioned influence of the duration of the rest interval) suggests that the slight plastic extension required for determining the initial stress-set curve has relieved most of the internal stress in the unannealed metal. The rise in most of the second-loading curves with an increase in the annealing temperature from  $70^{\circ}$  F to  $900^{\circ}$  F apparently indicates that this extension has not removed all of the internal stress, especially in the hard metal DH.

THE INFLUENCE OF PRIOR PLASTIC EXTENSION ON THE DERIVED PROOF STRESSES FOR FULLY ANNEALED 18 : 8 CHROMIUM-NICKEL STEEL

A specimen of the initially half-hard metal DM, which had been given a softening treatment at  $1,830^{\circ}$  F and had then been used in obtaining the experimental points at an abscissa representing  $1,830^{\circ}$  F in figure 23, was extended further by numerous small stages. After each of these stages, correlated stress-deviation and stress-set curves were determined. Because the forms of such curves for 18 : 8 alloy steels have been thoroughly illustrated in the previous report, these curves are not shown in this report. The derived proof stresses, however, have been used in studying the variation of these proof stresses with prior plastic extension. This relationship is shown in figure 24.

The experimental points in this diagram are distributed in pairs. The first three pairs are separated by relatively short intervals of plastic extension; the other pairs are separated by relatively long intervals. The influence of the extension spacing and of the duration of the rest interval causes an abrupt rise in the curves between the first and second experimental points of each pair. The relatively large rises at pairs 11-12, 19-20, and 23-24 evidently are due to the very short rest intervals before the determination of the second experimental points of these pairs. The rise in the curve at a pair of experimental points also tends to increase with an increase in the total plastic extension. In these respects, therefore, the 18 : 8 alloy is qualitatively similar to monel metal, Inconel, and aluminum-monel metal.

The oscillations due to the combined influence of the extension spacing and the duration of the rest interval

are superposed on a basic curve of variation of proof stress with prior plastic extension. The form of the basic curve may be determined approximately by assuming that the curve starts at the indicated origin and traverses the low points of the superposed oscillations. (The assumption that the basic curve follows approximately the low points of the oscillations would give a qualitatively correct form but not a correct position. For a correct position, the basic curve probably should traverse more nearly the midpoints of the oscillations.) The basic curves for the 0.001- and 0.003-percent proof stresses have an initial upward trend from the origin to point 7, at a prior plastic extension of about 2 percent. The trend is then reversed, and the curves descend to a minimum at point 13, at a prior plastic extension of about 16 percent. With further plastic extension, oscillations of the basic curve continue, with no general upward trend in the curve for the 0.001-percent proof stress, but with a slight upward trend in the curve for the 0.003 percent proof stress. The basic curves for the 0.01-, 0.03-, and 0.1-percent proof stresses evidently rise from the origin, at a gradually decreasing rate.

The initial rapid rise and descent of the 0.001- and 0.003-percent proof-stress curves for fully annealed 18:8 chromium-nickel steel is similar to the course of the curves for the annealed 18:8 alloy steel 2A-1 considered in reference 1. The initial course of these curves, however, is very different from the course of the proof stress-extension curves for the other fully annealed alloys that have been discussed in this report. All the proof stress-extension curves for fully annealed monel metal (figs. 2 and 4), and the lower three curves for Inconel (fig. 14), have an initial rapid descent to a minimum. Similar descent is found in the lower three curves for heat-treated aluminum-monel metal J (fig. 18).

The fully annealed monel metals G-12 and G-14, the fully annealed Inconel L-17.5, and the heat-treated aluminum-monel metal J probably were initially free from internal stress. The initial descent of the proof-stress-extension curves for these metals (figs. 2, 4, 14, and 18), therefore, probably is due to the predominant influence of increase of internal stress. As the annealed 18:8 alloy DM-18.3 also probably was initially free from internal stress, the initial rise of the proof-stress curves could not be due to relief of internal stress. The descent following the initial rise, however, must be due to an increase of internal stress. This relationship suggests that the internal stress increased continuously throughout the initial rise and descent of the basic curves but that the depressing influence of the increasing internal stress was overcome at first by the elevating influence of work-hardening. Eventually, the influence of the increasing internal stress predomi-

nated over the influence of the work-hardening, thus causing the proof-stress curves to descend.

The initial trend of a proof-stress-extension curve (for a metal initially free from internal stress) evidently depends on the relative magnitudes of the elevating influence of work-hardening and the depressing influence of increasing internal stress. A metal with a high initial rate of work-hardening tends to give a proof-stress-extension curve with an initial rise and descent, such as the lower two curves obtained with 18:8 alloy DM-18.3 (fig. 24). A metal with a lower initial rate of work-hardening tends to give a curve with an initial descent, such as the curves obtained with fully annealed monel metal, fully annealed Inconel, and heat-treated aluminum-monel metal.

**THE INFLUENCE OF PRIOR PLASTIC EXTENSION ON THE PROOF STRESSES FOR WORK-HARDENED 18:8 CHROMIUM-NICKEL STEEL ANNEALED FOR RELIEF OF INTERNAL STRESS**

The maximum relief of internal stress for 18:8 alloy, as shown in figure 23, is caused by annealing at about 900° F. Specimens of half-hard and hard 18:8 alloy, which had been annealed at 900° F and used in obtaining data for figure 23, were then extended by numerous small stages to the beginning of local contraction. After each of these stages, correlated stress-deviation and stress-set curves were determined. From the stress-set curves, which are not shown in this report, proof stresses have been derived. These proof stresses are plotted against plastic extensions in figure 25.

The experimental points in this figure are distributed in pairs. The influence of the rest interval and of the extension spacing has caused the second experimental point of each pair, with only one exception, to be higher than the first. The resultant oscillations in the curves as drawn make it difficult to determine the entire course of each of the basic curves. The course of such a curve may be established by determining all the experimental points with long prior rest intervals. In the absence of such a series of experimental points, however, the forms of the basic curves in figure 25 may be determined by assuming that these curves would traverse approximately the points that have been determined with a relatively long prior-rest interval. In such a study, consideration must be given to the possibility of a rebound of the basic curve between adjacent low points.

The initial trend of each basic curve in figure 25 may be readily determined. This trend is indicated by the relative positions of points 1 and 3. If point 3 is below point 1, a rise from point 1 to point 2 may be attributed to the influence of the relatively short rest interval prior to the determination of point 2. This is the probable reason for the rise from point 1 to point 2 in the 0.003-percent proof stress curve for half-hard metal DM-9 and in the lower three curves for hard metal DH-9. The initial trend of each of these curves, as indicated by the relatively low position of point 3, is downward.

The initial trend of every other curve in figure 25 is upward.

In the diagram for metal DM-9, the exceptionally high rebound from point 3 to point 4 (in the lower two curves), followed by the still greater recoil to point 5, may possibly be due to a rapid rise and fall of the basic curve. Additional experiments, therefore, are needed to determine whether the first minimum in these curves is at point 3 or point 5. In the diagram for metal DH-9, the basic curves for the 0.001-, 0.003-, and 0.01-percent proof stresses evidently reach a minimum at a prior plastic extension of about 0.5 percent, then rise rapidly throughout the further extent here represented. The most significant feature in figure 25 is the initial descent of the lower two curves for metal DM-9 and of the lower three curves for metal DH-9.

In the initial trend, the basic curves for metals DM-9 and DH-9 are similar to the curves for another work-hardened metal that had been annealed for relief of internal stress (monel metal G-8, fig. 10). The basic curves for metals DM-9 and DH-9 are also similar to the curves for the fully annealed monel metal (figs. 2 and 4), the fully annealed Inconel L-17.5 (fig. 14), and the heat-treated aluminum-monel metal J (fig. 18). Because all these alloys probably were nearly free from internal stress, the initial descent of the (lower) proof-stress-extension curve probably is due to the predominating influence of increase of internal stress.

**THE VARIATION OF THE MODULUS OF ELASTICITY WITH STRESS FOR FULLY ANNEALED 18:8 CHROMIUM-NICKEL STEEL**

After each stage of plastic extension of the specimen of annealed chromium-nickel steel represented in figure 24, a corrected stress-deviation curve was obtained. (The curves thus obtained are not shown in this report.) From each of these curves has been derived a graph representing the variation of the modulus of elasticity with stress. The stress-modulus lines thus obtained (fig. 26) are numbered consecutively in order of the corresponding prior plastic extensions. The plastic extension prior to the determination of each stress-modulus line is indicated by the abscissa of the correspondingly numbered experimental point in figure 27, which is derived from figure 26.

Stress-modulus lines 1 to 13 and line 15 are curved from the origin; the other stress-modulus lines are practically straight. Within a range of prior plastic extension from zero to about 15 percent (fig. 27), therefore, this alloy gives curved stress-modulus lines. After further plastic extension, the stress-modulus lines are straight.

Adjacent to each stress-modulus line is a number representing the linear stress-coefficient ( $C_0$ ), based on the initial slope. Stress-modulus line 1, as indicated by the value of zero for  $C_0$ , is practically vertical at the origin. Very low values of  $C_0$  have been found also for the initial curves obtained with fully annealed monel

metal (figs. 5 and 7) and fully annealed Inconel (fig. 15). A general discussion of the forms of the initial stress-modulus line and the initial stress-deviation curve, for fully annealed metals, is given in section X.

THE INFLUENCE OF PRIOR PLASTIC EXTENSION ON THE MODULUS OF ELASTICITY AND ON ITS STRESS COEFFICIENT FOR FULLY ANNEALED 18 : 8 CHROMIUM-NICKEL STEEL

The values of  $E_0$  and  $C_0$  given in figure 26 have been plotted as ordinates in figure 27, with abscissas representing prior plastic extensions.

Before the general trend of the curves in figure 27 is considered, attention will be given to the abrupt oscillations due to the combined influence of the extension spacing and the duration of the rest interval. In the curves for  $E_0$  and  $C_0$ , the abrupt oscillations (almost without exception) are qualitatively similar; each abrupt rise or drop in the curve for  $E_0$ , at a pair of experimental points, is accompanied by a similar abrupt change in direction in the curve for  $C_0$ . Most of the abrupt oscillations in the curves for  $E_0$  and  $C_0$ , however, are accompanied by opposite oscillations in the proof stress-extension curves (fig. 24). The oscillations in these curves for 18 : 8 chromium-nickel steel are similar to the oscillations in the curves for monel metal and Inconel.

The approximate course of the basic curve for  $E_0$  is indicated by the dotted line (fig. 27). This line is based chiefly on the experimental points obtained with relatively long prior rest interval. The basic  $E_0$  curve for this annealed 18 : 8 alloy, like the basic  $E_0$  curves for annealed monel metal (fig. 8) and annealed Inconel (fig. 16), has an initial rise, followed by descent at a decreasing rate. The approach to a horizontal direction, however, is much slower in the  $E_0$  curve for the 18 : 8 alloy than in the curves for the annealed monel metal and Inconel. Unlike the curves for monel metal G-12 (fig. 8), and possibly Inconel (fig. 16), moreover, the  $E_0$  curve for the 18 : 8 alloy (fig. 27) gives no evidence of reascent. The reasons for these forms of the  $E_0$  curve are given in section X.

The basic  $C_0$  curve for annealed 18 : 8 alloy (fig. 27) starts at a very low value of  $C_0$  (practically zero) and rises rapidly to a maximum at a prior plastic extension of about 15 percent. With further plastic extension, the curve has a general downward trend, at a gradually decreasing rate. The  $C_0$  curve, therefore, is qualitatively similar to the  $E_0$  curve. The  $C_0$  curve also is qualitatively similar to the  $C_0$  curves for annealed monel metal (figs. 6 and 8) and annealed Inconel (fig. 16).

The highest point in the  $C_0$  curve (fig. 27) corresponds approximately with the point of change of the stress-modulus line from a curve to a straight line (fig. 26). Throughout the rise of the  $C_0$  curve (fig. 27), the corresponding stress-modulus line is curved. The variation of the curvature of the stress-modulus line, within

this range of plastic extension, is illustrated by the diagram for metal DM-18:3 in figure 46. The  $C'$  curve in this diagram rises abruptly with slight plastic extension, and then takes a general downward course. The second experimental point of a pair tends to be at the bottom of an oscillation. The abrupt oscillations in this curve thus are qualitatively similar to the oscillations in  $E_0$  and  $C_0$  curves. The basic  $C'$  curve for the 18 : 8 alloy is qualitatively similar to the  $C'$  curves of monel metal and Inconel (in the same figure), and is also qualitatively similar to the basic curve for 18 : 8 alloy 2A-1. The curve for alloy 2A-1 is derived from data in reference 1. This curve differs quantitatively from the other curves in figure 46 in that it has a smaller initial rise and a more regular downward course from the maximum.

MODULUS-EXTENSION CURVES FOR WORK-HARDENED 18 : 8 CHROMIUM-NICKEL STEEL ANNEALED FOR RELIEF OF INTERNAL STRESS

The modulus-extension curves for half-hard 18 : 8 alloy DM-9 and hard 18 : 8 DH-9 are shown in figure 28. The specimens used in obtaining these diagrams were annealed (before test) at 900° F for maximum relief of internal stress. The experimental points in figure 28 are derived from a consecutive series of stress-modulus lines. The first pair of stress-modulus lines, for both half-hard and hard 18 : 8 alloy, are shown in figure 29. The initial stress-modulus line for the half-hard metal DM-9 is slightly curved and is nearly vertical at the origin. The stress-deviation line on which this stress-modulus line is based, therefore, is approximately a cubic parabola (sec. III). The initial stress-modulus line for hard metal DH-9 is nearly vertical but is straight. With further plastic extension, all the stress-modulus lines for both half-hard and hard metal (not shown in this report) are straight.

Because the initial stress-modulus line for half-hard metal DM-9 is curved from the origin (fig. 29), broken lines are drawn from point 1 to point 2 of the graphs for  $E_0$  and  $C_0$  in the diagram at the left of figure 28. For the same reason, the graph for  $E_{100}$  is not extended to the left of point 2.

At the pairs of experimental points in figure 28, there are few abrupt rises or descents in the curves for  $E_0$  and  $C_0$ . The abrupt changes generally are the same in direction for both the  $E_0$  and  $C_0$  curves and are opposite in direction to the corresponding changes in the proof stress-extension curves (fig. 25).

The basic  $E_0$  curve for half-hard material (fig. 28) probably rises from point 1 to point 2. This rise accompanies the change of the stress-modulus line from a curve to a straight line. (See DM-9 curves, fig. 29). Beyond point 2, the basic curve evidently descends at a decreasing rate. The basic  $E_0$  curve for hard metal DH-9 also descends at a gradually decreasing rate. The  $E_0$  curves for both half-hard and hard metal,

therefore, are similar in form to the  $E_0$  curves for fully annealed 18 : 8 alloy DM-18.3 (fig. 27).

The basic  $C_0$  curves for both half-hard and hard 18 : 8 alloy annealed for relief of internal stress (fig. 28) rise continuously, throughout the extent here shown. In the curve for half-hard metal DM-9, the rapid rise from point 1 to point 2 accompanies the change of the stress-modulus line from a curve to a straight line (fig. 29). These basic curves for work-hardened 18 : 8 alloy are similar in form to the curve obtained with another work-hardened alloy that had been annealed for relief of internal stress (monel metal G-8, fig. 12). The rising trend of these  $C_0$  curves probably characterizes work-hardened metal that has been suitably annealed for the relief of internal stress. The influence of internal stress on the  $C_0$  curve is discussed further in section X.

The intermediate curve in each of the diagrams in figure 28 represents the variations of the secant modulus corresponding to an arbitrarily selected value of the stress. In the diagram at the left, the curve for  $E_{100}$  shows the variations of the modulus corresponding to a tensile stress of 100,000 pounds per square inch. This curve has not been extended to the left of the point of change of the stress-modulus line from a curve to a straight line. In the diagram at the right, the curve for  $E_{200}$  shows the variations of the modulus corresponding to a tensile stress of 200,000 pounds per square inch.

THE EFFECT OF ANNEALING ON THE INITIAL PAIR OF STRESS-MODULUS CURVES FOR COLD-DRAWN 18 : 8 CHROMIUM-NICKEL STEEL

In figure 29 are shown the initial pair of stress-modulus lines for half-hard and hard 18:8 chromium-nickel steel, as received and after annealing at various temperatures. In the diagram for the half-hard metal DM, the second stress-modulus line for the metal annealed at 900° F is straight, at least in the lower part; all the other stress-modulus lines are slightly curved from the origin. The first curve of each pair gives a very low value of  $C_0$ ; the second curve gives a much higher value. Slight curvature is found in some of the stress-modulus lines for the five half-hard 18:8 alloys discussed in the previous report. Curvature generally is not found in the initial stress-modulus lines, but it may appear after slight plastic extension and disappear after more plastic extension.

In the diagram for the hard metal DH (fig. 29), all the stress-modulus lines are practically straight, at least in the lower part. Very low values of  $C_0$  are derived from both the stress-modulus lines for the metal as received, and the second stress-modulus line for the metal annealed at 900° F; a slightly higher value of  $C_0$  is derived the second stress-modulus line for the metal annealed at 900° F.

Much higher values of  $C_0$  are derived from all the other stress-modulus lines of this diagram. The low

values of  $C_0$  obtained with metals DM and DH as received are very different from the values obtained with the five 18:8 alloys discussed in reference 1. All five alloys, both in half-hard and hard condition, gave high values of  $C_0$ . With plastic extension, the value of  $C_0$  (for each of the five hard 18:8 alloys) decreased, but remained somewhat higher than the highest value given in figure 29. Possible reasons for this great difference in behavior between the five 18:8 alloys discussed in reference 1 and metals DM and DH discussed in this report are given in section IX.

THE EFFECT OF ANNEALING ON THE MODULUS OF ELASTICITY AND ON ITS STRESS COEFFICIENT FOR COLD-DRAWN 18 : 8 CHROMIUM-NICKEL STEEL

The values of  $E_0$  and  $C_0$  for the first stress-modulus curve of each pair in figure 29 have been used in deriving the curves for  $E_0$  and  $C_0$  in figure 30. These curves show the variation of the initial values of  $E_0$  and  $C_0$  with annealing temperature. An abscissa corresponding to 70° F has been used in plotting results for the metals as received.

The  $E_0$  curve in each diagram rises continuously with increase in the annealing temperature. The value of  $E_0$  is much higher for fully annealed metal (represented by the right end of each curve) than for the metal as received. A similar relationship was found for the five 18:8 alloys considered in the previous report. The curve of variation of  $E_0$  with annealing temperature for those alloys probably would be similar to the  $E_0$  curve for metals DM and DH (fig. 30).

The  $E_0$  curves for 18:8 alloys DM and DH (fig. 30), however, differ greatly in trend from the corresponding  $E_0$  curves for monel metal and Inconel (fig. 21). The reasons for this difference may be found in section X.

The  $C_0$  curves for metals DM and DH are low at the left, rise somewhat in the middle, and descend to a very low value at an abscissa representing fully annealed metal. The relatively high part of each curve is within the range of annealing temperature for relief of internal stress without important loss of strength. These curves apparently differ greatly from the corresponding curves for monel metal and Inconel (fig. 21), particularly in the range of temperature between 70° F and 900° F. Within this range, the curves for the 18:8 alloys rise, and the curves for monel metal and Inconel (as drawn) descend. The exact course of the  $C_0$  curves for monel metal and Inconel, however, is not established throughout the range of annealing temperature from 70° F to 800° F or 850° F. The rise and descent of the  $C_0$  curves for metals DM and DH, moreover, may not be the typical trend for 18:8 alloys. As previously stated, metals DM and DH give much lower values of both  $E_0$  and  $C_0$  than the values obtained with the five 18:8 alloys considered in the previous report.

The results of the annealing treatment at 482° F for 44 hours are represented (fig. 30) by diamond-shaped shaded points. These results show that the long time at this temperature has caused little change in  $E_0$  but has decreased  $C_0$  considerably below the corresponding values obtained by annealing for 30 minutes. The longer annealing time has decreased the curvature of the stress-strain line but (as shown in fig. 23) has had little effect on the proof stresses.

ASSEMBLED DATA ON THE INFLUENCE OF PLASTIC DEFORMATION AND OF ANNEALING ON  $E_0$  AND  $C_0$  FOR 18:8 CHROMIUM-NICKEL STEEL

The 18:8 alloy steels DM and DH differ from the five 18:8 alloys considered in the previous report not only in the initial values of  $C_0$  but also in the values for  $E_0$ . It has seemed desirable, therefore, to assemble for comparison the characteristic values of  $E_0$  obtained with all these alloys. In figure 30, consequently, have been plotted initial values of  $E_0$  and values obtained after tensile extension nearly to the beginning of local contraction. The two diagrams in this figure give information about the influence of plastic deformation and of annealing on the modulus of elasticity and on its stress coefficient. The 18:8 alloys discussed in the previous report are designated by numerals 1 to 5; following each of these numerals is a letter indicating the degree of hardness of the alloy as received; the fully annealed, half-hard, and hard alloys are designated, respectively, by the letters A, B, and C. Values obtained with half-hard and hard alloys are plotted in their respective diagrams. Values obtained with the alloys as received are plotted at an abscissa representing 70° F, values obtained with fully annealed alloys are plotted, in both diagrams, at an abscissa representing an annealing temperature of 1,830° F.

The initial values of  $E_0$  obtained with the 18:8 alloys considered in the previous report are much greater than the corresponding values obtained with alloys DM and DH (fig. 30). After tensile extension nearly to the beginning of local contraction, however, a lower value for  $E_0$  was obtained with the fully annealed alloy 2A than with the fully annealed alloy DM-18.3. The value for half-hard alloy 1B, after similar tensile extension, is about the same as the value obtained with alloy DM as received. (Alloy DM was not extended to the beginning of local contraction.) After similar tensile extension of the hard alloys 2C, 3C, 4C, and 5C, the values for  $E_0$  remain higher than the value obtained with alloy DH as received.

As the values for  $E_0$  and  $C_0$  are generally higher for the five alloys considered in the previous report than for alloys DM and DH, the values obtained with alloys DM and DH may be exceptionally low. These low values cannot be attributed to abnormality in chemical composition. The chemical composition of metals

DM and DH is within the range of composition of the five 18:8 alloys considered in reference 1, and differs little from the composition of alloy 2. The rapid rise of the proof stresses of these alloys with relief of internal stress (fig. 23), moreover, indicates that the low initial values of  $E_0$  and  $C_0$  for metals DM and DH (fig. 30) cannot be attributed to low internal stress. The influence of crystal orientation in causing such differences in  $E_0$  and  $C_0$  is considered in sections IX and X.

VII. THE TENSILE ELASTIC PROPERTIES OF 13:2 CHROMIUM-NICKEL STEEL AS AFFECTED BY PLASTIC DEFORMATION AND BY HEAT TREATMENT

DESCRIPTION OF THE 13:2 CHROMIUM-NICKEL STEEL

The stainless steels hitherto discussed in this report and in reference 1 are practically single-phase alloys. The elastic strength of these alloys may be increased by cold-work but not (to an important extent) by heat treatment. The stainless steel now to be considered, 13:2 chromium-nickel steel, may be strengthened either by cold-work or by heat treatment. In another important respect, moreover, this steel differs from the alloys previously considered. The space lattice of each of the alloys previously considered is face-centered cubic. The 13:2 chromium-nickel steel, either after strengthening heat treatment or in the softest condition, has a ferritic matrix. The space lattice of this matrix is body-centered cubic.

The steel used in this investigation was supplied in the form of round rods. The chemical composition is given in table I. The heat treatment given by the manufacturers consisted in heating to 1,240° F and cooling in the furnace. As no other heat treatment is mentioned by the manufacturers, probably no heat treatment intervened between the hot-rolling and the reheating to 1,240° F. Heating to about this temperature and cooling slowly is the most convenient treatment for softening. Heating to about 1,750° F causes the carbides to go into solution and thus makes the alloy (at that temperature) practically a single-phase austenitic alloy. As the transformation of this alloy on cooling is slow, only partial transformation occurs on cooling in air. Suitable heat treatment consists in cooling in air from 1,750° F, and reheating to the desired temperature for tempering.

In order to investigate the effect of heat treatment on the elastic properties, consequently, specimens were heated to 1,750° F, cooled in air, and reheated to various temperatures, ranging from room temperature to 1,750° F. After tempering, the specimens were cooled in the furnace.<sup>7</sup> Details of the heat treatment are given in table III.

<sup>7</sup> The elastic properties probably are not affected by the rate of cooling after tempering at temperatures up to about 1,240° F. Greater toughness, however, probably would be obtained by cooling in air.

## THE EFFECT OF TEMPERING ON THE INITIAL PAIR OF STRESS-SET CURVES AND ON THE DERIVED PROOF STRESSES FOR 13:2 CHROMIUM-NICKEL STEEL

With each of these specimens, an initial pair of correlated stress-deviation and stress-set curves were determined. The pairs of stress-set curves are shown in the lower row of figure 31. Corresponding pairs of stress-deviation curves are shown in the upper row.

The second stress-set curve of each pair is steeper than the first. This difference in steepness is very great in the first pair, which was obtained with a specimen that had been air-cooled from 1,750° F and not afterward reheated. The difference in steepness decreases with an increase in the tempering temperature, up to about 850° F. With further increase in the tempering temperature, the difference in steepness increases and is very great in the specimens that were tempered at 1,450° and 1,750° F. The pair designated A, like the first pair, was obtained with a specimen that had been cooled from 1,750° F. The indicated difference in the rate of cooling from this temperature accounts for the difference in steepness of corresponding curves of the two pairs. The pair designated B (heated to 1,240° F by the manufacturers), as would be expected, differs little from the pair obtained with a specimen that had been air-cooled from 1,750° F and tempered at 1,200° F.

The variation of steepness with annealing temperature is much greater for the first curve than for the second curve of a pair. These variations may best be studied by considering the influence of annealing temperature on the proof stresses. Proof stresses derived from the stress-set curves in figure 31 have been plotted as ordinates in figure 32, with the abscissas representing tempering temperatures. The diagrams designated "first loading" and "second loading" are derived from the first and second curves, respectively, of the pairs of stress-set curves of figure 31.

The course of each curve (fig. 32) is largely due to the variation of microstructure with the tempering temperature. The initial rise is largely due to hardening of the metal caused by transformation of retained austenite and precipitation of fine particles of carbide. At the maximum, which is the same for all curves in each diagram but not the same in the two diagrams, the microstructure consists of fine particles of carbide dispersed in a matrix of ferrite. The descent of the curves is due to the growth and the decrease in number of the carbide particles. The reascent, with an increase in the tempering temperature above about 1,250° F, is due to increasing re-resolution of the carbide particles and to partial reprecipitation in finer form during the cooling from the tempering temperature. The rate of cooling from the tempering temperature evidently is important when this temperature is above about 1,250° F.

The initial rise in the curves (fig. 32) is similar to the initial rise in the curves of variation of proof stresses of 18:8 alloy with annealing temperature (fig. 23). The

initial rise in the curves for the 18:8 alloy, and in the curves for monel metal and Inconel (fig. 20), is due chiefly to relief of internal stress. The relief of internal stress is also an important factor but is not the only factor, in the initial rise of the curves for 13:2 alloy (fig. 32), especially in the diagram representing first loading. The internal stress in this alloy is due not to cold-work but to the volume changes (caused chiefly by the partial transformation of the austenite) during the cooling in air from 1,750° F.

In the diagram for first loading, the ascent of the curves (between 70° F and 700° F to 800° F) is caused by two factors, the relief of internal stress and the variation of microstructure. The relative importance of these two factors varies with the amount of permanent set on which the proof stress is based. The influence of relief of internal stress is relatively large for the curves representing 0.001-, 0.003-, and 0.01-percent proof stresses and is small for the other two curves. As the slight plastic extension during the first loading causes important changes in internal stress, the following comparison of the diagrams representing first and second loading gives information about the relative importance of the variation of internal stress and the variation of microstructure as causes of the initial ascent of the curves.

In the diagram for first loading, the ascent of the curves is due to a change in both microstructure and in internal stress; in the diagram for second loading, the ascent probably is due almost entirely to a change in the microstructure. A comparison of the ascents of the lower curves in the two diagrams makes it possible to estimate approximately how much of the ascent of the curves in the diagram is due to relief of internal stress. In such a comparison, however, consideration should be given to the fact that the rise of the lower curves in the diagram for second loading probably has been diminished somewhat by restoration of internal stress during the first loading after annealing at 700° F to 800° F. As stated in section III, tensile extension of specimens in which the internal stress is zero or at a minimum, causes increase of internal stress and thus tends to lower the proof stresses. For this reason, the curves at the maximum in the diagram for second loading may have been somewhat depressed. This effect, however, probably is small. The total ascent of the curve for 0.003-percent proof stress (the best established of the lower curves) is slightly more than twice as great in the diagram for the first loading than in the diagram for the second loading. Somewhat more than half the ascent of this curve in the diagram for first loading, therefore, probably is due to relief of internal stress. The remainder of the ascent is due to a change of microstructure.

At an abscissa representing 1,750° F, in each diagram, are two series of experimental points. The

lower series represents results obtained with a specimen that had been heated to 1,750° F and cooled in the furnace. This specimen had not been previously heated to 1,750° F and cooled in air, as had all the specimens represented by the small circles. Such a prior treatment, however, would not have affected the results obtained by heating to the same temperature and cooling in the furnace. The upper series of experimental points, at the same abscissa, are merely repetitions of the experimental points plotted at 70° F. This repetition appears justified by the fact that tempering at 1,750° F and cooling in air would be merely a repetition of the treatment that was given to the specimen represented at an abscissa of 70° F.

Cooling in the furnace from 1,750° F evidently gives lower proof stresses than does cooling in air from the same temperature. By very slow cooling, the proof stresses may be decreased still more. Excessively slow cooling probably would permit a sufficient precipitation and growth of carbides to reduce the proof stresses to the values obtained by tempering at about 1,250° F. Tempering at about 1,250° F, however, is the most convenient treatment for softening.

The experimental points at 1,240° represent results obtained with this alloy as received. The report of heat treatment by the manufacturers indicates that this alloy was heated to 1,240° F and cooled in the furnace. No mention is made of any heat treatment intervening between the hot-rolling and the tempering. The proof stresses for this alloy (fig. 32) are about the same as if the alloy had been given a solution treatment, followed by air cooling, prior to the tempering at 1,240° F. This solution treatment, however (as shown below), had great effect on the values of  $E_0$  and  $C_0$ .

THE EFFECT OF HEAT TREATMENT ON THE INITIAL PAIR OF STRESS-MODULUS LINES, ON THE MODULUS OF ELASTICITY AND ON ITS STRESS-COEFFICIENT FOR 13:2 CHROMIUM-NICKEL STEEL

The initial pair of stress-modulus lines, obtained with specimens that had been given the previously described heat treatments, are shown in figure 33. These stress-modulus lines are derived from the stress-deviation curves in the upper row of figure 31. All the stress-modulus lines except the first line obtained after tempering at 1,200° F, are practically straight. In this respect, these stress-modulus lines obtained with a heat-treated alloy resemble the lines obtained with single-phase alloys that have been hardened by considerable plastic extension (figs. 11, 15, and 26). A noteworthy feature in figure 33 is the great difference in slope and in position at the origin, between the lines of pair B and the lines obtained by tempering at 1,200° F after air-cooling from 1,750° F. This difference is in accordance with the great difference in initial steepness and in curvature between the two corresponding pairs of stress-deviation lines (fig. 31). The lines of pair B in

figure 33 were obtained with a specimen of the alloy as received. The only heat treatment given to this metal (as reported by the manufacturers) was furnace-cooling from 1,240° F. The great difference in the slope of the lines of these two pairs, therefore, may be attributed to an effect of the solution treatment. A possible effect of this solution treatment is suggested in section IX.

The values of  $E_0$  and  $C_0$  obtained from the stress-modulus lines of figure 33 have been used in deriving a diagram to represent the variation of these indices with heat treatment. This diagram is shown in figure 34. The curve for  $E_0$  in this figure shows no evidence of general upward or downward trend throughout the entire range of tempering temperature. The curve for  $C_0$  shows no general upward or downward trend throughout the range of temperature from 70 to 1,450° F; between 1,450 and 1,750° F there is evidence of an upward trend. (The lower experimental point at 1,750° F, for reasons given in connection with fig. 32, is merely a repetition of the point at 70° F.) These curves are based entirely on values obtained with the specimens that had been heat treated by the authors.

At an abscissa representing 1,240° F are plotted the values of  $E_0$  and  $C_0$  obtained with the alloy as received. These points are far above the corresponding curves. The value of  $C_0$  is about 10 times the mean value obtained with the specimens heat treated by the authors.

The high values of  $E_0$  and  $C_0$  obtained with the alloy as received are not due to an unstable condition, removable by plastic extension. Even after plastic extension to the beginning of local contraction (fig. 38), the values of  $E_0$  and  $C_0$  remain higher than any of the values obtained with specimens that had been given the solution treatment (fig. 34). Although this solution treatment (heating to 1,750° F and cooling in air) probably caused some change in the distribution of the precipitated carbides, this change in microstructure was not enough to have an important effect on the proof stresses (fig. 32) and probably was not enough to have important effect on  $E_0$  and  $C_0$ . The great effect of the solution treatment on  $E_0$  and  $C_0$  probably may be attributed to an effect of this treatment on the crystal orientation. Difference in crystal orientation has been mentioned previously as a possible cause of differences in values of  $E_0$  and  $C_0$  for 18:8 alloy (sec. VI). The subject is discussed further in section IX.

When for any reason both  $E_0$  and  $C_0$  are higher for one metal than for another, it may be of interest to know the range of tensile stress within which the one metal remains superior to the other in effective modulus ( $E$ ). This information may be obtained by calculating the stress at which the effective modulus of elasticity would be the same for both metals. This stress  $S_c$  can be estimated by the use of two simultaneous equations, of the general form of equation (2). In these two

equations the values of  $E$  and  $S_c$  evidently are the same. If the ratio of the larger to the smaller values of  $E_0$  and  $C_0$  be represented by  $m$  and  $n$  respectively, the value of the stress at which the elastic strain is the same for the metal in the two conditions is given by

$$S_c = \frac{m-1}{C_0(mn-1)} \quad (9)$$

In this equation,  $C_0$  represents the smaller of the two values of this index.

The stress ( $S_c$ ) at which the effective modulus would be the same for the 13:2 alloy in the two conditions, may be estimated from equation (9) by using the values for  $E_0$  and  $C_0$  given in figure 34. The value for  $S_c$  thus obtained is about 85,000 pounds per square inch. Throughout a range of stress up to the highest indicated proof stress value (fig. 34), therefore, the 13:2 alloy as received is superior (in effective modulus of elasticity) to the alloy after air-cooling from 1,750° F and tempering at 1,200° F (fig. 32).

THE INFLUENCE OF PRIOR PLASTIC EXTENSION ON THE STRESS-SET CURVE AND ON THE DERIVED PROOF STRESSES FOR 13:2 CHROMIUM-NICKEL STEEL

With the specimens heat-treated by the authors, only the initial pair of stress-set (and stress-deviation) curves were determined. A specimen of the alloy as received, however, was extended by small stages to the beginning of local contraction; after each of these stages, correlated stress-deviation and stress-set curves were determined. The stress-set curves are shown in the lower row of figure 35. The proof stresses derived from these curves are plotted as ordinates in figure 36, with abscissas representing the prior plastic extensions. As shown in figure 36, all the extensions between determinations of the experimental points were small. The points, therefore, are not arranged in distinct pairs as they are in nearly all the previously discussed diagrams of this type.

After some of the stages of extension, a cycle of stress between 1,000 and 80,000 pounds per square inch was introduced before the determination of the next stress-set curve. This cycle invariably caused the next stress-set curve to be steeper than the preceding curve (fig. 35) and thus caused an experimental point following such a cycle to be the top of a wide vertical oscillation, especially in the curves for the 0.001- and 0.003-percent proof stresses (fig. 36). From these tops, the descent generally is abrupt, even when the next experimental point has been obtained with a short prior rest interval; increase in the duration of this rest interval tends to increase the extent of the drop. This effect of duration of the rest interval is illustrated by the results obtained with a relatively long prior rest interval.

Each of the four stress-set curves obtained with a long prior rest interval (fig. 35) is less steep than the curves immediately preceding and following, and each corresponding experimental point in figure 36 is at the bottom of a wide vertical oscillation.

The basic curves for the 0.01, 0.03, and 0.1 percent proof stresses evidently rise from the origin, at a decreasing rate. The course of the lower two basic curves cannot be followed with certainty because of the wide oscillations. The initial trend, however, can be determined qualitatively by considering the low points of the oscillations. A comparison of the heights of points 1 and 5 thus shows that the initial trend is upward. The steep rise and descent in the curve as drawn between points 1 and 5 probably is due to a steep rise and descent in the basic curve. The descent of the curve as drawn between points 3 and 5, however, probably is hastened by the influence of the long rest interval prior to the determination of point 5. The first minimum in the basic curve, therefore, may be at somewhat more than 1 percent prior plastic extension.

Because of the tempering at 1,240° F, this alloy as received probably was free from internal stress. Plastic extension of a metal initially free from internal stress tends to increase the internal stress from zero to a maximum (sec. III) and thus tends to cause the initial trend of the lower proof-stress-extension curves to be downward. Whether the actual initial trend is downward or upward, however, depends on the relative magnitudes of two opposing factors: the depressing influence of the increasing internal stress and the elevating influence of the work hardening.

Various indices have been used to represent the rate of work hardening. A valuable index is the extension at the beginning of local contraction (maximum load). As shown by an arrow in figure 36, however, the extension of 13:2 alloy E at maximum load is only about 7 percent. According to this index, therefore, the rate of work-hardening of this alloy is small. And yet the initial rise of the proof-stress curves suggests that the influence of the rate of work-hardening of this alloy predominated over the influence of increasing internal stress. It should be noted, however, that the 13:2 alloy contains hard particles in a relatively soft ferritic matrix. The rate of work-hardening that determines the initial course of the proof-stress-extension curve for such an alloy probably is the rate of work-hardening of the matrix. This rate, for the 13:2 alloy, is much greater than the rate of work-hardening of the alloy as a whole, which is represented by indices such as the extension at maximum load. The rate of work-hardening of the matrix of the 13:2 alloy evidently is great enough to predominate, at first, over the depressing influence of increasing internal stress.

THE INFLUENCE OF PRIOR PLASTIC EXTENSION ON THE MODULUS OF ELASTICITY AND ON ITS STRESS COEFFICIENT FOR 13 : 2 CHROMIUM-NICKEL STEEL

After each stage of plastic extension represented in figure 36, a corrected stress-deviation curve was determined; these curves are shown in the upper row of figure 35. From these curves are derived the stress-modulus lines shown in figure 37. All the stress-modulus lines are practically straight. The lines vary greatly in slope and in the indicated value of  $E_0$ , corresponding to the variations in curvature and the initial slope of the stress-deviation lines in figure 35. The influence of plastic extension on these variations is shown in figure 38.

The combined influence of duration of the rest interval and the intermediate cycle, introduced between some of the stages of plastic extension and the determination of the next stress-deviation curve, is qualitatively the same in the curves for  $E_0$  and  $C_0$  (fig. 38). Three of the points obtained with long prior rest interval are at the tops of oscillations in both curves; the other point obtained with long prior rest interval is at the top of an oscillation in the curve for  $E_0$  and is near a top in the curve for  $C_0$ . These oscillations are opposite in direction to corresponding oscillations in the proof-stress-extension curves (fig. 36). In this respect, the 13:2 alloy behaves like all the alloys previously discussed in this report and in the previous report.

The basic  $E_0$  curve probably descends continuously at a decreasing rate. The downward trend evidently continues at least to an extension of 7 percent, the point of maximum load. As the contraction beyond this point localizes very slowly, it was found possible to extend the curves considerably further. Beyond the point of maximum-load, however, the superposed oscillations tend to become erratic.

The curve for the 13:2 alloy differs in form from the curves for monel metal (figs. 6 and 8) and annealed Inconel (fig. 18), and is qualitatively similar to the curves for 18:8 alloy (figs. 27 and 28). The approach to a horizontal direction, however, is much more rapid in the curve for the 13:2 alloy than in the curves for the 18:8 alloys. The reasons for these differences in the form of the  $E_0$  curves are given in section X.

The basic  $C_0$  curve evidently has an initial rise to a maximum at prior plastic extension of about 1 percent. Beyond this maximum, the basic curve descends at a decreasing rate to a nearly constant value. The course of the basic curve for the 13:2 alloy, therefore, is qualitatively similar to the course of the  $C_0$  curve for annealed monel metal (figs. 6 and 8), annealed Inconel (fig. 18), and annealed 18:8 alloy (fig. 27). The reasons for the courses of these curves are given in section X.

Throughout the entire course of the  $C_0$  curve for 13:2 alloy (fig. 38) the indicated values of  $C_0$  are about 10

times the values obtained with the same alloy after air-cooling from 1,750° F and tempering (fig. 34).

VIII. THE TENSILE ELASTIC PROPERTIES OF COPPER AS AFFECTED BY PLASTIC DEFORMATION

SOME GENERAL CHARACTERISTICS OF COPPER AND A DESCRIPTION OF THE COPPER USED IN THIS INVESTIGATION

Because of the important differences that have been found in the elastic properties of the metals considered in this report, especially the differences in the curves for  $E_0$  and  $C_0$ , it is desirable to include in the investigation metals differing widely in composition, in elastic strength, and in the modulus of elasticity. Only thus is it possible to study adequately the interrelationship between the various factors affecting the elastic properties of metals. The alloys previously considered do not differ greatly in the modulus of elasticity or in elastic strength. Much lower values of the modulus of elasticity, however, are found for some commercial alloys, even for some that may be classed as high-strength alloys. The modulus of elasticity of copper and of some of its alloys is little more than half the values obtained with the metals previously considered. In strength also copper differs greatly from the metals previously studied; the tensile strength of fully annealed copper is little more than one third that of fully annealed monel metal or 18:8 alloy.

Because information about the elastic properties of copper was needed in connection with an investigation of creep of metals, a short study has been made of the elastic properties of this metal as affected by plastic extension. The results of this study, when compared with the results obtained with the much stronger metals previously considered, have thrown much light on the interrelationship of factors affecting the form of the stress-strain curve and the values of  $E_0$  and  $C_0$ . The results obtained with copper are therefore included in this report.

The copper used in this investigation is "oxygen free" copper. It was supplied in the form of cold-rolled round rods. A specimen of this copper was tested in the work-hardened condition. Additional specimens were annealed at 600° and 800° F, respectively. The lower temperature is just above the recrystallization range. Details of the annealing treatment are given in table III.

THE INFLUENCE OF PRIOR PLASTIC EXTENSION ON THE STRESS-SET CURVE AND ON THE DERIVED PROOF STRESSES FOR ANNEALED COPPER

The two specimens (N-6 and N-8) of fully annealed copper were extended by short stages to the beginning of local contraction; after each of these stages, a stress deviation curve and a stress-set curve were determined. These curves are shown in figures 39 and 41. Proof stresses derived from the stress-set curves are plotted

as ordinates in figures 40 and 42 respectively, with abscissas representing prior plastic extensions.

The first four stages of extension, as shown in figures 40 and 42, are short; the other stages are alternately long and short. The stress-set curves thus were determined in pairs. The first stress-set curve of each pair was determined after a relatively long rest interval; the second curve was determined after a short rest interval. The influence of the extension spacing and of the duration of the rest interval causes the second stress-set curve of each pair (figs. 39 and 41) to be steeper than the first, and thus causes the second experimental point of each pair in figures 40 and 42 to be higher than the first. In this respect, copper is similar to all the metals previously considered in this report.

The form of each basic curve in figures 40 and 42 can be determined qualitatively by tracing a curve from the origin approximately through the experimental points obtained with long prior rest intervals. The general trend of each basic curve, with the exception of the curves for the 0.001-percent proof stress, is continuously upward. In figure 42 the basic curve for the 0.001-percent proof stress evidently has an initial rise to a maximum, followed by a descent to a minimum at plastic extension between 2 and 5 percent. In figure 40, the initial course of the basic curve is less certain. A curve drawn from the origin through points 3, 5, and 7 would first rise, then descend, and again rise, all within a plastic extension of about 2 percent. It seems more probable, however, that this basic curve is similar to the corresponding curve in figure 42. Each of these two basic curves probably has an initial rise, followed by an abrupt descent to a minimum.

The initial trend of the basic curve for the 0.001-percent proof stress in figure 42, and probably in figure 40, is similar to the initial trend of corresponding curves obtained with fully annealed 18:8 chromium-nickel steel (fig. 24) and with 13:2 chromium-nickel that had been softened by tempering (fig. 36). An initial downward trend, however, is found in the corresponding (lower) curves for fully annealed monel metal (figs. 2 and 4), fully annealed Inconel (fig. 14), and heat-treated aluminum-monel metal (fig. 18). All these metals, because of the thermal treatment, must have been initially free from internal stress. Tensile extension of metals initially free from internal stress (sec. III), causes an increase of internal stress from zero to a maximum and thus tends to cause a descent of the lower proof-stress-extension curves to a minimum. This tendency, however, is opposed by the elevating tendency of the tensile work-hardening. When the rate of work-hardening is sufficiently high, the elevating influence of work-hardening at first predominates over the depressing influence of increasing internal stress and the proof-stress-extension curve has an initial rise. When the initial rate of work-hardening is not sufficient

to overcome the influence of increasing internal stress, the curve has an initial descent. Even if the influence of work-hardening predominates at first, the influence of increasing internal stress eventually predominates and the curve descends.

A high rate of work-hardening has been mentioned as the probable cause of the initial rise of the lower proof-stress-extension curves for fully annealed 18:8 alloy (fig. 24) and for the 13:2 alloy that had been softened by tempering (fig. 36). To the same cause may be attributed the rise of the curve for the 0.001-percent proof stress for annealed copper (fig. 42 and probably fig. 40).

An index of the general rate of work-hardening is the tensile extension at maximum load (beginning of local contraction). This extension is about 33 percent for annealed monel metal G-14, 34 percent for annealed monel metal G-12, 35 percent for annealed Inconel L-17.5, 11½ percent for heat-treated aluminum-monel metal J, 70 percent for annealed 18:8 alloy DM-18.3, 14 percent for tempered 13:2 alloy E, and 40 percent for annealed copper N-6 and N-8. With the exception of the 13:2 alloy,<sup>8</sup> the extension at maximum load is greater for the second four than for the first four metals.

The first four of this list of eight metals are metals whose (lower) proof-stress-extension curves have an initial descent; the second four are metals whose proof-stress curves have an initial rise.

The initial rate of work-hardening may be represented by the ratio between the yield stress after slight plastic extension and the initial yield stress. Such indices have been obtained from the curves for the 0.10-percent proof stress by determining the ratio between the proof stress at an extension of 3 percent and the initial proof stress. These indices for the eight metals previously mentioned are:

Monel metal G-14.....	1. 26
Monel metal G-12.....	1. 27
Inconel L-17.5.....	1. 44
Aluminum-monel metal J.....	1. 19
13 : 2 alloy E.....	1. 43
18 : 8 alloy DM-18.3.....	1. 74
Copper N-6.....	2. 22
Copper N-8.....	2. 29

The first four in this list give proof-stress-extension curves with initial descent; the second four give curves with initial rise. This index places the 13:2 alloy on the border line between the two groups. An index representing the matrix of this alloy, however, undoubtedly would be much higher, possibly nearly as high as that for the 18:8 alloy. The indices for the three single-phase metals in the second group of four are much higher than the indices for the three single-phase metals of the first groups of four. The evidence

<sup>8</sup> The low extension for the 13:2 alloy is due to a low rate of hardening of this alloy as a whole and does not indicate a low rate for the ferrite matrix. For this the rate of work-hardening probably is high.

therefore supports the view that the relationship between the rate of work-hardening and the rate of increase of internal stress determines the initial trend of the (lower) proof-stress-extension curves, when the initial internal stress is zero or a very low value.

**THE INFLUENCE OF PRIOR PLASTIC EXTENSION ON THE STRESS-SET CURVE AND ON THE DERIVED PROOF STRESSES FOR WORK-HARDENED COPPER**

The stress-deviation and stress-set curves obtained with work-hardened copper (N) are shown in the diagram at the right of figure 41. The proof stresses derived from the stress-set curves are plotted in the diagram at the right of figure 40, in which abscissas represent prior plastic extensions. The influences of duration of the rest interval and of the extension spacing evidently are qualitatively the same for this metal as for all the other metals considered in this report.

The lower two proof-stress-extension curves show wide oscillations. It is uncertain whether the basic curves, like the curves as drawn, have an initial rise and descent. If they do, work-hardened copper is similar (in this respect) to the other unannealed work-hardened metals considered in this report and in the preceding report.

**THE INFLUENCE OF PRIOR PLASTIC EXTENSION ON THE STRESS-MODULUS LINES FOR COPPER**

From the stress-deviation curves in the upper rows of figures 39 and 41 are derived curves of variation of the modulus of elasticity with stress (fig. 43). The initial stress-modulus line for annealed copper N-8, and lines 4 and 8 for annealed copper N-6, are practically straight; all the other stress-modulus lines are curved from the origin. Some adjacent stress-modulus lines in figure 43 differ greatly in curvature and in initial slope. Lines 1, 4, and 8 for metal N-6 are nearly straight, whereas the adjacent lines are strongly curved. Lines 4 and 8 for metal N-8 are vertical at the origin, whereas the adjacent lines are much less steep. With prior tensile extension, the stress-modulus line for annealed copper does not become straight, as it does for the metals previously considered. The curvature of some of these lines, especially some lines near the beginning of each series, is much greater than the curvature of any stress-modulus lines for the other metals<sup>9</sup> considered in this report.

The initial stress-modulus lines for metals N-6 and N-8 give very high values of  $C_0$ . The initial value of  $C_0$  for metal N-8 is the highest value obtained with the metals considered in this report.

The influence of prior plastic extension on the curvature of the stress-modulus line is shown in figure 47. In this figure, abscissas represent prior plastic exten-

sions and ordinates represent values of  $C'$ , the index of curvature of the stress-modulus line. The experimental points in figure 47 are numbered to correspond to the stress-modulus lines in figure 43. The initial value of  $C'$  (fig. 47) is zero for copper N-6 and is very small for copper N-8. With slight plastic extension,  $C'$  rises rapidly to a very high maximum and then descends rapidly. (The fact that this maximum is much higher for N-8 than for N-6 may possibly be attributed to the somewhat softer condition of N-8 because of the higher annealing temperature.) This rise and descent is followed by two smaller abrupt rises and descents and then by a slow downward trend, at gradually decreasing rate and with gradually decreasing oscillation. These curves for annealed copper are similar in general form to the previously discussed curves of the same type obtained with other metals (fig. 46). All these curves have an initial rise followed by less rapid descent. The initial rise and descent are abrupt for all these metals, except in the curve for the annealed 18 : 8 alloy 2A-1, derived from data presented in reference 1. In one important respect, however, the curves for annealed copper (fig. 47) differ from the curves for the other metals (fig. 46). The quadratic stress coefficient of the modulus does not become zero, at least within the range of tensile extension. Even after more severe cold-working, as illustrated by the curved stress-modulus lines for cold-rolled copper N (fig. 43),  $C'$  has not decreased to zero.

**THE INFLUENCE OF PRIOR PLASTIC EXTENSION ON THE MODULUS OF ELASTICITY AND ON ITS STRESS COEFFICIENT FOR COPPER**

The values of  $E_0$  and  $C_0$  derived from the stress-modulus curves in figure 43 are plotted as ordinates in figures 44 and 45, with abscissas representing the prior plastic extensions.

The abrupt rises or descents at pairs of experimental points, with few exceptions, are qualitatively the same in the curves for  $E_0$  and  $C_0$ . In both curves, moreover, these abrupt rises or descents are generally opposite in direction to the abrupt rises or descents in the proof-stress-extension curves (figs. 40 and 42). Copper is similar in this respect to all the other metals considered in this report.

The basic  $E_0$  curve (figs. 44 and 45) first descends rapidly at a decreasing rate and reaches a minimum at a slight plastic extension. With further extension, the curve rises at first rapidly and then at decreasing rate throughout the whole range of tensile extension. At the beginning of local contraction, the modulus of elasticity has risen almost to the initial value. As shown in the diagram for unannealed, cold-rolled copper at the right of figure 44, the  $E_0$  curve continues to rise slightly with tensile extension. The  $E_0$  curve for copper, therefore, differs greatly from the curve obtained with any other metal considered in this report. As

<sup>9</sup> In such a comparison, allowance must be made for the differences in the ordinate scales of corresponding diagrams.

the  $E_0$  curves in figures 44 and 45 are similar in form, and as these two curves were obtained with specimens that had been annealed at two different temperatures, the form of the modulus-extension curve for annealed copper is well established.

These curves for copper are the only modulus-extension curves (in this report) that give unmistakable evidence of a reascent. The curves for annealed monel metal G-12 (fig. 8) and annealed Inconel (fig. 16) apparently have a slight reascent. The curve for annealed 18:8 alloy (fig. 27) after an initial rise descends continuously at a decreasing rate. The course of the  $E_0$  curve for annealed copper must be due to the influence of two or more variables. The reascent of the curve, as shown in sections IX and X, is probably due to a change of crystal orientation.

The basic  $C_0$  curve for annealed copper N-6 and N-8 (figs. 44 and 45) descends rapidly from the origin, at a decreasing rate, and reaches a minimum at a prior extension of a few percent. With further plastic extension, the curve evidently rises at a gradually decreasing rate and eventually becomes practically horizontal. The basic  $C_0$  curve is qualitatively similar to the basic  $E_0$  curve. The  $C_0$  curve for copper differs greatly from the  $C_0$  curves for annealed monel metal (figs. 6 and 8), annealed Inconel (fig. 16), aluminum-monel metal (fig. 19), annealed 18:8 alloy (fig. 27), and 13:2 chromium-nickel steel (fig. 34). The differences in form of the  $E_0$  and  $C_0$  curves for different metals are due to the combined influence of three variables, which are discussed in section X.

The variation of  $C'$  with plastic extension of unannealed, cold-rolled copper N is shown in the small diagram at the right of figure 47. The course of this curve, when compared with the course of the  $C'$  curves for annealed copper, indicates that  $C'$  eventually tends to decrease with increase in the degree of cold-work but probably does not disappear as it does with initially harder metals. With a harder metal, such as annealed monel metal, annealed Inconel, or annealed 18:8 alloy, as shown in figure 46,  $C'$  disappears after moderate tensile extension. With a still harder metal, such as the tempered 13:2 chromium-nickel steel E, even the initial stress-modulus line is straight (fig. 37).

## IX. CRYSTAL ORIENTATION AND ITS INFLUENCE ON ELASTIC PROPERTIES

### THE DIRECTIONAL VARIATION OF THE MODULUS OF ELASTICITY OF SINGLE CRYSTALS

The great differences in form of the modulus-extension curves for single-phase face-centered cubic metals (figs. 6, 8, 16, 27, 44, and 45) indicate that during plastic extension the modulus is influenced by two or more variables. One of these variables is crystal orientation. Plastic deformation tends to change the orientation of the grains from a random to a preferred orientation.

Because of directional variation of the modulus of elasticity of a metal crystal, the change to a preferred orientation may greatly affect the mean modulus of elasticity of a polycrystalline aggregate.

In the study of the directional variation of the modulus of elasticity of metal crystals, attention will be confined to the two types of space lattice represented by the metals considered in this report. These are face-centered and body-centered cubic lattices. The directional variation of the modulus in these lattices is illustrated by the diagrams in figures 49 to 52, which are adaptations of diagrams in reference 2. These diagrams are drawn with spherical coordinates having their origins at the intersection of the three mutually perpendicular axes of symmetry. The surface shown in each figure is the locus of all points representing (by distance and direction from the origin) values of the modulus of elasticity. The axes represented in each figure are the cubic axes of crystal symmetry.

In the discussion of crystal orientation, use will be made of the Miller indices of crystal planes and directions. A crystal plane is thus represented by the reciprocals of the ratios of the intercepts of the three principal axes. A cubic plane is thus represented by (100), an octahedral plane by (111), and a dodecahedral plane by (110). A crystal direction is designated by the plane to which the direction is normal. In order to distinguish a direction from a plane, use is made of a form of bracket symbol. Thus, a direction making equal angles with all three principal axes is denoted by [111], the direction of a cubic axes of symmetry by [100], and the dodecahedral direction by [110]. In figures 49 to 52, however, the principle crystal directions are denoted by letters, the significance of which is indicated in the legend of figure 49.

A typical diagram of variation of the tensile modulus of elasticity ( $E$ ) of a face-centered cubic metal is the diagram for gold (fig. 49). The modulus for this metal is least in the direction of the cubic axis (C) and greatest in the direction of the octahedral axis (O). The ratio between these maximum and minimum values for gold, as given in reference 2, is 2.71. For copper and silver (see reference 2), the ratios are 2.85 and 2.55, respectively. Diagrams for copper and silver, therefore, would be similar to the diagram for gold (fig. 49). The diagram for aluminum (fig. 50), however, is very different in form. As indicated by this nearly spherical diagram, the ratio of values of the modulus in the octahedral (O) and the cubic (C) directions is not far from 1.0. The value given in reference 2 is 1.2. The diagram for aluminum probably is exceptional among the diagrams for pure metals with face-centered cubic lattices.

A diagram for a body-centered cubic metal, alpha iron, is shown in figure 51. This diagram is similar in form to the diagram for gold (fig. 49). The ratio

of values of the modulus of elasticity in the octahedral (O) and cubic (C) directions is given in reference (2) as 2.15. For tungsten; another body-centered cubic metal, the corresponding ratio is given as 1.0. A diagram for tungsten, like the diagram for aluminum (fig. 50), evidently is nearly a sphere.

The directional variation of the shearing modulus ( $G$ ), as illustrated by the diagram for alpha iron in figure 52, is evidently opposite to the variation of the tensile modulus. The maximum value of the shearing modulus is in the direction of the cubic axis, which is the direction of minimum value of the tensile modulus. The minimum value of the shearing modulus is in the direction of the octahedral axis, which is the direction of maximum value of the tensile modulus. The ratios of the maximum to the minimum values of the shearing modulus for alpha iron, gold, copper, and silver are 1.93, 2.28, 2.48, and 2.26, respectively. These ratios are slightly less than the corresponding ratios for the tensile modulus. For aluminum and tungsten, which give nearly spherical diagrams of directional variation of the tensile modulus, the ratio of maximum to minimum values of the shearing modulus is small, 1.16 for aluminum and 1.0 for tungsten. Shearing-modulus diagrams for these metals evidently would be nearly spherical.

When the directional variation of the modulus of elasticity is as great as it is for copper or alpha iron, the orientation of the crystals may have great effect on the modulus of elasticity of a polycrystalline aggregate. Change from random to preferred orientation may greatly affect the mean value of the modulus of elasticity. Consideration, therefore, must be given to the influence of plastic deformation on the orientation of grains in a polycrystalline aggregate.

#### CYLINDRICAL AND PARALLELEPIPEDAL DEFORMATION

In the study of the influence of plastic deformation on crystal orientation, it is convenient to consider two types of uniform deformation. One of these types is cylindrical deformation; the other is parallelepipedal deformation.

Cylindrical deformation causes equal percentage changes in two dimensions and a necessarily opposite change in the third dimension. In cylindrical deformation, therefore, the ratio between two of the dimensions remains unchanged, although the external form is not necessarily cylindrical. Cylindrical deformation may be produced by tensile extension, by drawing, by rolling of rod or wire, or by axial compression of a cylinder.

Parallelepipedal deformation is illustrated by the deformation of a cube into a rectangular parallelepiped, whose three principal dimensions are unequal. The unidirectional rolling of plate or sheet is the most common example of this type of deformation. Although the width of the sheet remains practically unchanged

by rolling, the ratios of the three dimensions change greatly. Another example of parallelepipedal deformation is the deformation of single crystals under unidirectional loading. Such deformation is by slip on crystallographic planes. Slip generally starts on only one series of planes and in one direction on each plane. This slip causes change of direction of the plane with reference to the direction of loading and change of an initially circular to an elliptical cross section. Deformation of single crystals by unidirectional loading, therefore, is parallelepipedal. Single crystals, however, can be subjected to cylindrical deformation. The orientation thus produced generally differs from the orientation produced by unidirectional loading.

#### THE INFLUENCE OF PLASTIC DEFORMATION ON CRYSTAL ORIENTATION OF FACE-CENTERED CUBIC METALS

Tensile extension of specimens cut from single crystals of aluminum, as shown by Taylor and Elam (reference 3), causes a [112] direction of the crystal to approach and finally to reach the direction of tensile loading. (The [112] direction is indicated approximately by letters E in fig. 49.) These results have been confirmed by investigations by others.

Cylindrical extension of single crystals of face-centered cubic metals, however, causes a different kind of crystal orientation, as has been shown by a recent investigation by Vacher (reference 4). Cylindrical specimens of copper, some consisting of single crystals and some of two crystals, were swaged cold to various degrees of reduction, ranging from 30 to 95 percent. If the octahedral axis initially made the smaller angle with the axis of the specimen, the crystal approached the octahedral [111] orientation; otherwise, it approached the cubic [100] orientation. The orientation caused by cylindrical extension of single crystals, therefore, differs greatly from the orientation caused by unidirectional tension.

The cause of this difference is the lateral restraint necessary for cylindrical extension of single crystals. If either an octahedral axis or a cubic axis is in the direction of extension, either three or four planes of slip and either six or eight directions of slip, respectively, are symmetrically placed with reference to the direction of extension, and the resolved shearing stresses in these symmetrically placed directions are equal. If this alinement could be maintained during tensile extension, the extension would be by cylindrical deformation and not by the usual parallelepipedal deformation of single crystals by tensile extension. This alinement, however, is metastable for tensile extension; a small deviation from alinement would cause still further deviation. A small lateral restraint, however, would preserve the alinement and thus keep either the cubic axis or the octahedral axis in the direction of the specimen axis. When neither the octahedral

axis nor the cubic axis is initially in the direction of the specimen axis, extension with lateral restraint (as by swaging) evidently causes approach to either octahedral or cubic orientation.

In a polycrystalline aggregate under cylindrical deformation, each crystal is under lateral restraint by adjacent crystals and thus undergoes cylindrical rather than parallelepipedal deformation. Cylindrical extension of a polycrystalline aggregate of a face-centered cubic metal, therefore, might be expected to cause some of the crystals to assume the cubic orientation and others to assume the octahedral orientation. Such a duplex orientation of polycrystalline aggregates was found long before the recent investigation of cylindrical extension of single crystals. It was shown by Ettisch, Polanyi, and Weissenberg (references 5 and 6) that hard-drawn wires of face-centered cubic metals have both cubic and octahedral orientations (double-fiber texture). Sachs and Schiebold (reference 7), however, found that aluminum has almost entirely the octahedral orientation. This conclusion was confirmed by Schmid and Wassermann (reference 8), who also showed that the orientation textures of face-centered cubic metals are qualitatively similar but that they differ considerably in the proportions of [111] and [100] orientations. They found the following proportions:

	<i>Percentages</i>	
	[100]	[111]
Aluminum.....	0	100
Copper.....	40	60
Gold.....	50	50
Silver.....	75	25

Schmid and Wassermann also found that the amount of preferred orientation in wire is small in the outer layer but increases toward the center. In the outer layers, moreover, the preferred crystal axes are not exactly in the direction of the wire axis but make a small angle, so that the orientation is conical rather than longitudinal. This angle, however, decreases toward the center and, at a certain depth, the orientation becomes longitudinal. Vargha and Wassermann (reference 9) found that the orientation texture is the same in the interior of both drawn and rolled wires and that the same duplex orientation is produced by tensile extension.

Cold-drawn wires of nickel were found by Greenwood (reference 10) to have a double-fiber texture, consisting of [100] and [111] orientations with the [111] orientation predominating. As binary alloys of nickel and copper form a continuous series of solid solutions, all these alloys in the form of rod or wire would be expected to have qualitatively similar texture. Cold-drawn rods of monel metal, essentially a nickel-copper alloy, are said (reference 11) to have a double-fiber texture, with the [111] orientation greatly predominating.

Compression of single crystals of aluminum was investigated by Taylor (reference 12). The results were reported to indicate a preferred orientation with a dodecahedral [110] direction parallel to the direction of compression. Investigation by others has led to a similar conclusion as to the preferred orientation after cylindrical compression of either single crystals or polycrystalline aggregates. Recent papers by Barrett and Levenson (reference 13) and by Barrett (reference 14), however, have led these authors to somewhat different conclusions. They report that the deformation texture of axially compressed cylinders, either of single crystals or polycrystalline aggregates, does not consist of a single preferred orientation. They find a rather wide range of orientations of which the mean orientation is [110]. Single crystals and grains of a polycrystalline aggregate assume a range of orientations, with fragmentation of crystals probably starting at the beginning of deformation and increasing with the deformation. No grains or fragments were found with [111] orientation and very few with [100] orientation. The orientation generally ranged from [110] to about [113]. The preferred orientation is viewed in references 13 and 14 as a dynamic equilibrium between opposing tendencies, a tendency to approach [110] orientation and a tendency toward random orientation.

Rolling of plate or sheet produces parallelepipedal deformation with one dimension practically unchanged, one dimension greatly reduced, and one dimension greatly increased. Several investigators (references 15, 16, and 17) have suggested that the preferred orientation thus produced in the direction of the reduced dimension is the same as the orientation produced by unidirectional compression and that the orientation in the direction of extension (direction of rolling) is the same as the orientation produced by unidirectional tension. Contradictory results, however, have been reported in investigations of the orientation of rolled plate or sheet. Many of these apparent contradictions, however, probably are due to nonuniform deformation throughout the cross section. There is now general agreement as to the preferred orientation of plate or sheet that has been carefully rolled in one direction.

The preferred orientation of rolled plate or sheet, of polycrystalline face-centered cubic metals, consists approximately of a [112] orientation in the direction of rolling and a dodecahedral [110] orientation in the direction of decrease of thickness. The preferred orientation in the direction of rolling evidently is the same as that of a single crystal extended by unidirectional tension. The orientation in the direction of decrease of thickness evidently is the same as that of either a single crystal or a polycrystalline aggregate in the direction of unidirectional compression.

Few investigations have been made of the orientation produced by rolling single crystals. Piekus and

Mathewson (references 18 and 19) have recently studied the effect of compressing single crystals by means of a device used by Wever and Schmid (references 16 and 17). This device is a mold in which the metal is so compressed that the deformation is similar to that caused by rolling. As the thickness decreases, the width is kept unchanged, and extension is in only one direction. Results of investigation by Pickus and Mathewson with alpha brass, a face-centered cubic alloy, led them to the conclusion that a [112] direction tends to rotate into the direction of extension and a [110] direction into the direction of compression. These results indicate that the orientation produced by deformation of the rolling type is the same for single crystals as for polycrystalline aggregates. This orientation is different from the orientation produced by cylindrical deformation.

#### THE INFLUENCE OF PLASTIC DEFORMATION ON THE CRYSTAL ORIENTATION OF BODY-CENTERED CUBIC METALS

The most common body-centered cubic metals are alpha iron, chromium, molybdenum, and tungsten. Carbon steels are body-centered cubic unless the composition and heat treatment are such as to produce austenite (gamma iron), a face-centered cubic metal. A body-centered cubic metal alloyed with iron tends to produce a body-centered cubic alloy; a face-centered cubic metal (such as nickel or manganese), if alloyed in sufficient percentage, may cause the alloy to be face-centered cubic. The space lattice of steels containing iron, carbon, chromium, and nickel therefore depends on the proportions of these elements. If the ratio of nickel to chromium is sufficiently high, as in the 18:8 chromium-nickel steel, the alloy is face-centered cubic. Otherwise, as in the 13:2 chromium-nickel steel, the alloy (after ordinary heat treatment) is body-centered cubic.

As shown by Ettisch, Polanyi, and Weissenberg (reference 5) and confirmed by a number of other investigators (reference 20), cold-drawn iron gives preferred [110] orientation in the axial direction. A recent investigation by Barrett and Levenson (reference 21) leads to the same conclusion. Dodecahedral [110] orientation with no trace of other textures was found after severe plastic extension by drawing, or by swaging followed by drawing. This orientation was found with iron, iron-silicon alloys, and iron-vanadium alloy and was found with both single crystals and polycrystalline aggregates. The single crystals generally became fragmented whether or not constraint was imposed (by adjacent crystals or by the die walls).

Unidirectional compression of cylinders of alpha iron has been investigated by Barrett (reference 22). Some cylinders were cut from single crystals; others were cut from polycrystalline aggregates. The orientation produced by compression of the single crystals was

found to depend on the initial orientation. If either a [100] direction or a [111] direction initially made a small angle (less than about  $17^\circ$ ) with the axis of the specimen, the crystal orientation changed so as to decrease the angle and finally brought that crystal direction into alignment with the axis of the cylinder. If neither the [100] nor the [111] direction initially made a small angle with the axis of the cylinder, the crystal formed differently oriented portions, [100] and [111] orientations, and thus ceased to be a single crystal. Polycrystalline aggregates of iron, when compressed in the form of cylinders, were found to have duplex texture consisting of both [100] and [111] orientations.

Cylindrical *compression* of body-centered cubic metals evidently causes qualitatively the same preferred orientation that is caused by cylindrical *extension* of face-centered cubic metals. Cylindrical *extension* of body-centered cubic metals causes the same orientation [110] that is caused approximately by cylindrical *compression* of face-centered cubic metals.

Somewhat different orientation of body-centered cubic metals is caused by parallelepipedal deformation. Many investigations have been made of the preferred orientation in cold-rolled iron and steel plate or sheet. Contradictory results have been reported. A few investigators have reported two, or even three, superposed textures. Kurdjenow and Sachs (reference 23) found evidence of both [100] and [111] directions normal to the plate or sheet. Most investigators, however, now generally agree that the texture consists chiefly of a dodecahedral [110] direction in the direction of rolling and a cubic [100] direction normal to the plate or sheet. There is a considerable range of angular deviation, however, about each of these directions. The range of deviation tends to decrease with decrease in the thickness by rolling (references 24 and 25). Thin cold-rolled plate or sheet thus has a [110] direction in the direction of rolling and another [110] direction parallel to the width of the sheet. These [110] directions are the directions of greatest (relative) extension.

The orientation in the direction of rolling, consequently, is the same as the orientation in the direction of the axis of a cold-drawn or rolled rod or wire or of a specimen extended by unidirectional tension. In a direction normal to the plane of the sheet, however, the orientation is not the same as the previously discussed duplex orientation in the direction of axial compression of an iron cylinder (reference 22).

Preferred orientation may be found not only in cold-worked metal but also in hot-worked metal. Gensamer and Vukmanic (reference 20) have investigated the orientation of iron sheet that had been rolled at  $780^\circ\text{C}$ . and  $910^\circ\text{C}$ . The texture was found to be qualitatively similar to that of cold-rolled sheet. In the sheet rolled at  $910^\circ\text{C}$ ., however, the texture was less distinct than in the sheet rolled at  $780^\circ\text{C}$ .

## THE EFFECT OF ANNEALING ON CRYSTAL ORIENTATION

At one or more stages in severe cold-working, the metal sometimes must be annealed so as to permit the desired additional cold work. It is therefore important to know the effect of such annealing, on preferred orientation. Consideration must also be given to the possibility of changes of orientation due to annealing for relief of internal stress.

In the consideration of the effect of annealing on preferred orientation, attention will be first given to face-centered cubic metals. It has been shown that cylindrical extension of polycrystalline face-centered cubic metals generally causes a duplex texture, with both [100] and [111] directions in the direction of extension. Annealing such a metal tends to cause a decrease in the number of crystals with [111] orientation and an increase in the number of crystals with [100] orientation. Farnham and O'Neill (reference 26) obtained such a result by annealing hard-drawn copper wires. Even after annealing at a temperature too low to cause recrystallization, 130° C (266° F), they found appreciable change in the proportion of the [100] and [111] orientations. After annealing at 280° C (536° F), a temperature that caused complete recrystallization, the orientation was found to be almost entirely cubic. Similar results have been obtained by other investigators with other face-centered cubic metals.

Annealing aluminum after plastic extension, according to reference 8, caused no new preferred orientation. Annealing at temperatures above 500° C, however, was said to give a random orientation. Burgers and Louwse (reference 27) found that, when single crystals of aluminum are deformed by compression and then recrystallized (at 600° C), new grains appear with orientations different from those of the parent crystal. Polycrystalline aluminum, after axial compression, was reported to have a [110] orientation and to retain this orientation after recrystallization. A different conclusion, however, was recently reached by Barrett (reference 14). He found that the deformation and recrystallization textures of axially compressed high-purity aluminum are of the same type. Practically the same results were obtained whether the compressed cylinders were single crystals or polycrystalline aggregated. The texture obtained, as previously stated, consists of a range of orientation with mean orientation approximately [110].

Collins and Mathewson (reference 28) state that no simple relation was found that would rationalize the relation of the orientation of a recrystallized aluminum grain to that of the original crystal.

Cold-rolled sheet of face-centered cubic metals, as previously stated, generally has a [112] direction in

the direction of rolling and a dodecahedral [110] direction normal to the surface. Recrystallization tends to cause a new orientation with cubic axes in the direction of rolling, in the direction of the normal to the surface, and in the direction of the width of the sheet. Such results have been obtained by Göler and Sachs (references 29, 30, and 31), with copper, silver and gold. They also found that the tendency to reorientation on annealing differs greatly for different face-centered cubic metals. With recrystallized silver, alpha brass, and alpha bronze, they found a [112] direction in the direction of rolling and a [113] plane in the plane of rolling. Recrystallization therefore caused no change in the longitudinal orientation but caused approach to [100] orientation in the direction of the normal to the surface. The tendency to reorientation on annealing evidently is much less for these metals than for copper, nickel, gold and probably for other face-centered cubic metals. With aluminum sheet, Göler and Sachs (reference 32) found no new preferred orientation after annealing.

The same authors (reference 30) also point out that the effect of annealing on crystal orientation is sensitive to impurities and to slight variations in treatment. Two specimens of copper with practically the same rolling texture had very different textures after apparently the same annealing treatment. One specimen had random orientation, the other had a new preferred orientation. Farnham and O'Neill (reference 26) also found that impurities in copper may greatly affect the tendency to change from a deformation texture to a recrystallization texture.

The recrystallization texture of body-centered metals has been studied almost entirely with sheet material. The texture of body-centered polycrystalline metals after rolling in sheet form consists, as previously stated, of a [110] direction in the direction of rolling and in the direction of the width of the sheet, and a [100] direction normal to the surface. The recrystallization texture of iron has been studied by Barrett (reference 24), by Gensamer and Lustman (reference 33), and by others. They found that recrystallization causes rotation of the rolling texture about 15° to 17° each way about the normal to the surface of the sheet. (Such rotation may be visualized with the help of the diagram in fig. 51.)

Cold-rolled or drawn rod or wire of body-centered cubic metals has been shown, as previously stated, to have a [110] direction in the direction of the axis of the rod or wire and generally a random radial orientation. It seems probable that recrystallization of a rod or a wire would cause rotation of the deformation texture, just as it causes rotation of the texture of a plate or sheet.

#### THE DIRECTIONAL VARIATION OF THE ELASTIC STRENGTH OF A SINGLE CRYSTAL

It is important to know the influence of crystal orientation not only on the modulus of elasticity and on its stress coefficient but also on elastic strength. It can be shown that crystal orientation has qualitatively similar effects on elastic strength and on the modulus of elasticity. The directional variation of the elastic limit in a face-centered cubic crystal has been calculated by E. Schmid (reference 34) on the basis of his observation that the critical shear stress (stress necessary to cause slip, resolved in the direction of slip), is constant and independent of the normal stress on the plane of slip. The results of his calculations are represented by the diagram in figure 53. The elastic limit evidently is greatest in an octahedral direction, the direction in which the modulus of elasticity is greatest. The ratios of values of the elastic limit in the cubic, the dodecahedral, and the octahedral directions are 1:1:1.5. The directional variation of the elastic limit, therefore, is less than the directional variation of the modulus of elasticity for metals such as those represented in the diagrams of figures 49 and 51.

With 100 percent preferred orientation, a bar or sheet would become practically a single crystal, and its elastic limit in any direction would be very low. For practical purposes, grains with preferred orientation should be intermingled with grains having random orientation.

#### THE INFLUENCE OF CRYSTAL ORIENTATION ON THE FORM OF THE MODULUS-EXTENSION CURVE

The great directional variation of the modulus of elasticity of most metals (figs. 49 and 51) suggests that change of crystal orientation may have considerable effect on the variation of the modulus with plastic extension. The effect of change from random to preferred orientation evidently would depend on the type of preferred orientation. If the preferred orientation is of the duplex type, the variation of the modulus of elasticity with prior plastic extension would depend on the relative numbers of grains approaching the [111] and [100] orientations. Increase in the proportion of grains with [111] orientation would tend to cause increase in the modulus of elasticity; increase in the proportion of grains with [100] orientation would tend to cause decrease in the modulus of elasticity.

Of the metals considered in this report, copper and monel metal tend to form a duplex texture with predominance of [111] orientation. As Inconel is an alloy containing more than 80 percent of nickel and as nickel tends to form a preferred orientation with predominance of the [111] orientation, Inconel probably tends toward predominance of the [111] orientation. No information has as yet been found about the preferred orientation of the 18:8 alloy. The 13:2 alloy, because of its

ferritic matrix, probably tends to form a [110] orientation. Change of orientation of monel metal, copper, Inconel, and 13:2 alloy from random to preferred, therefore, probably would tend to cause increase of the modulus of elasticity. Change from a recrystallization texture, with further plastic extension, probably would have a similar effect. The effect of change of orientation during plastic extension, however, is only one factor affecting the form of the modulus-extension curve. The form of this curve depends on the interrelationship of three important variables, which will now be considered.

#### X. THE STRESS-STRAIN CURVE AS AFFECTED BY PRIOR PLASTIC EXTENSION AND BY ASSOCIATED VARIABLES

##### THE FORM OF THE STRESS-DEVIATION CURVE FOR ANNEALED OR TEMPERED METALS

As a basis for study of the influence of prior plastic extension on the form of the stress-strain (or stress-deviation) curve, attention should first be given to the form of the stress-deviation curve for a fully annealed metal or for a metal that has been heat treated so as to be free from the influence of cold-work and internal stress. The form of the stress-deviation curve may be deduced from the form and the slope of the stress-modulus line. When the stress-modulus line is straight, the corresponding stress-deviation curve is a quadratic parabola. When the stress-modulus line is curved, the stress-deviation curve may be approximated either by superposition of a cubic parabola on a quadratic parabola or by a single parabola whose exponent is between 2 and 3.

In table IV are listed the forms of stress-deviation curves and the derived indices of curvature for various metals that have been either fully annealed or tempered. One of these metals, 13:2 chromium-nickel steel E, consists of ferrite and carbides; the others are single-phase metals. The forms of the stress-deviation curves and the derived indices are listed for both first and second loading. Attention will be given first to the initial curves for single-phase metals.

The initial stress-deviation curves for two of the single-phase metals listed in table IV, monel metal G-12 and 18:8 alloy DM-18.3, are cubic parabolas. The curve for monel metal G-14 is nearer to a cubic than to a quadratic parabola. The curve for copper N-6 is a quadratic parabola, and the curve for copper N-8 is nearly a quadratic parabola. The curve for the annealed 18:8 alloy 2A-1, discussed in reference 1, is intermediate between a quadratic and a cubic parabola. The stress-strain curve obtained with Inconel is straight. As stated in section IV, however, this curve is based on too few experimental points to give conclusive evidence as to the typical form of the stress-deviation curve for annealed Inconel. If the nearly vertical

stress-modulus line ( $C_0=0$ ) for this metal actually is slightly curved, as appears probable, the stress-deviation curve is a cubic parabola.

On second loading, the stress-deviation curves for monel metal G-14 and Inconel L-17.5 are cubic parabolas, thus giving confirmatory evidence as to the tendency of the curves for annealed monel metal and Inconel to be approximately cubic parabolas. The second-loading curves for the 18:8 alloys and for copper are intermediate curves between a quadratic and a cubic parabola.

The curves for the 13:2 alloy, both on first and second loading, are quadratic parabolas (fig. 35). They thus resemble the curves obtained with cold-worked single-phase alloys, such as monel metal, Inconel, and 18:8 alloy (figs. 9, 13, and 22). The strengthening of the ferrite matrix of the 13:2 alloy by carbides, like the strengthening of a metal by cold-work, evidently tends to make the stress-deviation curve a quadratic parabola.

With prior plastic extension of the annealed single-phase metals discussed in this report, with the exception of copper,  $C_0$  first increases. This fact is illustrated by the initial rise of the curves for  $C_0$  in figures 6, 8, 16, and 27. Within the range of extension that causes this increase of  $C_0$ ,  $C'$  rises rapidly and then descends, as illustrated by the curves in figure 46. The relationship between  $C'$  and  $C_0$ , however, varies as illustrated by the curves in figure 48. As  $C_0$  increases with plastic extension,  $C'$  first increases and then decreases. In this respect, all these curves in figure 48 are similar. They are also similar in form to the curves in figure 46.

The ratio of  $C'$  to  $C_0$ , which is indicated by the ratio of ordinate to abscissa in figure 48, evidently tends to decrease with increase of  $C_0$  and hence with increase in prior plastic extension. This decrease of  $C'/C_0$  is an indication of decrease in the order of the parabola. Point 1 in the curve for 18:8 alloy DM-18.3 thus indicates that the corresponding stress-deviation curve is a cubic parabola. Point 14 indicates that the corresponding curve is a quadratic parabola. The intermediate points indicate various orders intermediate between a quadratic and a cubic parabola.

While the order of the parabola tends to decrease (probably continuously) until the curve becomes a quadratic parabola, the curvature evidently first increases and then decreases.

#### FACTORS AFFECTING THE VARIATION OF $E_0$ AND $C_0$ WITH PLASTIC EXTENSION OF COPPER

The form of the basic  $E_0$  curve for copper (figs. 44 and 45) indicates that the variation of the modulus with plastic extension is influenced by at least two factors acting simultaneously. At least one factor evidently tends to cause descent of the curve at a decreasing rate; at least one factor tends to cause ascent at a decreasing rate. At first, the depressing influence is dominant

and the curve descends; the elevating influence then becomes dominant and the curve rises. The reascent of the curve for copper may be attributed to the change of crystal orientation with plastic extension. Approach to the preferred orientation with plastic extension of a copper rod, as shown in section IX, tends to cause increase of the tensile modulus of elasticity. The factor tending to cause descent of the modulus-extension curve will be considered later.

Curves of variation of the modulus of elasticity with extension have been reported by other investigators. Kuntze (reference 35), in an investigation of the elastic properties of copper, obtained curves qualitatively similar to the  $E_0$  curves in figures 44 and 45.<sup>10</sup> He attributed the initial descent of the curve for annealed copper to increasing internal stress and the subsequent ascent of the curve to the influence of "pure plastic deformation" (deformation free from the influence of varying interval stress). These conclusions, as will be shown, are incorrect. The effects of internal stress and pure plastic extension are opposite to those surmised by Kuntze. Furthermore, the course of the  $E_0$  curve is affected by an additional important factor, the change of crystal orientation.

Curves qualitatively similar to the curves in figures 44 and 45 have also been obtained by Kawai (reference 36) with copper, nickel, and aluminum. With Armco iron and mild steel, however, he obtained curves that descend continuously at a decreasing rate. A similar effect of the plastic extension of steels was reported by Honda and Yamada (reference 37). The modulus values obtained by Kawai, however, are not values of  $E_0$  but are based on a range between variable maximum and minimum values of stress and strain. No study was made of the form of the stress-strain curve.

The initial descent of the curves for copper, nickel, and aluminum as well as the continuous descent of the curves for steels were attributed by Kawai to increasing internal stress. He thus expressed agreement with the views of Heyn (reference 38), Sachs (reference 39), and Honda and Yamada (reference 37),<sup>11</sup> that introduction of internal stress decreases the modulus of elasticity. His views evidently are also in agreement with the previously mentioned incorrect views of Kuntze (reference 35). The ascent of the curves for copper, nickel, and aluminum was attributed by Kawai to change of crystal orientation. According to his views, therefore, the course of the modulus-extension curve is due to the combined influence of two factors, increasing internal stress and change of crystal orientation. He thus overlooked one of the three important factors affecting the course of the modulus-extension curve. The factor overlooked by Kawai, however, is

<sup>10</sup> As the curves plotted by Kuntze represent the variations of the "Dehnungszahl," the reciprocal of Young's modulus of elasticity, these curves are inverted with reference to the  $E_0$  curves in figs. 44 and 45.

<sup>11</sup> Agreement with these views of Kawai is not apparent in reference 37.

different from the previously mentioned factor overlooked by Kuntze (reference 35).

Kawai classified the stress-modulus curves for body-centered and face-centered cubic metals in two distinct types, the one having a descent followed by a rise, the other having a continuous descent. In order to explain these two types, the assumption was made that approach to preferred orientation tends to cause less increase of the modulus when the lattice is body-centered than when it is face-centered. As illustrated by the curves in figures 6, 8, 12, 16, 27, 38, 44, and 45, however, the modulus-extension curves cannot be placed in two distinct classes. Furthermore, approach to the preferred orientation (sec. IX) of some face-centered cubic metals tends to cause decrease of the modulus.

Erroneous views as to the influence of internal stress have been reached because attention has been confined to the slope of the stress-strain curve at some indefinite point. Study of the variation of the modulus of elasticity with plastic extension should envisage the entire stress-strain curve; it therefore should include in its scope  $E_0$ ,  $C_0$ , and  $C'$ . By such study, it can be shown that introduction of internal stress does not generally cause decrease of  $E_0$ . Internal stress, however, is one of three important factors affecting the form of the modulus-extension curve, though it is not the cause of the descent of the curves in figures 44 and 45.

The descent of these curves is due to an important factor not mentioned by Kawai. This factor is probably connected with the structural changes (other than change of orientation) that cause work-hardening of a metal, such changes as slip on crystal planes, lattice distortion, grain fragmentation, etc. The factor that tends to depress the  $C_0$  curves, therefore, will be termed the "work-hardening" factor. The three important variables affecting the course of a modulus-extension curve are: crystal orientation, internal stress, and the work-hardening factor. Although all three factors may affect the course of the curve simultaneously, a short curve may manifest the influence of only one factor; a long curve may manifest successively the influence of two factors, or even of all three factors.

The  $C_0$  curves for copper (figs. 44 and 45) are qualitatively similar to the  $E_0$  curves. This similarity indicates that the same two influences cause the descent and the rise of both these curves. The descent of the  $C_0$  curves, therefore, is due to the dominant influence of the work-hardening factor; the reascent is due to the dominant influence of the change of crystal orientation.

#### THE DIRECTIONAL VARIATION OF THE STRESS-COEFFICIENT OF THE MODULUS OF ELASTICITY

No published information has been found regarding the variation of the curvature of the stress-strain line with the direction in a metal crystal. The reascent of the  $C_0$  curves for copper accompanying the reascent of

the  $E_0$  curves (figs. 44 and 45), however, suggests that the variation of  $C_0$  with the direction in a metal crystal is qualitatively similar to the variation of  $E_0$ . Evidence tending to substantiate this view may be found by comparing certain values of  $E_0$  and  $C_0$  for different metals of the same type, and for the same metal after different heat treatments.

In section VI, it is shown that the values of both  $E_0$  and  $C_0$  obtained with 18:8 chromium-nickel steels DM and DH are much lower than the values obtained with the five 18:8 alloys considered in reference 1. This difference in elastic properties cannot be attributed to difference of chemical composition and probably not to difference of microstructure or to difference in internal stress. The difference in elastic properties possibly is due to a difference in crystal orientation.

The 13:2 chromium-nickel steel E (sec. VII) gave much higher values of both  $E_0$  and  $C_0$  after tempering at 1,240° F. by the manufacturers than after the high-temperature-solution treatment by the authors. These differences cannot be attributed to a difference in microstructure or to a difference of internal stress but possibly may be attributed to a difference of crystal orientation. After treatment by the manufacturers, the 13:2 alloy probably retained the deformation texture; after the solution treatment by the authors, the alloy possibly acquired a recrystallization texture. The recrystallization texture of a body-centered cubic alloy, as stated in section IX, is generally derived from the deformation texture by rotation of the crystals about 15° in each direction from the preferred orientation [110]. Such rotation from a [110] direction toward a [100] direction, as shown in figure 51, would decrease the modulus of elasticity of the grains in the longitudinal direction. It is thus possible to account for the lower value of  $E_0$  obtained with the 13:2 alloy after the high-temperature-solution treatment. To the same cause may possibly be attributed the lower value of  $C_0$ .

The evidence obtained with the 18:8 alloys, with the 13:2 alloy, and with copper, therefore, indicates that the directional variation of the modulus of elasticity is accompanied by a qualitatively similar variation of the linear stress coefficient of the modulus, and hence is accompanied by a qualitatively similar variation of the degree of curvature of the stress-strain curve. When the directional variation of  $E_0$  is of the usual type (represented by figs. 49 and 51),  $C_0$  possibly is greater in a [111] direction than in a [110] direction and much greater in a [110] direction than in a [100] direction.

#### THE THREE FACTORS AFFECTING VARIATION OF $C_0$ AND $C'$ WITH PRIOR PLASTIC EXTENSION

In the study of the factors affecting the variations of stress-strain curve with prior plastic extension, attention will first be given to the factors affecting  $C_0$ . The  $C_0$  curves to be considered first are the curves obtained

with metals that are initially free, or practically free, from internal stress. With plastic extension of these metals, internal stress is a generally increasing variable. The simplest  $C_0$  curves for such metals are obtained with work-hardened metals that have been annealed for relief of internal stress. In these short curves, only one factor is dominant, the influence of increasing internal stress.

Curves of this kind were obtained with monel metal G-8 and Inconel L-8.5 (fig. 12) and with 18.8 alloys DM-9 and DH-9 (fig. 28). Relief of internal stress by heat treatment, as shown by comparison of the corresponding diagrams for annealed and unannealed metals in figure 12, reduced  $C_0$  for each metal to a very low value. With plastic extension after the annealing, however, the  $C_0$  curves for all these annealed metals rise rapidly at a decreasing rate. This rise evidently is due to restoration of internal stress.

The next curves to be considered are the longer  $C_0$  curves obtained with the fully annealed metals G-12 and G-14 (figs. 6 and 8), L-17.5 (fig. 16), and DM-18.3 (fig. 27). Each  $C_0$  curve for these metals has an initial rise followed by descent at a decreasing rate. A similar curve, obtained with the annealed 18:8 alloy 2A-1, is shown in figure 15 of reference 1. These curves, unlike the  $C_0$  curves for copper (figs. 44 and 45), are dominated first by an elevating influence, then by a depressing influence. The elevating influence is internal stress, the same factor that causes the rise of the  $C_0$  curves for metals G-8 (fig. 12), L-8.5 (fig. 12), and DM-9 and DH-9 (fig. 28); the depressing influence is the work-hardening factor. The dominance of the internal-stress factor is within the extension range of the rapid rise of internal stress.

Although these curves are not dominated by the third factor, change of crystal orientation, their course is somewhat affected by this factor. Change of crystal orientation with plastic extension tends to increase the modulus of elasticity of monel metal (sec. IX) and probably of Inconel, which contains a large percentage of nickel. Such a change of crystal orientation of these metals, like increase of internal stress, would tend to elevate the  $C_0$  curve. This elevating factor, however, is initially less rapid than the change of internal stress. The reorientation factor does not usually become dominant until the depressing influence of the work-hardening factor has become considerably weakened. Even then, it does not become dominant in the  $C_0$  curves for annealed monel metal, Inconel, and 18:8 alloys (figures 6, 8, 16 and 27). The initial rise of these curves consequently is due to the dominant influence of internal stress.

If internal stress in these alloys were as high at the beginning of plastic extension as it is after extension of 15 percent or more, the  $C_0$  curves probably would start at very high values of  $C_0$  and would descend con-

tinuously at a decreasing rate. The curves thus would manifest the influence of the work-hardening factor alone.

Increasing internal stress with prior plastic extension moreover, probably is the cause of the initial increase of the quadratic stress coefficient  $C'$  (figs. 46 and 47). The rise and the descent of the  $C'$  curves, like the rise and the descent of the  $C_0$  curves, is due to the influence of two factors. At first the influence of increasing internal stress is dominant and the curves rise; soon the influence of the work-hardening factor becomes dominant and the curves descend. Dominance of the work-hardening factor begins sooner in the  $C'$  curves than in the  $C_0$  curves.

The basic  $C_0$  curve for the 13:2 chromium-nickel steel (fig. 38) is similar to the  $C_0$  curves for annealed monel metal (figs. 6 and 8), Inconel (fig. 16), and 18:8 alloy (fig. 27) in that each curve rises initially to a maximum and descends at a decreasing rate. This metal, after tempering at 1,240° F. by the manufacturers, probably retained its dodecahedral [110] deformation texture (sec. X); the crystal orientation, therefore, would change little with tensile extension. Tensile extension, however, would be expected to cause initial rapid rise of internal stress. The initial rise of the  $C_0$  curve (fig. 38) can therefore be ascribed to the dominant influence of increasing internal stress. The descent at a decreasing rate is due to dominance of the work-hardening factor. In the long, nearly horizontal part of the basic curve, the two opposing factors evidently are nearly in balance.

The descent from the maximum is much less in this curve than in the curves for the three single-phase alloys. This relationship suggests that the work-hardening factor may vary with the rate of work-hardening of the metal. A  $C_0$  curve influenced solely by the work-hardening factor would be the reverse in form of a curve of variation of the 0.1-percent proof stress with prior plastic extension. The greater the ascent of the proof stress-extension curve, the greater probably would be the descent of the corresponding curve of variation of  $C_0$  under the influence of the work-hardening factor alone.

The  $C_0$  curves for annealed copper (figs. 44 and 45) do not manifest an effect of internal stress. Variation of internal stress, nevertheless, probably has some effect on the course of these curves. The absence of an initial rise of the  $C_0$  curve may be attributed to the relative softness of this metal. Because of the softness of copper, initial work-hardening with plastic extension is rapid and the increase of internal stress is rather slow. The work-hardening factor thus predominates over the internal stress factor and prevents an initial rise of the  $C_0$  curve. In the absence of influence of change of crystal orientation, the  $C_0$  curve for copper probably would descend continuously at a decreasing rate.

The factors affecting the  $C_0$  curve are generally less easily distinguished in the curves for unannealed work-hardened metals than in the curves for fully annealed metals, because slight plastic extension of the work-hardened metals generally causes rapid decrease of internal stress and thus tends to cause initial descent of the  $C_0$  curve to a minimum. (With further plastic extension, the internal stress increases and thus tends to elevate the  $C_0$  curve). The work-hardening factor tends to cause continuous descent of the  $C_0$  curve, although the influence of this factor may be slight if the metal was severely cold-worked prior to the tensile extension. Two factors therefore tend to cause initial descent of the  $C_0$  curve for unannealed work-hardened metals. The third factor, change of crystal orientation, tends to elevate the  $C_0$  curve for most metals but tends to depress the curve for a few metals, such as silver (sec. IX). This factor may have important influence, even though cold-working prior to the tensile extension has been severe.

The  $C_0$  curve for unannealed work-hardened monel metal G (fig. 12) shows no definite trend. The absence of downward trend of this curve probably is due to approximate balance between the depressing influence of relief of internal stress and the elevating influence of increase in [111] crystal orientation. As the reduction of cross section by cold-drawing was only about 40 percent, the change of crystal orientation probably was far from complete. Approach to preferred orientation during tensile extension, consequently would tend to elevate the  $C_0$  curve and thus would oppose the depressing tendencies due to decrease of internal stress and to the work-hardening factor.

The  $C_0$  curve for unannealed, cold-drawn Inconel L (fig. 12) descends at a generally decreasing rate, at least to an extension of about 2 percent. Similar curves, obtained with work-hardened 18 : 8 alloys, are shown in figures 11 and 19 of reference 1. The descent of these curves with slight plastic extension probably is due chiefly to relief of internal stress.

Relief of internal stress tends to decrease  $C_0$ , whether the relief is caused by slight plastic extension or by annealing. The effect of relief by annealing is revealed by comparison of the initial values of  $C_0$  for monel metal G and G-8 and for Inconel L and L-8.5 (fig. 12). Caution is necessary, however, in attributing the observed effects of such annealing to only one of the three important factors affecting  $C_0$ . Annealing for relief of internal stress generally affects more than one of these factors. It generally causes some decrease in hardness in single-phase alloys such as monel metal and Inconel, as illustrated by comparison of the 0.1-percent proof-stress curves for annealed and unannealed metals in figure 10. It may also cause structural changes in some alloys. To such changes may be attributed the fact that  $C_0$  is higher for 18 : 8 alloys DM and DH after

annealing at 900° F. than for the unannealed, work-hardened alloys (fig. 30). That relief of internal stress by the annealing at 900° F. was not the cause of this increase of  $C_0$  is indicated by the rise of the  $C_0$  curves for these alloys with restoration of internal stress during plastic extension (fig. 28).

#### FACTORS AFFECTING THE VARIATION OF $E_0$ WITH PRIOR PLASTIC EXTENSION

The same three factors that determine the variation of  $C_0$  with plastic extension determine the variation of  $E_0$ . The effects of two of these factors, the work-hardening factor and the change of crystal orientation, on the  $E_0$  curve for copper (figs. 44 and 45) have been discussed. The effect of each of these factors on the  $E_0$  curve was found to be similar to the effect on the  $C_0$  curve. Supplementary evidence that change of crystal orientation affects these two curves similarly, was also discussed previously. In the following discussion, reference will be made to additional evidence as to the influence of the reorientation factor and the work-hardening factor on the  $E_0$  curve.

There is considerable evidence that internal stress, like the other two factors, tends to affect the  $C_0$  and  $E_0$  curves similarly. This evidence will be presented first, and attention will then be called to some apparent contradictions.

The steep ascent and descent of the  $E_0$  curves for annealed Inconel (fig. 16) and for annealed 18:8 alloy (fig. 27), accompanying a similar course of the corresponding  $C_0$  curves, suggests that the  $E_0$  and  $C_0$  curves for these alloys are dominated by the same two factors. The rise and the descent of these  $C_0$  curves has been attributed (sec. X) to dominance of increasing internal stress followed by dominance of the work-hardening factor. The rise and the descent of the  $E_0$  curves, therefore, probably is due to successive dominance of these two factors.

Additional evidence that increase of internal stress tends to elevate both the  $E_0$  and  $C_0$  curves is found in the diagram for fully annealed monel metal G-12 (fig. 8). The rise of the  $C_0$  curve is accompanied by an initial rise of the  $E_0$  curve. As the rise of the  $C_0$  curve has been attributed to dominant influence of increasing internal stress, the initial rise of the  $E_0$  curve may be attributed to the same factor. The descent of the  $E_0$  curve from the maximum, like the descent of the  $C_0$  curve, probably is due to dominance of the work-hardening factor. The reascent of the  $E_0$  curve probably is due to dominant influence of change of crystal orientation. The elevating influence of this factor evidently is much stronger for this metal than for Inconel. The  $E_0$  curve for annealed Inconel (fig. 16) shows only slight evidence of reascent after the depressing influence of the work-hardening factor has been considerably weakened.

The  $E_0$  curve for annealed monel metal G-14 (fig. 6), unlike the curve for annealed monel metal G-12 (fig. 8), does not reveal the successive influence of all three factors. The slow initial rise of the curve may be due to the combined influence of increasing internal stress and change of crystal orientation. After this rise, the influence of the work-hardening factor evidently becomes dominant and the curve descends at a decreasing rate. Dominance of any one factor in the  $E_0$  curve for annealed monel metal is evidently slight.

No tendency to reascent is found in the  $E_0$  curve for annealed 18:8 alloy (fig. 27). The continuous descent of this curve from its maximum suggests the possibility that the change of crystal orientation of this alloy may involve decrease, rather than an increase, in the proportion of grains with [111] orientation. Such a change would tend to depress the  $E_0$  curve (and probably the  $C_0$  curve). Although this alloy is predominantly face-centered cubic, it contains a large proportion of naturally body-centered cubic elements (iron and chromium). The proportion of grains with [111] and [100] orientations, consequently, may be different from the proportion in an alloy (such as monel metal) of two face-centered cubic metals. The rapid continuous descent of the  $E_0$  curve for the 18:8 alloy, however, may be primarily due to strength of the work-hardening factor, in accordance with the high rate of work-hardening of this alloy.

The evidence previously presented indicates that *increase* of internal stress tends to cause increase of both  $C_0$  and  $E_0$ . The evidence now to be considered indicates that *decrease* of internal stress tends to cause decrease of both  $C_0$  and  $E_0$ .

Slight plastic extension of unannealed, severely cold-worked metal, as shown in the previous report and as illustrated by a number of examples in this report, tends to cause decrease of internal stress. In the diagram for unannealed, work-hardened Inconel L (fig. 12), the effect of such relief of internal stress is revealed by the rapid initial descent of both the  $C_0$  and  $E_0$  curves. (This rapid effect, obtained with severely cold-worked metal, cannot be attributed to the work-hardening factor.) *Annealing* this same cold-drawn alloy for relief of internal stress has a similar effect, which is revealed by a comparison of the initial values of  $E_0$  and  $C_0$  in the diagrams for Inconel L and L-8.5 (fig. 12). The relief of internal stress by annealing has decreased both  $C_0$  and  $E_0$ .

The initial values of  $E_0$  and  $C_0$  for unannealed work-hardened Inconel L (fig. 12) are much higher than the values obtained by the tensile extension of fully annealed Inconel L-17.5 (fig. 16). The maximum values obtained by this tensile extension were attained when the extension reached about 2 percent. With further extension,  $E_0$  reached a minimum about equal to the initial value for annealed Inconel; the curve then gives

some indication of reascent, probably under the influence of change of crystal orientation. At the beginning of local contraction (at about 35-percent extension), however,  $E_0$  is far below the value obtained with unannealed, cold-drawn Inconel L (fig. 12) and is also far below the maximum value for annealed Inconel L-17.5 (fig. 16). Cold-drawing the fully annealed Inconel, after tensile extension of 35 percent, probably would cause further increase of  $E_0$ . The reorientation factor alone, however, probably would be insufficient to increase  $E_0$  and  $C_0$  to the values found for cold-drawn Inconel L. These high values probably are due to high internal stress induced by drawing. Comparison of the diagrams for annealed Inconel L-17.5 and unannealed cold-drawn Inconel L therefore gives support to the view that increase of internal stress tends to cause increase of both  $C_0$  and  $E_0$ .

Additional evidence that variation of internal stress tends to cause qualitatively similar variation of  $E_0$  may be found by referring to the oscillations superposed on the basic curves of variation of  $E_0$  and  $C_0$  with prior plastic extension. The oscillations at pairs of experimental points, as mentioned frequently in previous discussion, generally are qualitatively the same for corresponding  $E_0$  and  $C_0$  curves. Although variations of the rest interval affect the magnitude of each oscillation, the oscillations are obtained even when all the rest intervals are long. The second experimental point of a pair, in both the  $E_0$  curve and the  $C_0$  curve, generally is lower than the first. As this abrupt decrease of  $C_0$  can be attributed to nothing else than decrease of internal stress, the accompanying abrupt decrease of  $E_0$  may be attributed to the same factor. The relatively long plastic extension prior to determination of the first experimental point of a pair evidently tends to cause increase of internal stress, and the short plastic extension prior to determination of the second experimental point tends to cause decrease of internal stress. These variations of internal stress evidently tend to cause similar variation of both  $C_0$  and  $E_0$ .

Attention will now be given to some instances of increase of  $C_0$  associated with decrease of  $E_0$ . An example of this relationship is found in the diagram for 13:2 chromium-nickel steel E (fig. 38). The rise of the  $C_0$  curve, under the dominant influence of increasing internal stress, is associated with a descent of the  $E_0$  curve. This fact does not necessarily imply, however, that increase in internal stress in this metal *tends* to cause decrease of  $E_0$ . As the work-hardening factor is dominant throughout the descending portion of the  $C_0$  curve, a natural surmise is that the continuous descent of the  $E_0$  curve is due to dominant influence of the same factor. According to this surmise, the influence of increasing internal stress is dominant in the ascent of the  $C_0$  curve but the work-hardening factor is dominant in the corresponding portion of the  $E_0$  curve.

Such a relationship is compatible with the view that increasing internal stress *tends* to elevate both the  $C_0$  and  $E_0$  curves.

Other examples of increase of  $C_0$  associated with decrease of  $E_0$  are found in the diagrams for three metals that have been annealed for relief of internal stress, Inconel L-8.5 (fig. 12), 18:8 alloy DM-9 (fig. 28), and 18:8 alloy DH-9 (fig. 28). Although the  $C_0$  curves ascend under the dominant influence of restoration of internal stress, the  $E_0$  curves descend. This relationship does not necessarily mean, however, that increasing internal stress *tends* to cause decrease of  $E_0$  for these metals. There is no apparent reason for such difference (in influence of internal stress) between these metals and the same metals in the fully annealed condition (figs. 16 and 27). The descent of the  $E_0$  curves for Inconel L-8.5 (fig. 12) and for 18:8 alloys DM-9 and DH-9 probably is due to dominant influence of the work-hardening factor. This view is supported by the fact that the descent of these curves is associated with ascent of the corresponding (0.10 percent) proof-stress-extension curves (figs. 10 and 25).

The opposite trends of these  $E_0$  and  $C_0$  curves is explainable on the assumption that increasing internal stress tends to increase both  $C_0$  and  $E_0$  and that the work-hardening factor is dominant in the  $E_0$  curve but not in the  $C_0$  curve. The effect of the internal stress factor on  $E_0$  or  $C_0$  can be represented by a curve rising at a decreasing rate, and the effect of the work-hardening factor can be represented by a curve descending at a decreasing rate. By superposition of two such curves, the resultant curve sometimes has an initial rise followed by descent and sometimes descends continuously from the origin. This difference in form of the resultant curve depends on quantitative, not on qualitative, differences in the component curves. The forms of all the modulus-extension curves, therefore, are explainable on the assumption that variation of internal stress tends to cause similar variation of both  $C_0$  and  $E_0$ .

THE TILT OF THE STRESS-STRAIN CURVE AS AFFECTED BY INTERNAL STRESS, CRYSTAL REORIENTATION, AND THE WORK-HARDENING FACTOR

By the "tilt" of the stress-strain curve is meant the inclination of the curve as a whole, up to the yield point. The stress-strain curve up to the yield point may be viewed as the ascending portion of a hysteresis loop. An index of the tilt of such a loop is the inclination of a straight line drawn from the origin to the vertex. The successive loops of a series, as shown in the preceding report, may vary greatly in maximum width yet change very little in tilt. Such a change in width involves an increase in the curvature of the ascending curve and in the slope of the curve at the origin. Increase in the width causes an increase of both  $C_0$  and  $E_0$ ; decrease in the width causes a decrease in both these indices.

It has been shown that each of the three important factors tends to cause similar changes in both  $C_0$  and  $E_0$ . Each of the factors, therefore, evidently tends either to increase or to decrease the width of the hysteresis loop. Consideration will now be given to the influence of each factor on the tilt of the stress-strain curve. Information as to the variation of tilt with prior plastic extension may be obtained by comparing the modulus-extension curves for  $E_{30}$ ,  $E_{50}$ , or  $E_{100}$  with the corresponding curves for  $E_0$ . In the following comparison, attention will be confined to metals that were not in the work-hardened condition prior to the tension test.

The trend of a curve of variation of  $E_Y$  (the secant modulus at the yield point) with prior plastic extension would be qualitatively similar to the trend of the corresponding curve of variation of  $E_{30}$ ,  $E_{50}$ , or  $E_{100}$ . The trend of a basic  $E_{30}$ ,  $E_{50}$ , or  $E_{100}$  curve therefore indicates qualitatively the influence of prior plastic extension on the tilt of the stress-strain curve. In the diagram for annealed 18:8 alloy steel (fig. 27), the trend of the  $E_{50}$  curve is downward, at least throughout the extent here shown. A similar trend of the  $E_{50}$  curve, throughout its entire extent, is found in the diagram for 13:2 chromium-nickel steel (fig. 38). In the diagrams for annealed monel metal (figs. 6 and 8) and annealed Inconel (fig. 18), the trend of the  $E_{50}$  curves is upward. An upward trend of the  $E_{30}$  curves is also found in the diagrams for annealed copper (figs. 44 and 45). An upward trend is found when the corresponding  $E_0$  curve reveals an elevating influence of the reorientation factor. A downward trend is found when the  $E_0$  curve shows no elevating influence of this factor. The evidence therefore appears to indicate that the reorientation factor tends sometimes to tilt the stress-strain curve backward, and that the work-hardening factor tends to tilt the curve forward.

The influence of the internal-stress factor on the tilt of the stress-strain curve is indicated by comparison of the abrupt superposed oscillations in the  $E_{30}$ ,  $E_{50}$  or  $E_{100}$  curve with the corresponding oscillations in the  $E_0$  curves. The oscillations are either absent in the former curves or are much less than in the latter curves. Practically no superposed oscillations, at pairs of experimental points, are found in the  $E_Y$  curves (not shown in this report). The evidence therefore indicates that abrupt variations of internal stress, although they cause similar abrupt variations of  $E_0$  and  $C_0$ , cause practically no change in the tilt of the stress-strain curve.

According to the available evidence, therefore, the work-hardening factor tends to tilt the stress-strain curve forward and to decrease its curvature. When the reorientation factor tends to increase  $E_0$ , it also tends to tilt the stress-strain curve backward and to increase its curvature. When the reorientation factor tends to

decrease  $E_0$ , it also tends to tilt the stress-strain curve forward and to decrease its curvature. The internal-stress factor affects the curvature but probably has little effect on the tilt of the stress-strain curve.

### CONCLUSIONS

The following conclusions apply to all the metals considered in this report except as indicated.

1. An incomplete view of the tensile elastic properties of a metal is obtained by considering either the stress-strain or the stress-set relationship alone. Consideration should be given to both relationships.

2. In a study of elastic properties, consideration should be given to the influence of hysteresis and of positive and negative creep.

3. Both the stress-set relationship and the stress-strain relationship are much influenced by the duration of the rest interval and by the extension spacing. The influence of duration of the rest interval is associated with negative creep.

4. Curves of variation of the proof stresses with prior plastic extension often have many wide, abrupt oscillations superposed on a more gradual wavelike curve. The wide oscillations are generally associated with varying duration of the rest interval and with variation in the extension spacing of the experimental points. The complexity of form of the proof-stress-extension curve may be attributed in part to variation of internal stress with plastic extension.

With prior plastic extension, the proof stresses representing permanent set values of 0.03 and 0.1 percent generally increase continuously. With prior plastic extension, the 0.001- and 0.003-percent proof stresses generally do not increase or decrease continuously but either increase to a maximum or decrease to a minimum; beyond this maximum or minimum, these proof stress-extension curves oscillate with little or no general upward trend. The 0.01-percent proof stress may follow a course similar to either the two lower or the two upper proof stresses.

6. The initial trend of the two lower proof-stress-extension curves, and sometimes of the 0.01-percent proof-stress-extension curve, depends on the initial change of internal stress and on the rate of work-hardening. Increase of internal stress tends to cause descent, and work-hardening tends to cause ascent, of the lower proof-stress-extension curves.

7. When the initial internal stress is high, as it generally is in unannealed, severely cold-worked metal, tensile extension tends to cause decrease of internal stress to a minimum. When the initial internal stress is zero or at a minimum, as it is in metals that have been fully annealed or annealed for relief of internal stress, tensile extension tends to cause increase of internal stress to a maximum.

8. With plastic extension of unannealed, work-hardened metals, the 0.001- and the 0.003-percent proof stresses generally increase considerably to a maximum, reached at a small percentage of plastic extension, and then decrease to a minimum. Further extension causes irregular oscillations in the proof-stress-extension curve.

9. With plastic extension of fully annealed metals, or of metals that have been annealed for relief of internal stress, the increasing internal stress tends to depress, and the work-hardening tends to elevate, the proof-stress-extension curve. If the rate of work-hardening of the metal is not high, the influence of the increasing internal stress predominates and the curve has an initial descent to a minimum. If the rate of work-hardening is high, as in annealed 18:8 chromium-nickel steel, the influence of the work-hardening at first predominates and the curve has an initial rise. Later, however, the influence of the increasing internal stress predominates, and the curve descends to a minimum.

10. From corresponding stress-strain and stress-set curves may be derived corrected stress-strain curves to represent approximately the variation of elastic strain with stress. From the corrected stress-strain curves may be derived curves of variation of the secant modulus with stress.

11. The stress-modulus line for fully annealed single-phase metals is generally curved. With prior plastic extension, the curvature generally first increases, then decreases. With high-strength single-phase alloys, such as 18:8 alloy, monel metal, and Inconel, the curvature of the stress-modulus line generally is negligible after prior extension of more than about 10 percent or 15 percent, and sometimes after considerably less prior extension. For half-hard and hard alloys of this type, the stress-modulus line is generally straight.

12. The stress-modulus line for an alloy that is sufficiently hardened by finely dispersed hard particles, such as carbides (as an example 13:2 chromium-nickel steel), is straight.

13. The stress-modulus line for an annealed, relatively soft metal, such as copper, is strongly curved. With prior plastic extension, the curvature first increases then decreases. Even after severe cold work, however, the stress-modulus line may be slightly curved.

14. Straightness of the stress-modulus line indicates that the corresponding stress-strain line is a quadratic parabola. The curvature of the parabola may be measured either by the slope ( $k$ ) of the stress-modulus line or by the linear stress coefficient ( $C_0$ ) of the modulus. The modulus at zero stress ( $E_0$ ) may be obtained by extrapolating the stress-modulus line to zero stress.

15. When the stress-modulus line is curved from the origin, a second constant ( $C'$ ) is needed to represent the curvature of the stress-modulus line.

16. For some fully annealed metals and for some other metals that are free from effects of cold-work,  $C_0$  is zero, and the stress-strain line, consequently, is a cubic parabola. The stress-strain line corresponding to a curved stress-modulus line may be viewed either as the result of superposition of a cubic parabola on a quadratic parabola or as a single parabola whose exponent ranges between 2 and 3. For a metal sufficiently hardened by alloying or by cold-work, the stress-strain line generally is a quadratic parabola.

17. Increase in the rest interval tends to *decrease* the slope of the stress-set curve and thus to decrease the proof stresses. Increase in the rest interval tends to *increase* the initial slope ( $E_0$ ) and the curvature ( $C_0$ ) of the "corrected" stress-strain curve.

18. The effect of increase of the rest interval on  $E_0$ ,  $C_0$ , and the proof stresses, is opposite to the effect of relief of internal stress. The effect of the rest interval is apparently some kind of softening effect, which (at least for a while) predominates over any beneficial effect of relief of internal stress by negative creep.

19. When  $E_0$ ,  $C_0$ ,  $C'$ , and the five proof stresses are known, a fairly good picture is available of the elastic strength in tension.

20. Because of the great directional variation of the modulus of elasticity of a metal crystal, change of orientation of the grains of a polycrystalline aggregate may greatly affect the course of the modulus-extension curve. With most face-centered cubic metals, cylindrical extension causes such change of crystal orientation that  $E_0$  tends to increase. Some face-centered cubic metals, however, exhibit the opposite tendency. With body-centered cubic metals, change from random to preferred orientation tends to cause some increase in  $E_0$ . Annealing may greatly affect the crystal orientation and thus may affect the modulus-extension curve.

21. The directional variation of the stress-coefficient ( $C_0$ ) of the modulus of elasticity of a metal crystal probably is similar to the directional variation of the modulus of elasticity ( $E_0$ ).

22. Change of crystal orientation with plastic extension, therefore, tends to have qualitatively the same effect on  $E_0$  and  $C_0$ .

23. The curves of variation of  $C_0$  and  $E_0$  with prior plastic extension are continuously affected by three important factors: Internal stress, crystal orientation, and the work-hardening factor. Change in dominance from one factor to another is accompanied by reversal in curvature. By the "work-hardening" factor is meant the influence of the structural changes (slip of crystallographic planes, lattice distortion, etc.) other than change of crystal orientation.

24. The work-hardening factor always tends to cause decrease of both  $E_0$  and  $C_0$ .

25. A variation of internal stress tends to cause a similar variation of  $C_0$ .

26. A variation of internal stress tends to cause a similar variation of  $E_0$ .

27. The reorientation factor tends to elevate the modulus-extension curves for copper, monel metal, and Inconel, has a slight tendency to elevate the curve for 13 : 2 chromium-nickel steel, and shows no tendency to elevate the curves for 18 : 8 alloys.

28. Variations of  $E_0$  and  $C_0$ , especially variations due to the influence of the rest interval and of the extension spacing, generally are accompanied by opposite variations in the proof stresses, especially the 0.001- and 0.003-percent proof stresses.

29. The tilt of the stress-strain curve as a whole (up to the yield point) generally varies with the prior plastic extension. The work-hardening factor tends to tilt the stress-strain curve forward and to decrease its curvature. When the reorientation factor tends to increase  $E_0$ , it also tends to tilt the stress-strain curve backward and to increase its curvature. The internal-stress factor, although it tends to affect the curvature, probably has little effect on the tilt of the stress-strain curve.

30. Annealing of 18 : 8 chromium-nickel steel at about 900° to 950° F for relief of internal stress causes great improvement in the proof stresses, especially the 0.001- and 0.003-percent proof stresses. Annealing for a longer time at a lower temperature, about 36 hours at about 480° F, causes practically no increase in the proof stresses above the values that would be obtained by annealing at the same temperature for 30 minutes. The longer duration of anneal, however, causes considerable decrease in  $C_0$ .

31. Heat treatment of the 13 : 2 chromium-nickel steel at 700° to 900° F causes great improvement in the proof stresses.

32. Annealing cold-worked monel metal and Inconel for relief of internal stress causes great improvement in elastic strength without important loss in tensile strength.

33. Aluminum-monel metal can be given high elastic strength by suitable heat treatment.

34. By slight prestretching of a metal having high internal stress, the reduction of the internal stress is comparable with that caused by suitable annealing. Slight prestretching of a metal that has been annealed for relief of internal stress, however, generally tends to increase the internal stress to a high value.

## REFERENCES

1. McAdam, D. J., Jr., and Mebs, R. W.: Tensile Elastic Properties of 18 : 8 Chromium-Nickel Steel as Affected by Plastic Deformation. T. R. No. 670, N. A. C. A., 1939.
2. Schmid, Erich, and Boas, W.: Kristallplastizität. Julius Springer (Berlin), 1935.
3. Taylor, G. I., and Elam, C. F.: The Distortion of an Aluminum Crystal during a Tensile Test. Proc. Roy. Soc. (London), ser. A., vol. 102, no. A. 719, March 1, 1923, pp. 643-667.
4. Vacher, Herbert C.: Development of a Fibrous Texture in Cold-Worked Rods of Cooper. Res. Paper 1210, Nat. Bur. Standards Jour. Res., vol. 22, no. 6, June, 1939, p. 651-668.
5. Ettisch, M., Polanyi, M., and Weissenberg, K.: Über Faserstruktur bei Metallen. Zeitschr. f. Phys., Bd. 7, Nr. 3, Nov. 3, 1921, S. 181-184.
6. Ettisch, M., Polanyi, M., and Weissenberg, H.: Faserstruktur hartgezogener Metalldrähte. Zeitschr. Phys. Chem., Bd. 99, Nr. 5, Dec. 9, 1921, S. 332-337.
7. Sachs, G., and Schiebold, E.: Rekristallisation und Entfestigung im Röntgenbild. Zeitschr. f. Metallkunde, Bd. 17, Nr. 12, Dec. 1925, S. 400-402.
8. Schmid, E., and Wassermann, G.: Über die Textur hartgezogener Drähte. Zeitschr. f. Phys., Bd. 42, Nr. 11-12, May 16, 1927, S. 779-794.
9. Vargha, G., and Wassermann, G.: Über des Einfluss des Formgebungsverfahren auf die Kristallgleichrichtung in Drähten. Zeitschr. f. Metallkunde, Bd. 25, Nr. 12, Dec. 1933, S. 310-313.
10. Greenwood, G.: Fibre Texture in Nickel Wires. Zeitschr. f. Krist., Bd. 72, Nr. 3, Nov. 1929, S. 309-317.
11. Fraser, O. B. J.: Private communication from O. B. J. Fraser, Director of Technical Service of Mill Products, International Nickel Co., Aug. 2, 1939.
12. Taylor, G. I.: The Distortion of Crystals of Aluminum under Compression. Pt. II. Distortion by Double Slipping and Changes in Orientation of Crystal Axes during Compression. Proc. Roy. Soc. (London), ser. A, vol. 116, no. A. 773, Sept. 1, 1927, pp. 16-38.
13. Barrett, C. S., and Levenson, L. H.: The Structure of Aluminum after Compression. Tech. Pub. No. 1104, Metals Technology, vol. 6, no. 6, Sept. 1939, 15 pages.
14. Barrett, C. S.: Recrystallization Texture of Aluminum after Compression. Tech. Pub. No. 1141, Metals Technology, vol. 7, no. 1, Jan. 1940, 18 pages.
15. Wever, F.: Über die Walzstruktur kubisch kristallisierender Metalle. Zeitschr. f. Phys., Bd. 28, Nr. 2, Sept. 24, 1924, S. 69-90.
16. Wever, F., and Schmid, W. E.: Beiträge zur Kenntnis der Textur kaltverformter Metalle. Mitteilung K. W. Inst. f. Eisenforschung, Bd. 11, Nr. 7, 1929, S. 109-122.
17. Wever, F., and Schmid, W. E.: Texturen kaltverformter Metalle. Zeitschr. f. Metallkunde, Bd. 22, Nr. 4, Apr. 1, 1930, S. 133-140.
18. Pickus, N., and Mathewson, C.: On the Theory of the Origin of Rolling Textures in Face-Centered Cubic Metals. Jour. Inst. Metals, vol. 64, no. 821, 1939, pp. 237-258.
19. Pickus, N., and Mathewson, C.: Plastic Deformation and Subsequent Recrystallization of Single Crystals of Alpha Brass. Trans. Am. Inst. Min. and Met. Eng., vol. 133, 1939, pp. 161-181.
20. Gensamer, M., and Vukmanic, P. A.: Preferred Orientations in Hot-Rolled Low-Carbon Steel. Trans. Am. Inst. Min. and Met. Eng., vol. 125, 1937, pp. 507-511.
21. Barrett, C. S., and Levenson, L. H.: Structure of Iron after Drawing, Swaging, and Elongating in Tension. Tech. Pub. No. 1038, Metals Technology, vol. 6, no. 2, Feb. 1939, 17 pages.
22. Barrett, C. S.: Structure of Iron after Compression. Tech. Pub. No. 977, Metals Technology, vol. 5, no. 7, Oct. 1938, 29 pages.
23. Kurdjumow, G., and Sachs, G.: Walz- und Rekristallisationstextur von Eisenblech. Zeitschr. f. Phys., Bd. 62, Nr. 9-10, June 25, 1930, S. 592-599.
24. Barrett, C. S., Ansel, G., and Mehl, R. F.: Preferred Orientations in Iron-Silicon Alloys. Trans. Am. Inst. Min. and Met. Eng., vol. 125, 1937, pp. 516-528.
25. Gensamer, M., and Mehl, R. F.: Preferred Orientations Produced by Cold-Rolling Low-Carbon Sheet Steel. Tech. Pub. no. 704, Metals Technology, vol. 3, no. 4, June 1936, 14 pages.
26. Farnham, G., and O'Neill, H.: Crystal Reorientation on Heating Drawn Copper Wires. Jour. Inst. Metals, vol. 55, no. 2, 1934, pp. 201-208.
27. Burgers, W. G., and Louwerson, P. C.: Über den Zusammenhang zwischen Deformationsvorgang und Rekristallisationstextur bei Aluminium. Zeitschr. f. Phys., Bd. 67, Nr. 9-10, Feb. 14, 1931, S. 605-678.
28. Collins, J. A., and Mathewson, C. H.: Plastic Deformation and Recrystallization of Aluminum Single Crystals. Tech. Pub. No. 1145, Metals Technology, vol. 7, no. 1, Jan. 1940, 2 pages.
29. Göler, V., and Sachs, G.: Walz- und Rekristallisationstextur regulär flächenzentrierter Metalle. I. Zeitschr. f. Phys., Bd. 41, Nr. 11-12, March 14, 1927, S. 873-888.
30. Göler, V., and Sachs, G.: Walz- und Rekristallisationstextur regulär flächenzentrierter Metalle. II. Zeitschr. f. Phys., Bd. 41, Nr. 11-12, March 14, 1927, S. 889-906.
31. Göler, V., and Sachs, G.: Walz- und Rekristallisationstextur regulär flächenzentrierter Metalle. III. Zeitschr. f. Phys., Bd. 56, Nr. 7-8, July 29, 1929, S. 477-484.
32. Göler, V., Sachs, G.: Walz- und Rekristallisationstextur regulär flächenzentrierter Metalle. IV. Zeitschr. f. Phys., Bd. 56, Nr. 7-8, July 29, 1929, S. 485-494.
33. Gensamer, M., and Lustman, B.: Preferred Orientations Produced by Recrystallizing Cold-Rolled Low-Carbon Sheet Steel. Trans. Am. Inst. Min. and Met. Eng., vol. 125, 1937, pp. 501-506.
34. Schmid, E.: Zur Fließgefahr von Metallkristallen. Zeitschr. f. Metallkunde, Bd. 19, Nr. 4, April 1927, S. 154-157.
35. Kuntze, W.: Abhängigkeit der elastischen Dehnungszahl "α" des Kupfers von der Vorbehandlung. Zeitschr. f. Metallkunde, Bd. 20, Nr. 4, April 1928, S. 145-150.
36. Kawai, T.: The Effect of Cold-Working on Young's Modulus of Elasticity. Sci. Rep., Tohoku Imperial Univ., vol. 19, No. 2, May 1930, pp. 209-234.
37. Honda, K., and Yamada, R.: On the Change of Elastic Constant in Metals Caused by Cold-Working. Sci. Rep., Tohoku Imperial Univ., vol. 17, No. 3, June 1928, pp. 723-742.
38. Heyn, E.: Internal Strains in Cold-Wrought Metals, and Some Troubles Caused Thereby. Jour. Inst. Metals, vol. 12, pt. 2, 1914, pp. 3-37.
39. Sachs, G.: Innere Spannungen in Metallen. VDI Zeitschr., Bd. 71, Nr. 43, Oct. 22, 1927, S. 1511-1516.

## BIBLIOGRAPHY

- Boas, W., and Schmid, E.: Zur Deutung der Deformationstexturen von Metallen. *Zeitschr. f. tech. Phys.*, 12. Jahrg., Nr. 2, 1931, S. 71-75.
- Brick, R. M.: Correlation of Deformation and Recrystallization Textures of Rolled 70:30 Brass. *Tech. Pub. No. 1144, Metals Technology*, vol. 7, no. 1, Jan. 1940, 20 pages.
- Burgers, W. G., and Snoek, J. L.: Über die Walz- und Rekristallisationstextur des Nischeisens. *Zeitschr. f. Metallkunde*, Bd. 27, Nr. 7, July 1935, S. 158-160.
- Dahl, O., and Pawlek, F.: Walz- und Rekristallisationstexturen bei Eisen-Nickel-Legierungen in Zusammenhang mit den magnetischen Eigenschaften II. *Zeitschr. f. Metallkunde*, Bd. 28, Nr. 8, Aug. 1936, S. 230-233.
- Dushman, S.: Cohesion and Atomic Structure. 4th Marburg Lect., *A. S. T. M. Proc.*, vol. XXIX, pt. 2, June 1929, pp. 7-64.
- Glocker, R.: Über Deformation- und Rekristallisationstexturen von Metallen. *Zeitschr. f. Phys.*, Bd. 31, Nr. 5-6, Feb. 19, 1925, S. 386-410.
- Göler, V., and Sachs, G.: Walz- und Rekristallisationstextur regulär flächenzentrierter Metalle. V. *Zeitschr. f. Phys.*, Bd. 56, Nr. 7-8, July 29, 1929, S. 495-502.
- Greenwood, G.: On the Cold-Working of Platinum Wires and the Fibrous Texture Thereby Produced. *Zeitschr. f. Krist.*, Bd. 78, Nr. 3-4, June 1931, S. 242-250.
- Hollabaugh, C. B., and Davey, W. P.: Preferred Orientation Produced by Cold Rolling in Surface of Sheets of Aluminum, Nickel, Copper and Silver. *Metals & Alloys*, vol. 2, nos. 4 and 5, Oct. 1931, pp. 246-250, and Nov. 1931, pp. 302-312.
- Houwink, R.: *Elasticity, Plasticity and Structure of Matter*. Cambridge Univ. Press, 1937. (With a chapter on the Plasticity of Crystals by Dr. W. G. Burgers.)
- Joffe, A.: *The Physics of Crystals*. McGraw-Hill Book Co., Inc., 1928.
- McLachlan, D., and Davey, W.: An X-Ray Study of Preferred Orientations in Pure Cold-Rolled Iron-Nickel Alloys. *Trans. Am. Soc. Metals*, vol. 25, no. 4, 1937, pp. 1084-1109.
- Owen, E., and Preston, G.: The Effect of Rolling on the Crystal Structure of Aluminum. *Proc. Phys. Soc.*, vol. 38, pt. 2, no. XVII, 1926, pp. 132-147.
- Pawlek, T.: Walz- und Rekristallisationstexturen bei Eisen-Nickellegierungen in Zusammenhang mit den Magnetischen Eigenschaftern. *Zeitschr. f. Metallkunde*, Bd. 27, Nr. 7, July 1935, S. 160-165.
- Polányi, M.: Über Strukturänderungen in Metallen durch Kaltbearbeitung. *Zeitschr. f. Phys.*, Bd. 17, Nr. 1, July 30, 1923, S. 42-53.
- Schmid, E., and Wassermann, G.: Über die Rekristallisation von Kupfer Draht. *Zeitschr. f. Phys.*, Bd. 40, Nr. 6, Dec. 14, 1926, S. 451-455.
- Taylor, G. I.: The Distortion of Crystals of Aluminum under Compression. III. *Proc. Roy. Soc. (London)*, ser. A, vol. 116, no. A 773, Sept. 1, 1927, pp. 39-60.
- Taylor, G. I.: Resistance to Shear in Metal Crystals. *Trans. Faraday Soc.*, vol. XXIV, Part 2, Feb. 1928, pp. 121-125.
- Taylor, G. I.: The Mechanism of Plastic Deformation of Crystals. I. *Proc. Roy. Soc. (London)*, ser. A, vol. 145, no. A 854, June 2, 1934, pp. 362-387.
- Taylor, G. I.: The Mechanism of Plastic Deformation of Crystals. II. *Proc. Roy. Soc. (London)*, ser. A, vol. 145, no. A 855, July 2, 1934, pp. 388-404.
- Taylor, G. I.: Plastic Strain in Metals. *Jour. Inst. Metals*, vol. 62, no. 1, 1938, pp. 307-324.
- Taylor, G. I., and Elam, C.: The Plastic Extension and Fracture of Aluminum Crystals. *Proc. Roy. Soc. (London)*, ser. A, vol. 108, no. A 745, May 1, 1925, pp. 28-51.
- Taylor, G. I., and Farren, W.: The Distortion of Crystals of Aluminum under Compression. *Proc. Roy. Soc. (London)*, ser. A, vol. 111, no. A 759, July 2, 1926, pp. 529-551.
- Wassermann, G.: Untersuchungen an Eisen-Nickellegierungen mit Würfeltextur. *Zeitschr. f. Metallkunde*, Bd. 28, Nr. 9, Sept. 1936, S. 262-271.

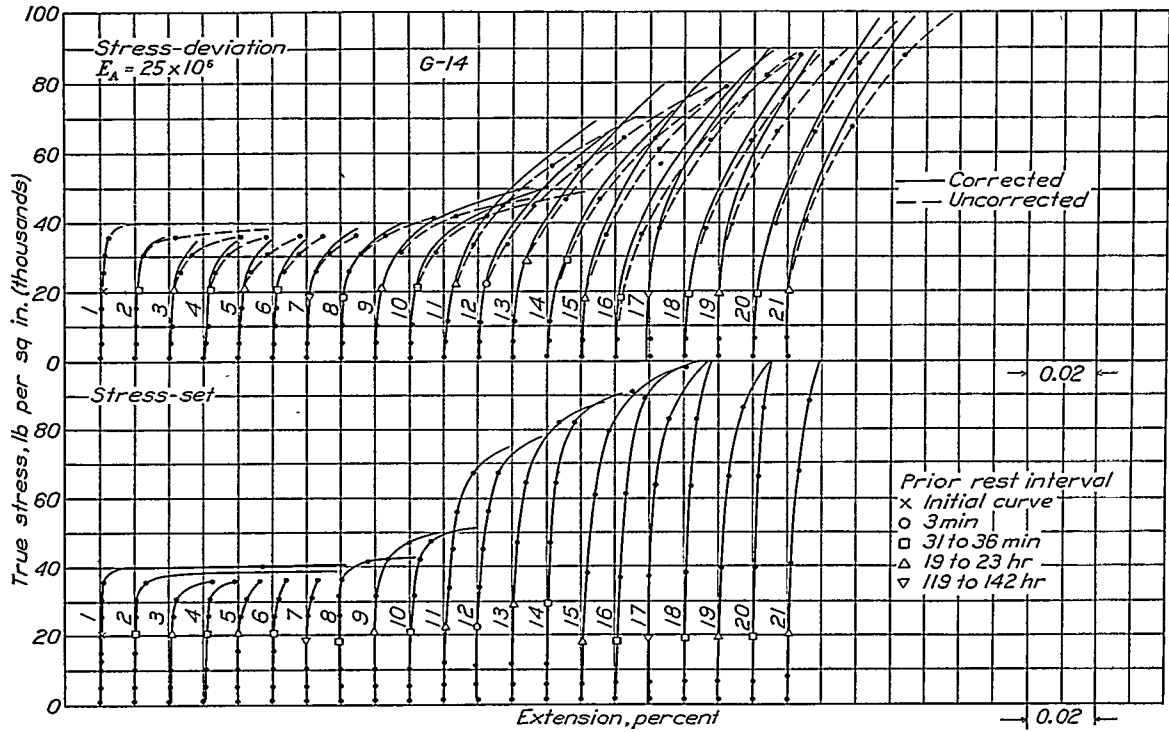


FIGURE 1.—Influence of prior plastic extension on stress-deviation and stress-set curves for monel metal G-14; cold-drawn; annealed at 1,400° F.

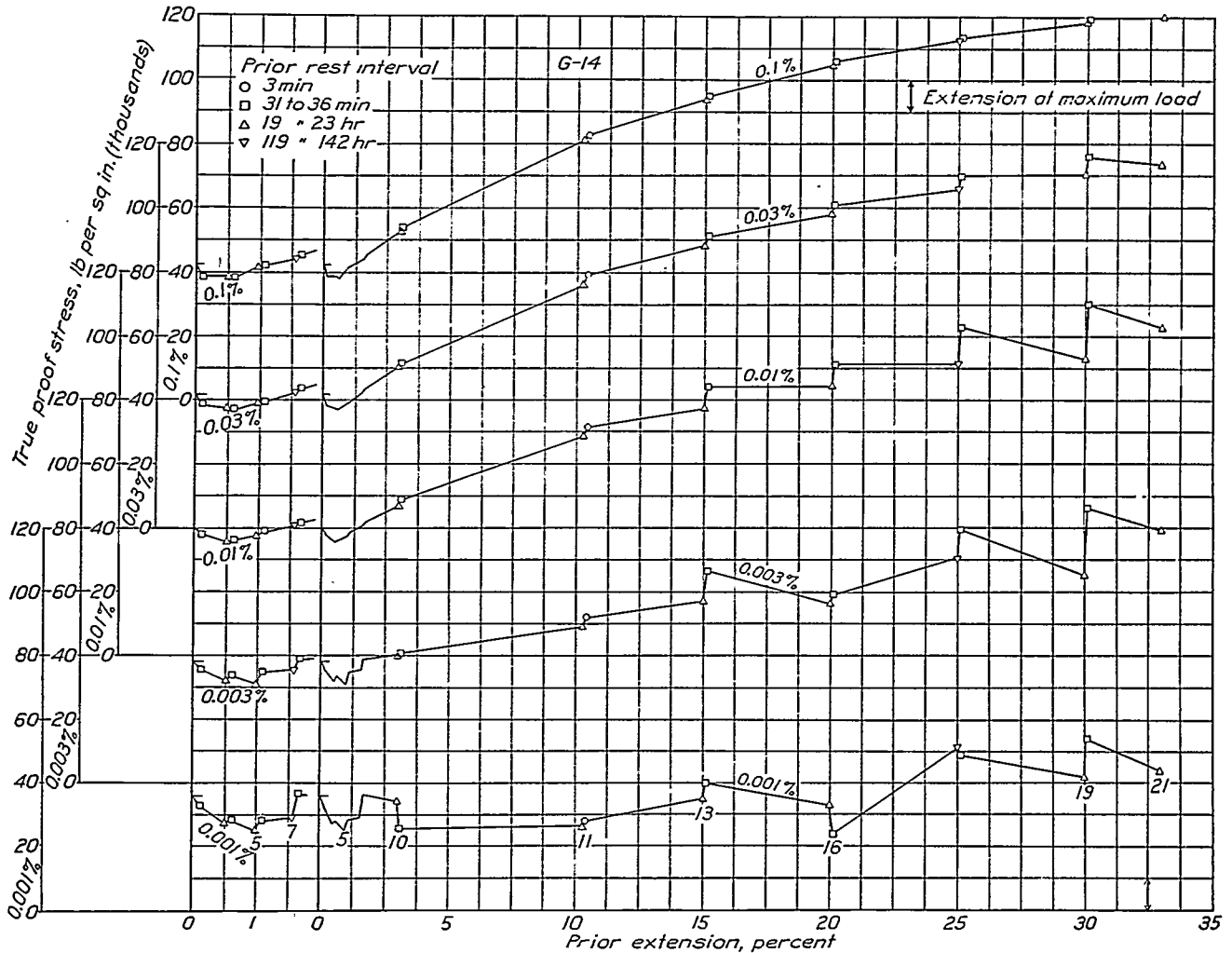
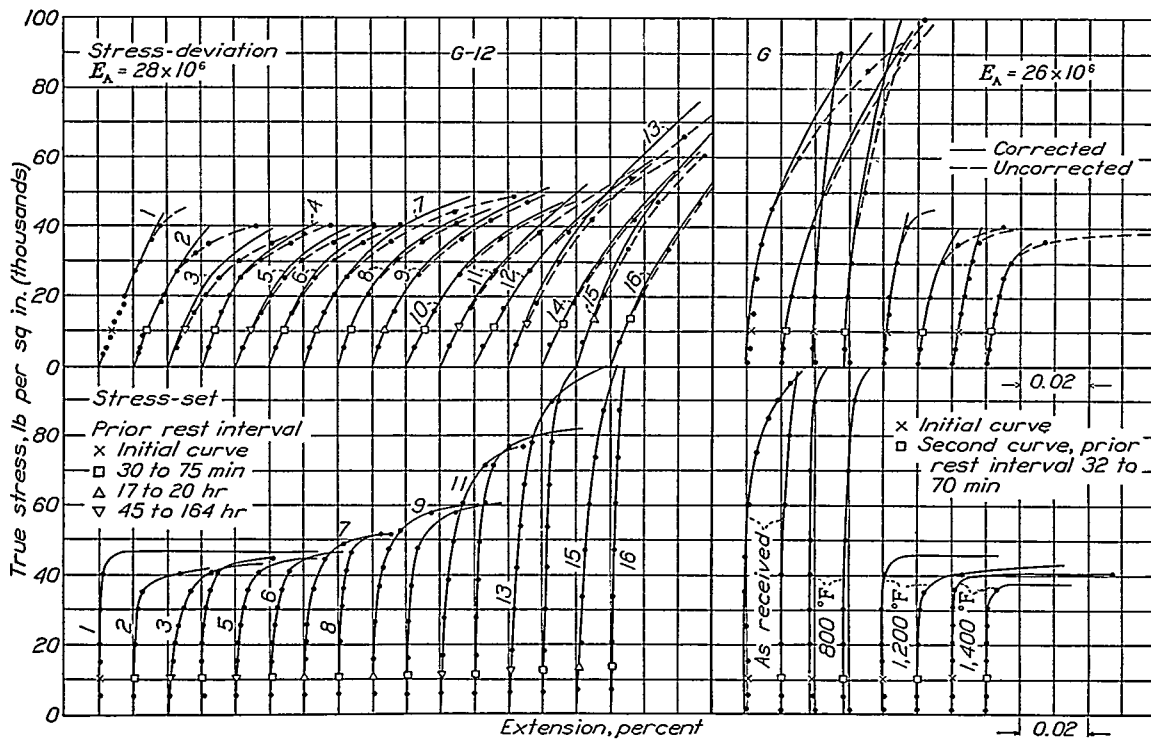


FIGURE 2.—Influence of prior plastic extension on proof stresses for monel metal G-14; cold-drawn; annealed at 1,400° F.



Monel metal G-12; cold-drawn; annealed at 1,200° F.  
 Monel metal G; cold-drawn; annealed at indicated temperature.

FIGURE 3.—Influence of prior plastic extension on stress-deviation and stress-set curves for monel metal.

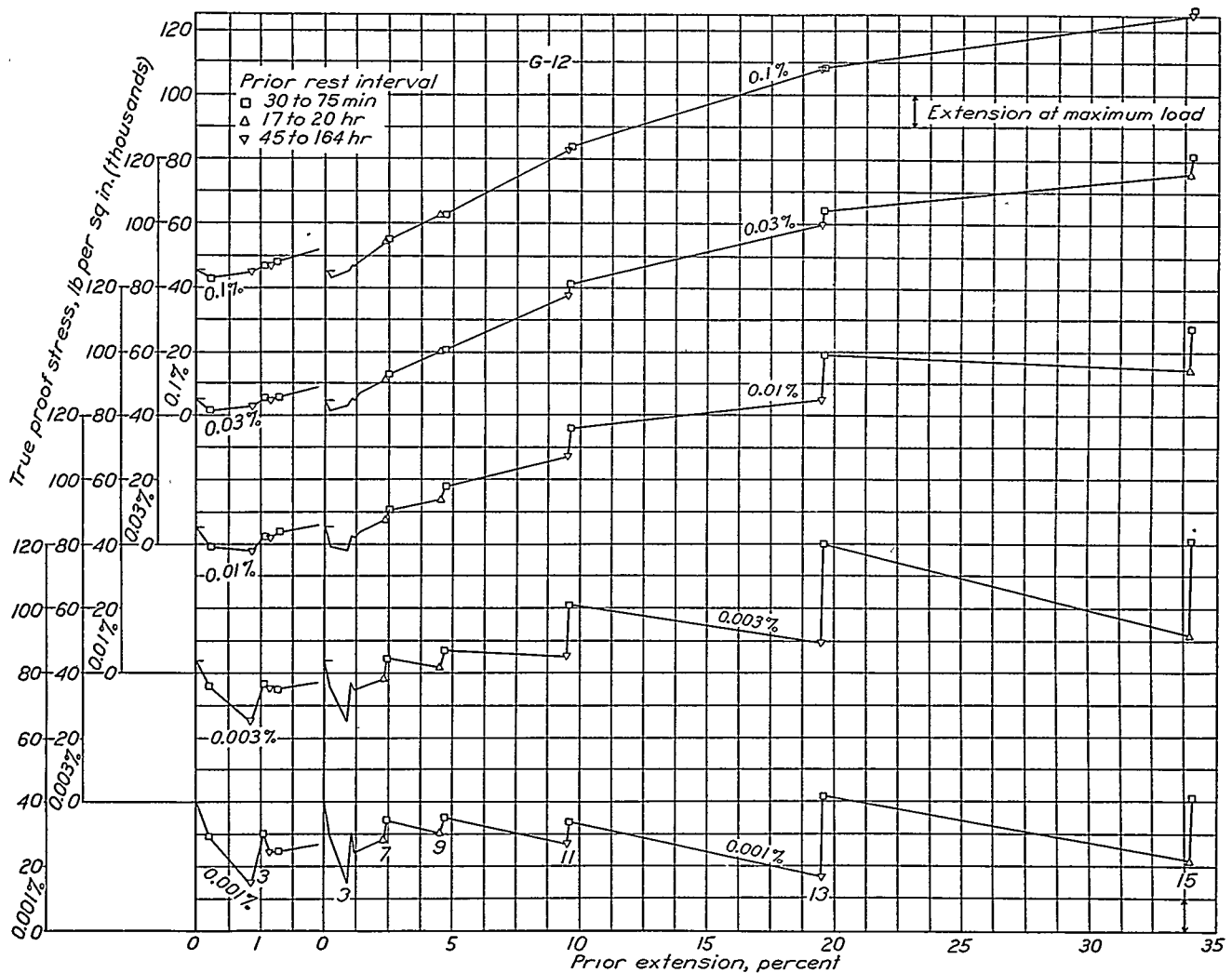


FIGURE 4.—Influence of prior plastic extension on proof stresses for monel metal G-12; cold-drawn; annealed at 1,200° F.

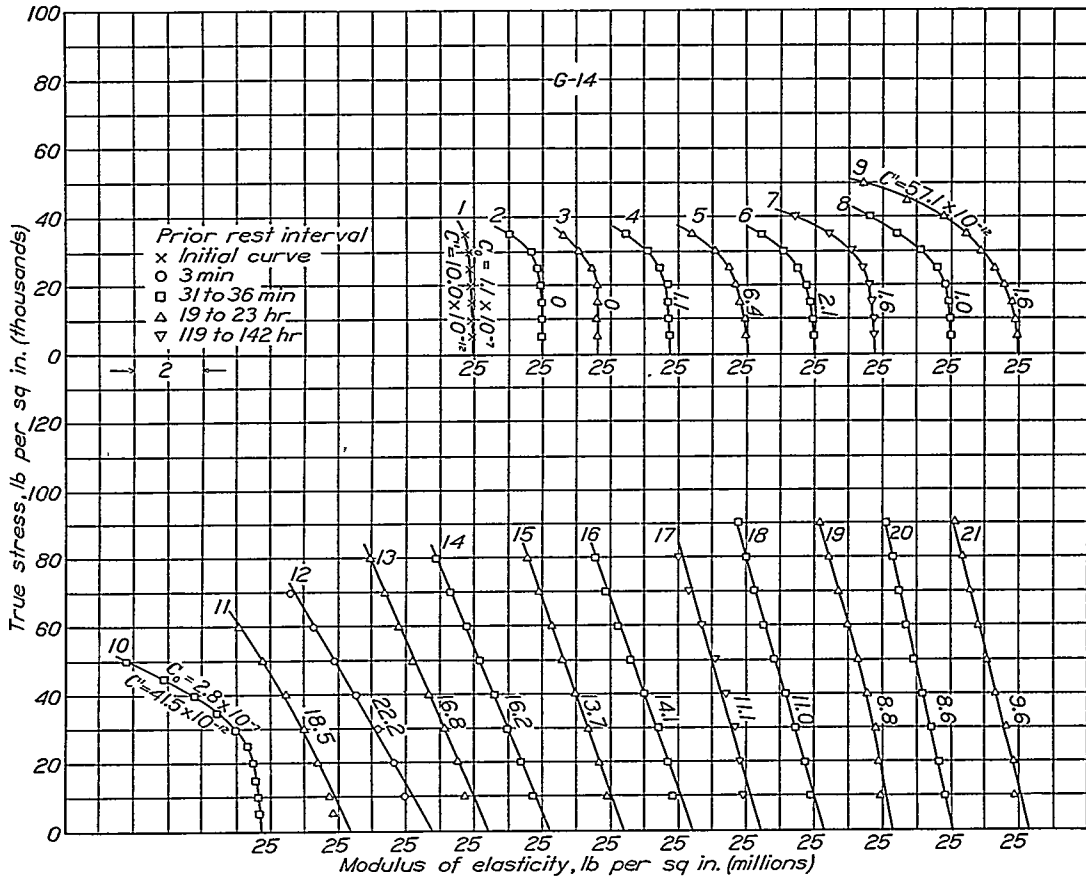


FIGURE 5.—Influence of prior plastic extension on the stress-modulus line for monel metal G-14; cold-drawn; annealed at 1,400° F.

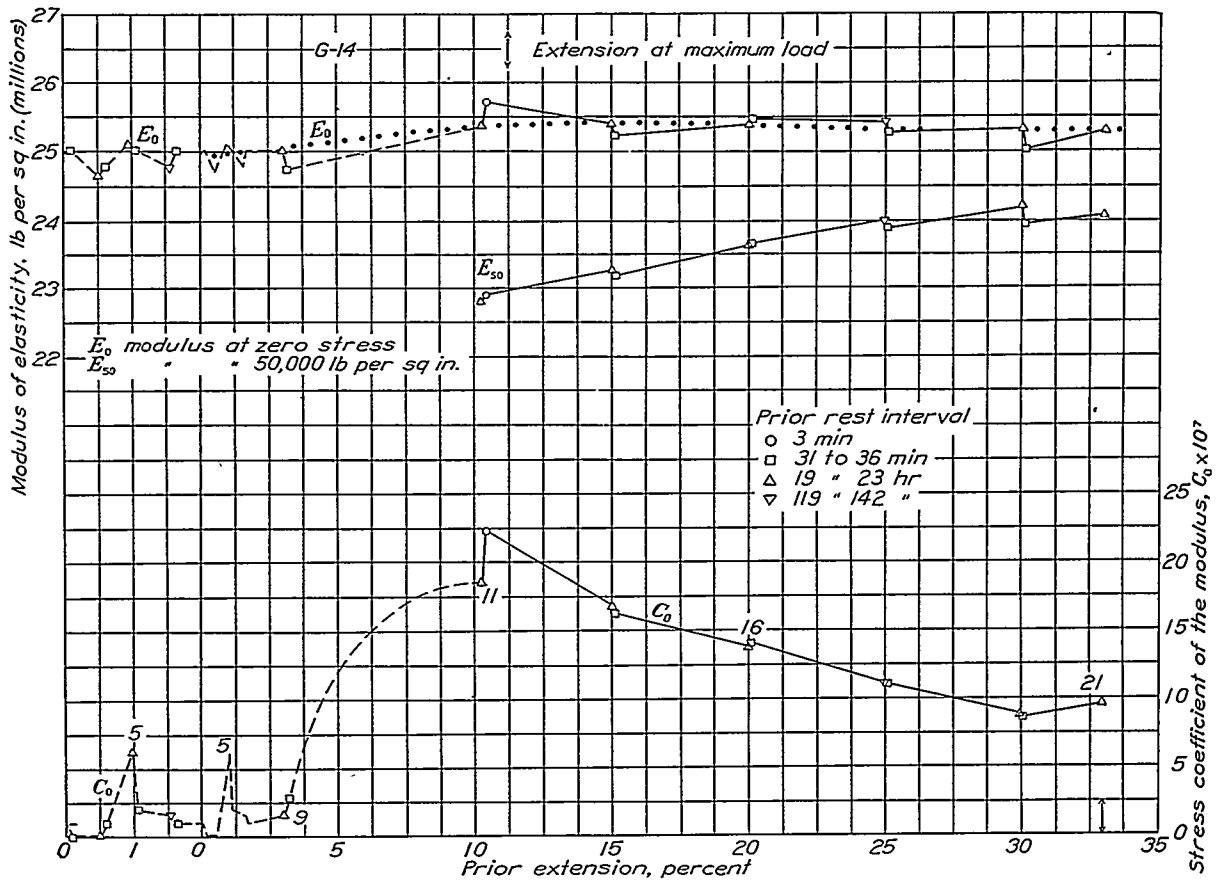


FIGURE 6.—Influence of prior plastic extension on the modulus of elasticity and on its stress coefficient for monel metal G-14; cold-drawn; annealed at 1,400° F

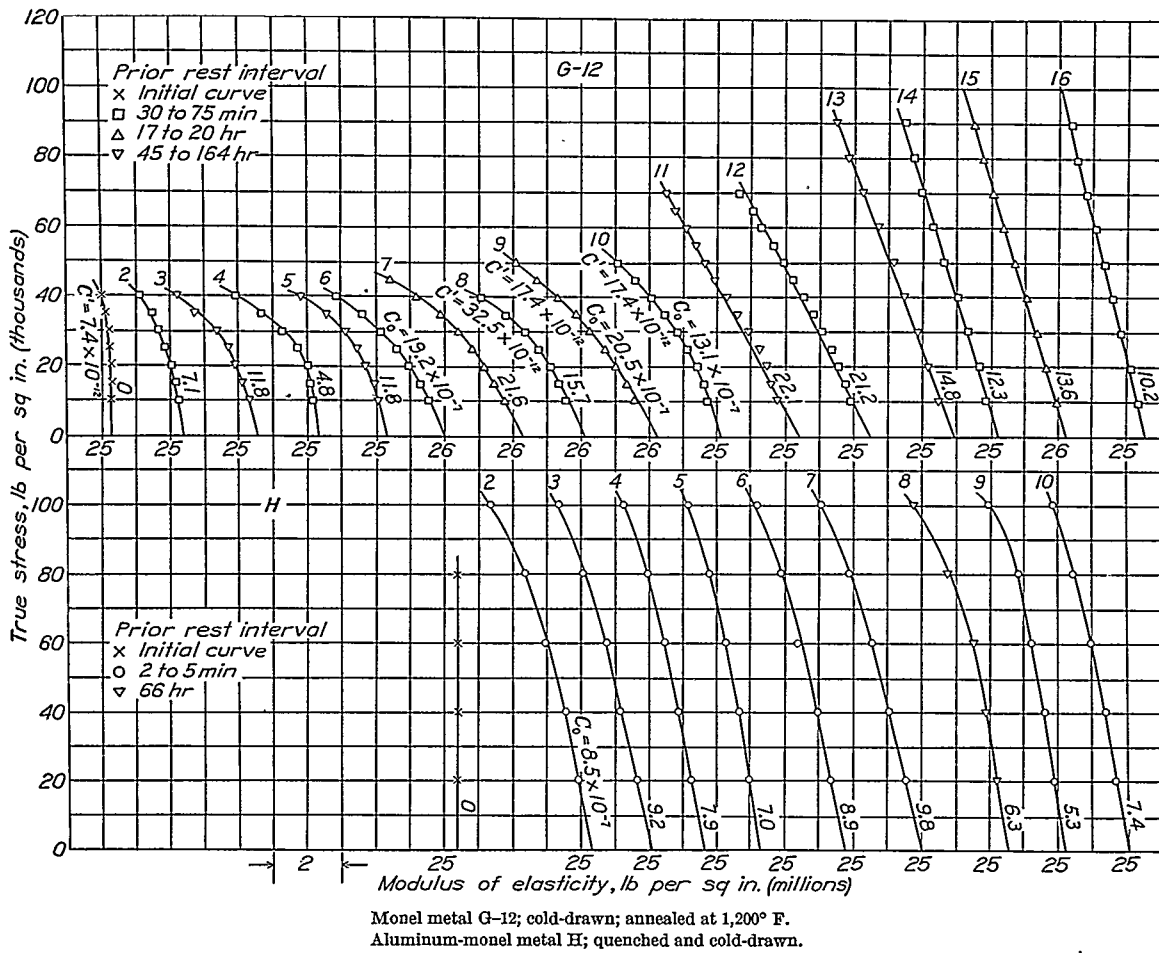


FIGURE 7.—Influence of prior plastic extension on the stress-modulus line for annealed monel metal G-12 and work-hardened aluminum-monel metal H.

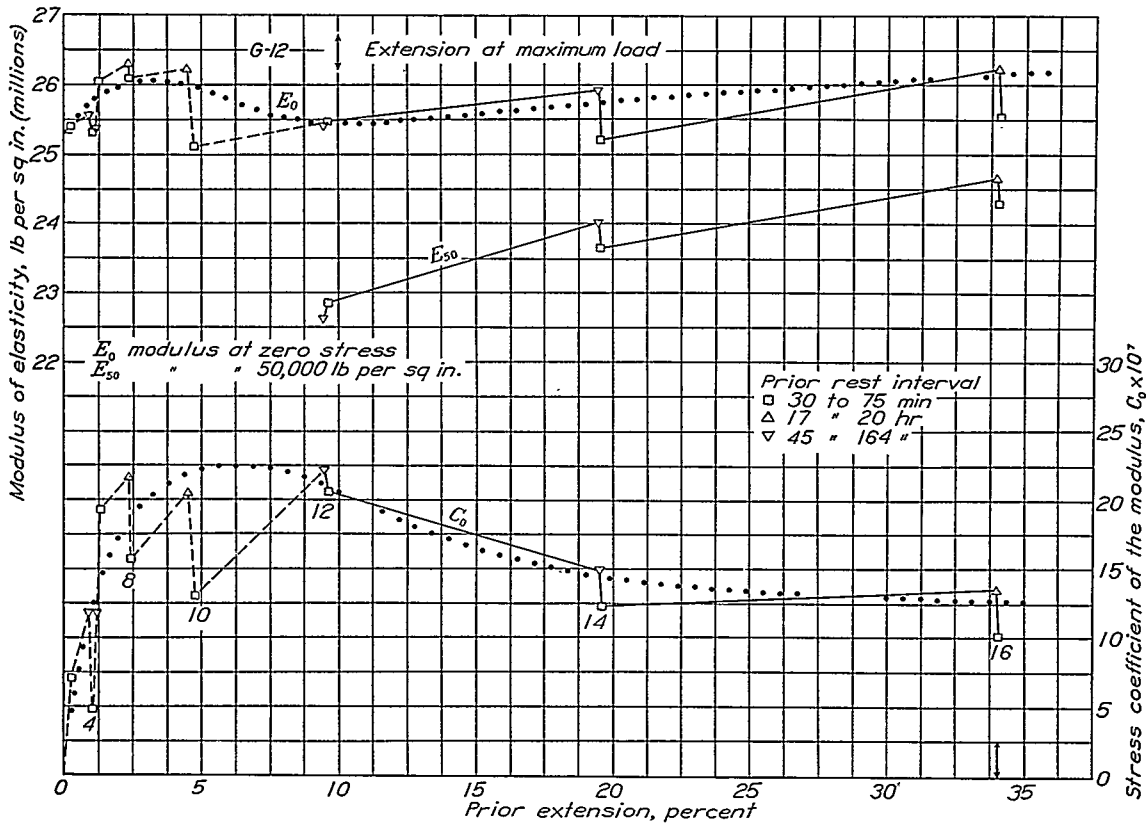


FIGURE 8.—Influence of prior plastic extension on the modulus of elasticity and on its stress coefficient for monel metal G-12; cold-drawn; annealed at 1,200° F.

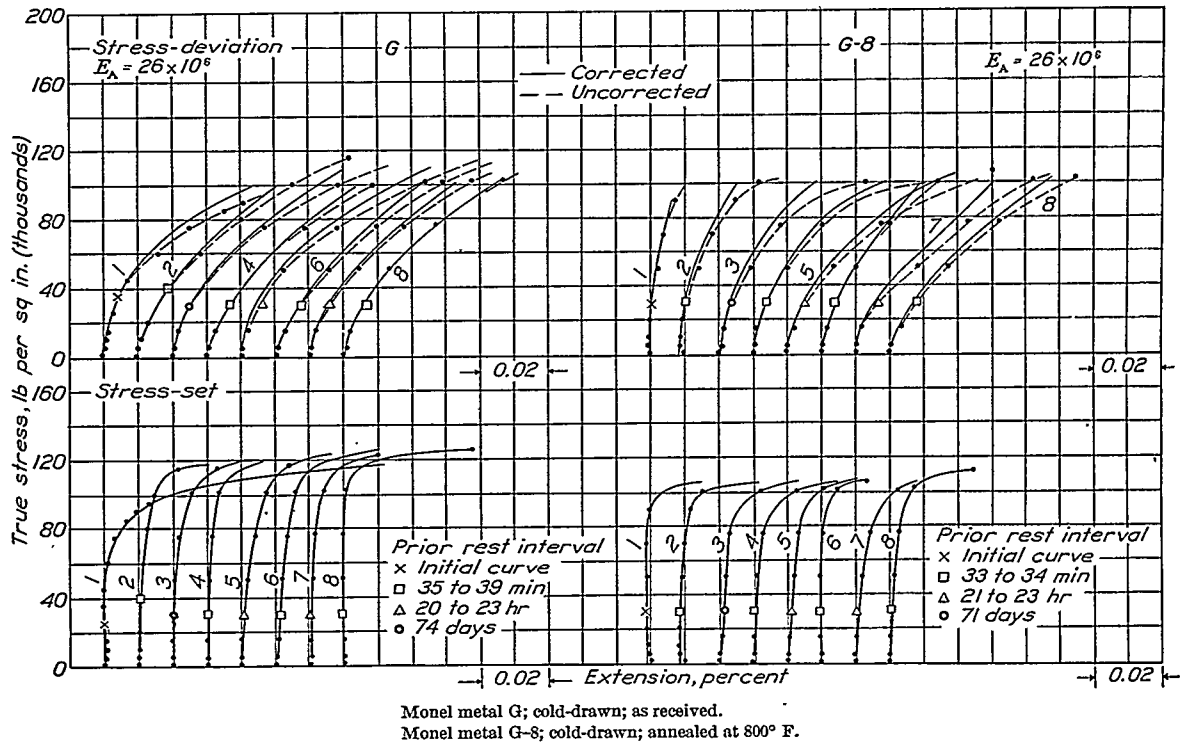
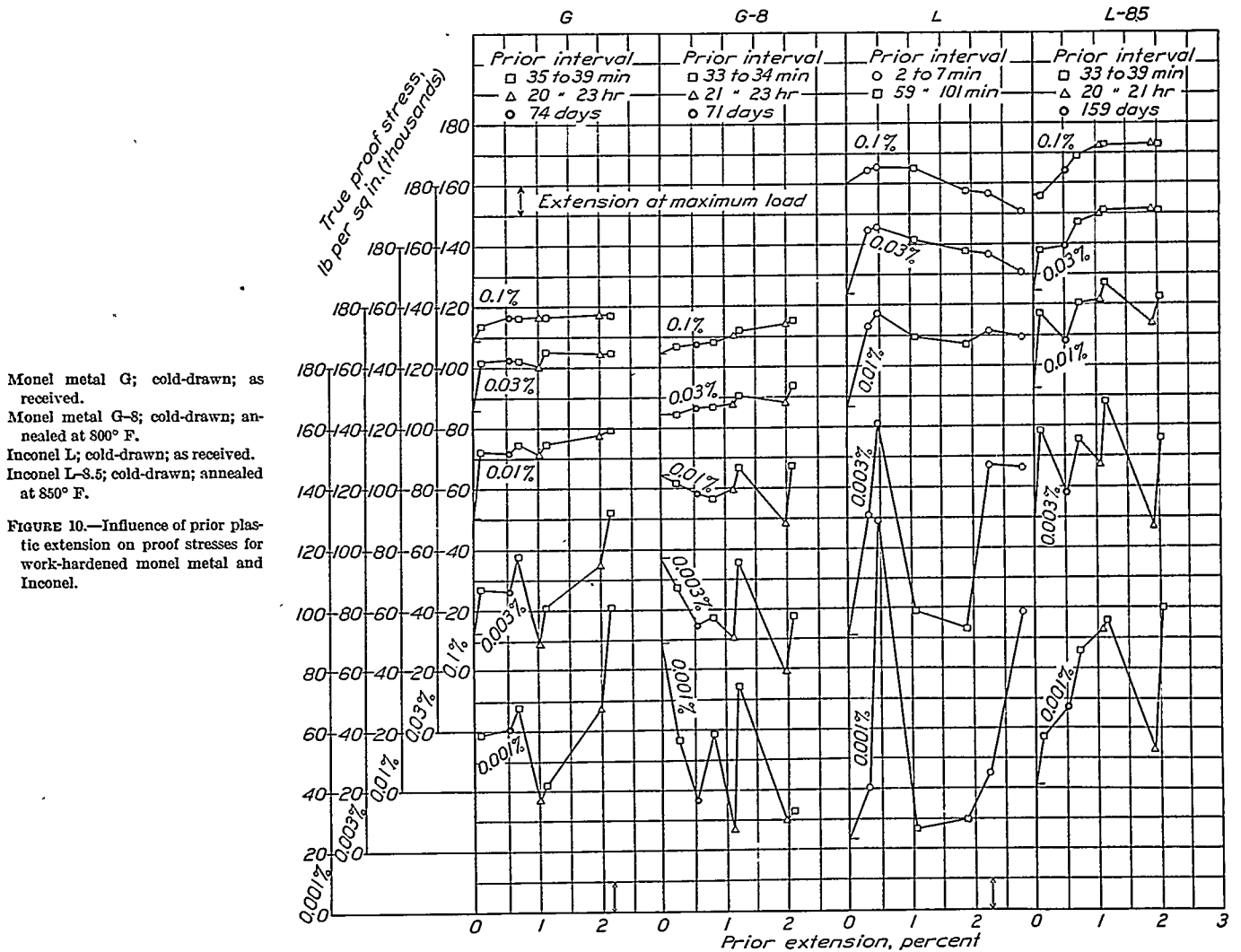
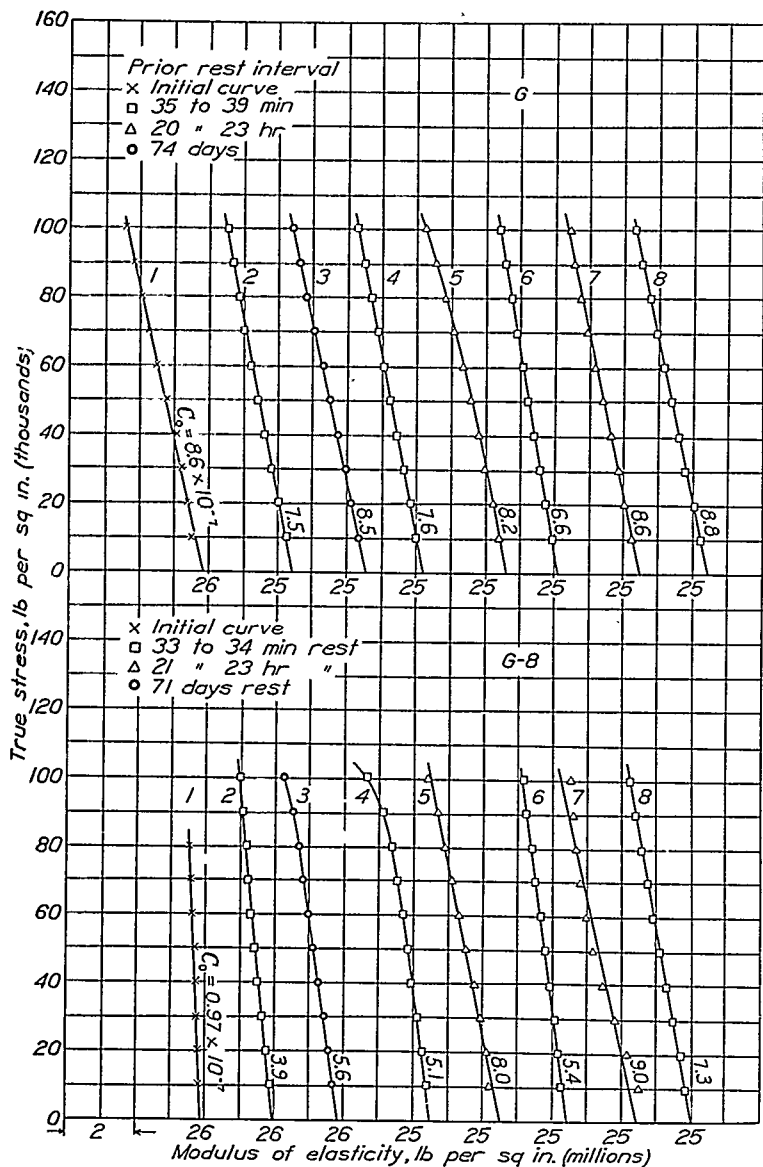


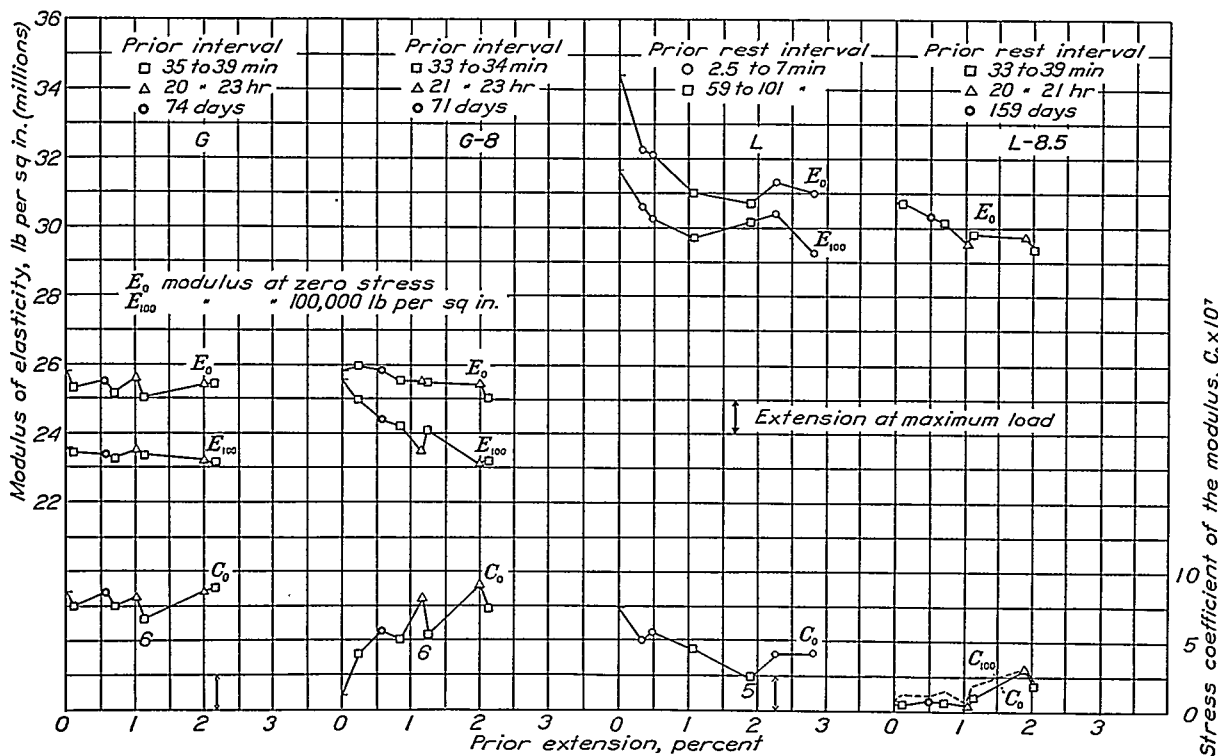
FIGURE 9.—Influence of prior plastic extension on stress-deviation and stress-set curves for work-hardened monel metal.

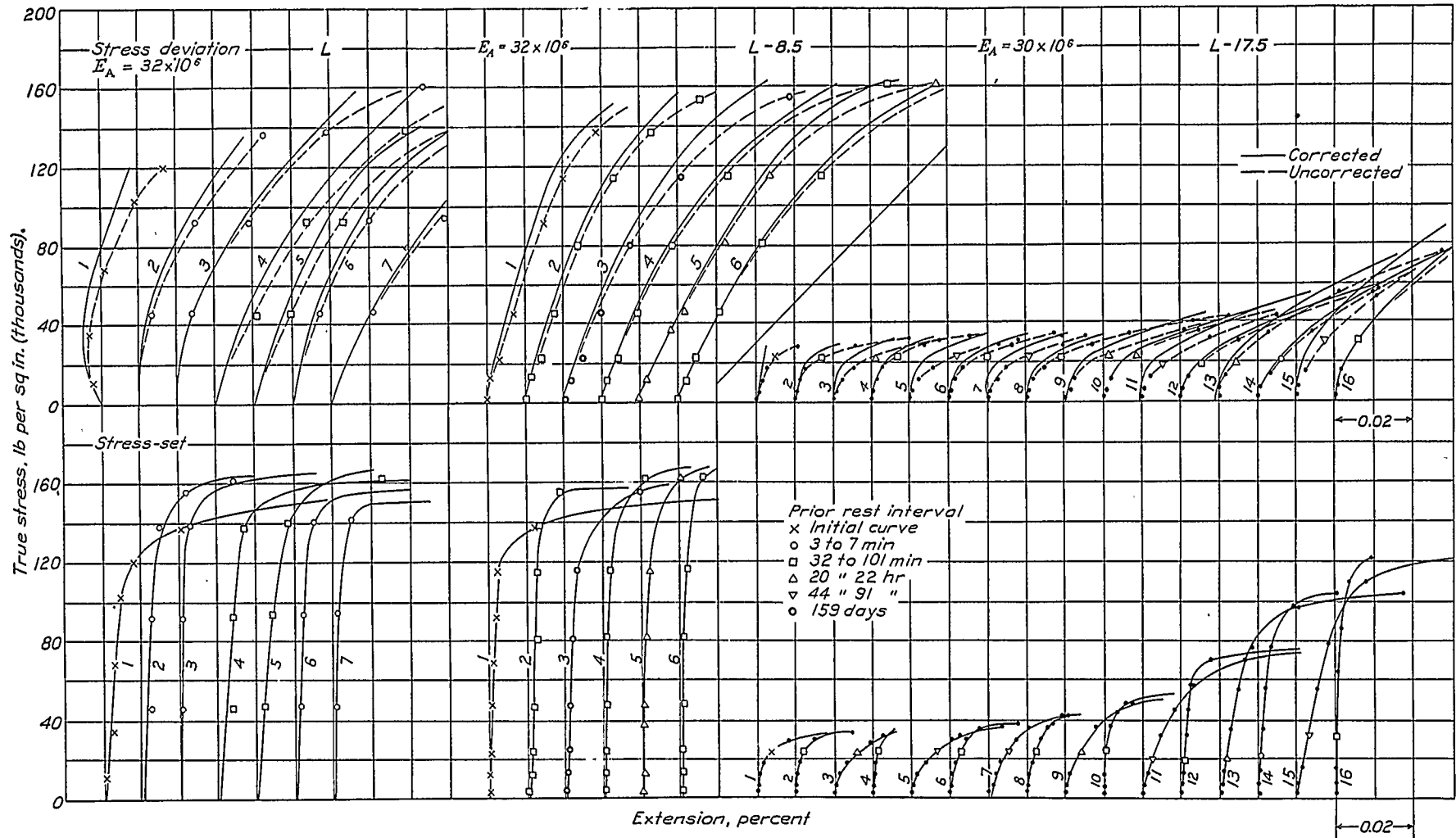




Monel metal G; cold-drawn; as received.  
 Monel metal G-8; cold-drawn; annealed at 800° F.  
 FIGURE 11.—Influence of prior plastic extension on the stress-modulus line for work-hardened monel metal.

Monel metal G; cold-drawn; as received.  
 Monel metal G-8; cold-drawn; annealed at 800° F.  
 Inconel L; cold-drawn; as received.  
 Inconel L-8.5; cold-drawn; annealed at 850° F.  
 FIGURE 12.—Influence of prior plastic extension on the modulus of elasticity and on its stress coefficient for work-hardened monel metal and Inconel.





Inconel L; cold-drawn; as received.  
 Inconel L-8.5; cold-drawn; annealed at 850° F.  
 Inconel L-17.5; cold-drawn; annealed at 1,750° F.

FIGURE 13.—Influence of prior plastic extension on stress-deviation and stress-set curves for Inconel.

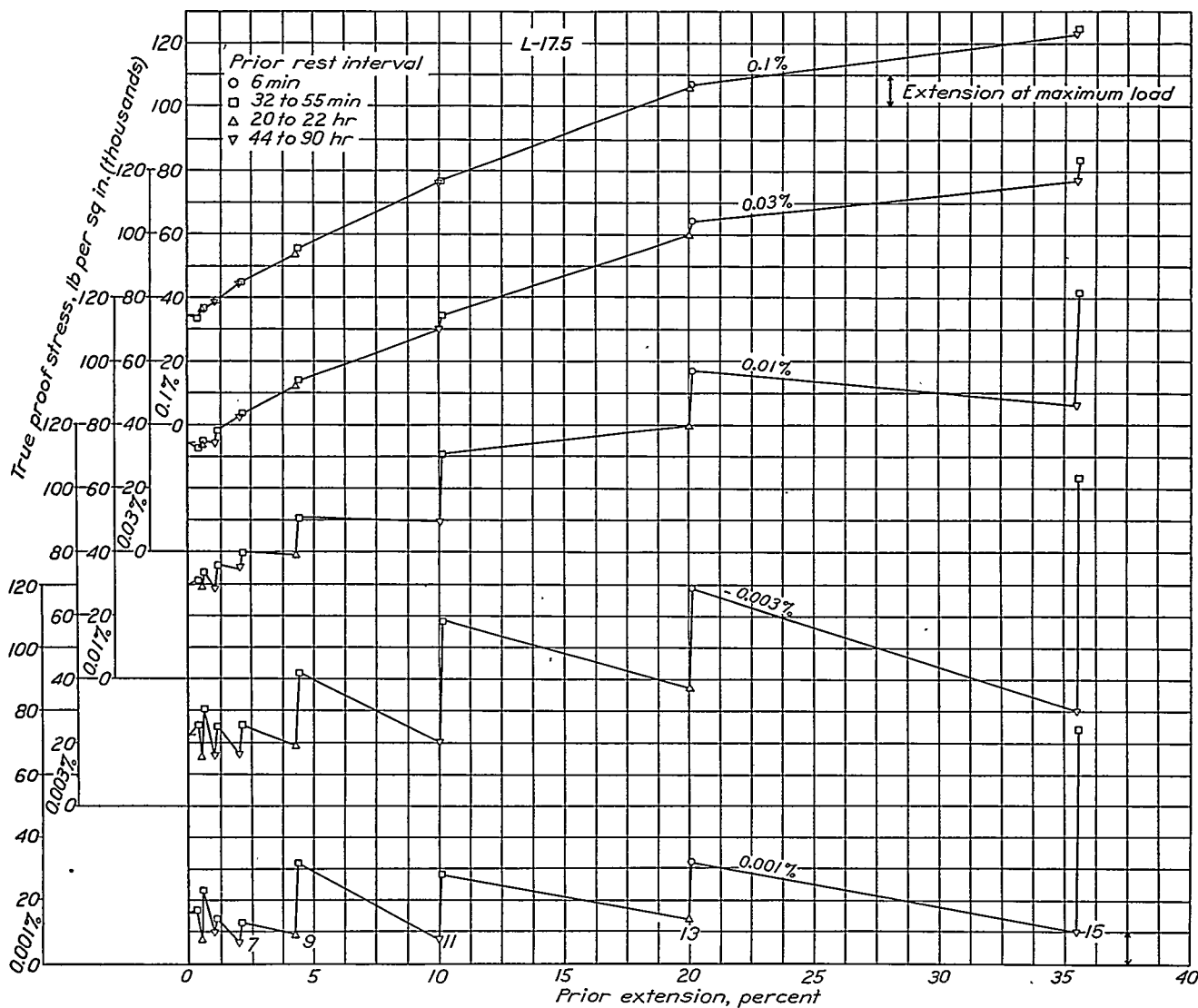
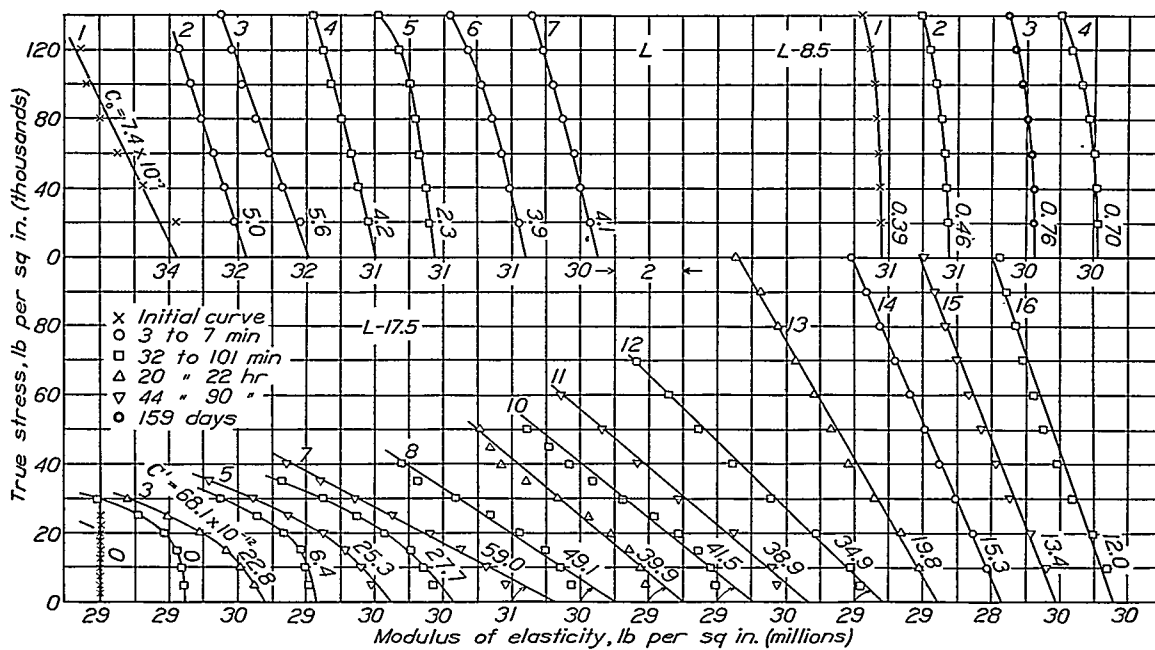


FIGURE 14.—Influence of prior plastic extension on proof stresses for Inconel L-17.5; cold-drawn; annealed at 1,750° F.



Inconel L; cold-drawn; as received.

Inconel L-8.5; cold-drawn; annealed at 850° F.

Inconel L-17.5; cold-drawn; annealed at 1,750° F.

FIGURE 15.—Influence of prior plastic extension on the stress-modulus line for Inconel.

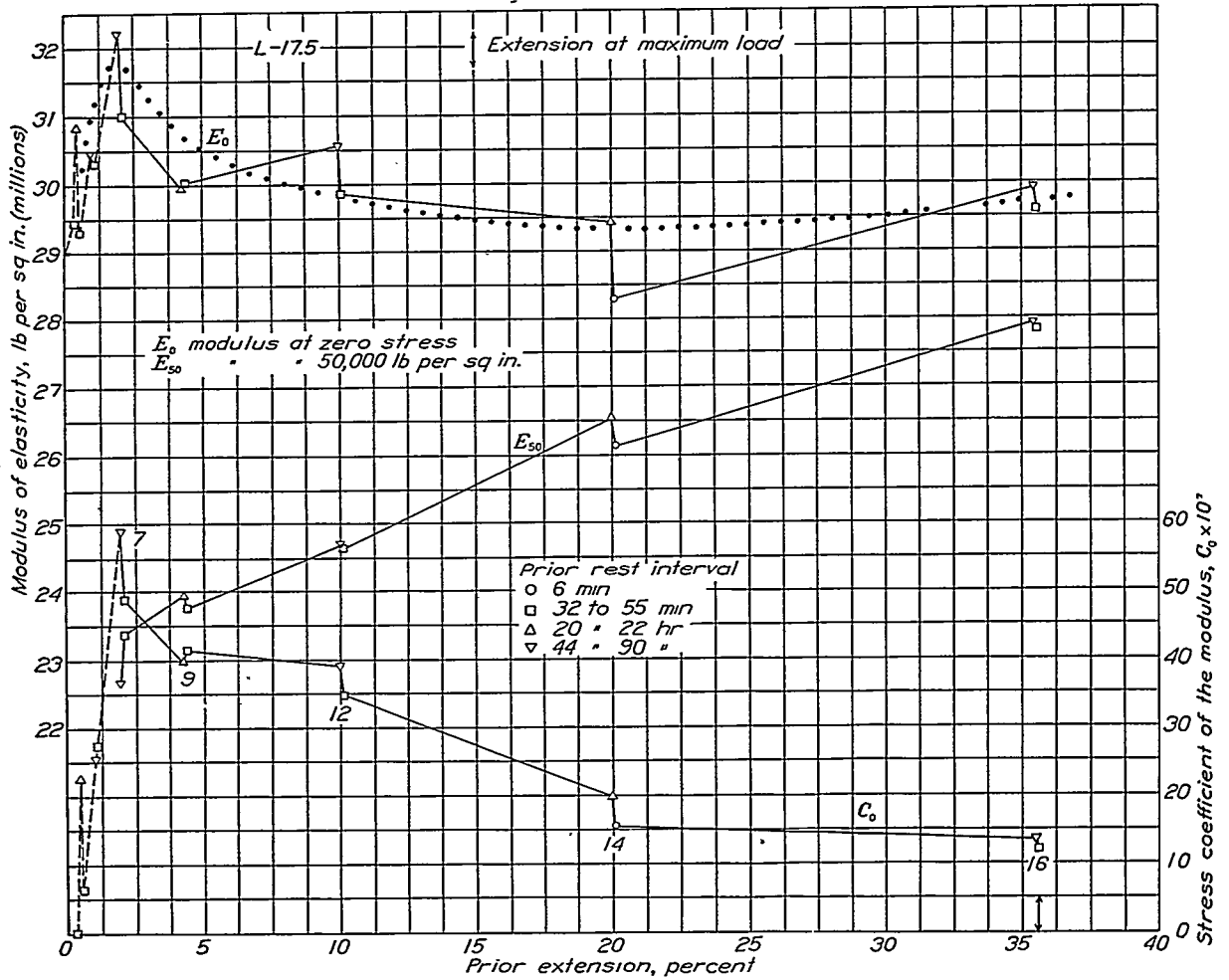
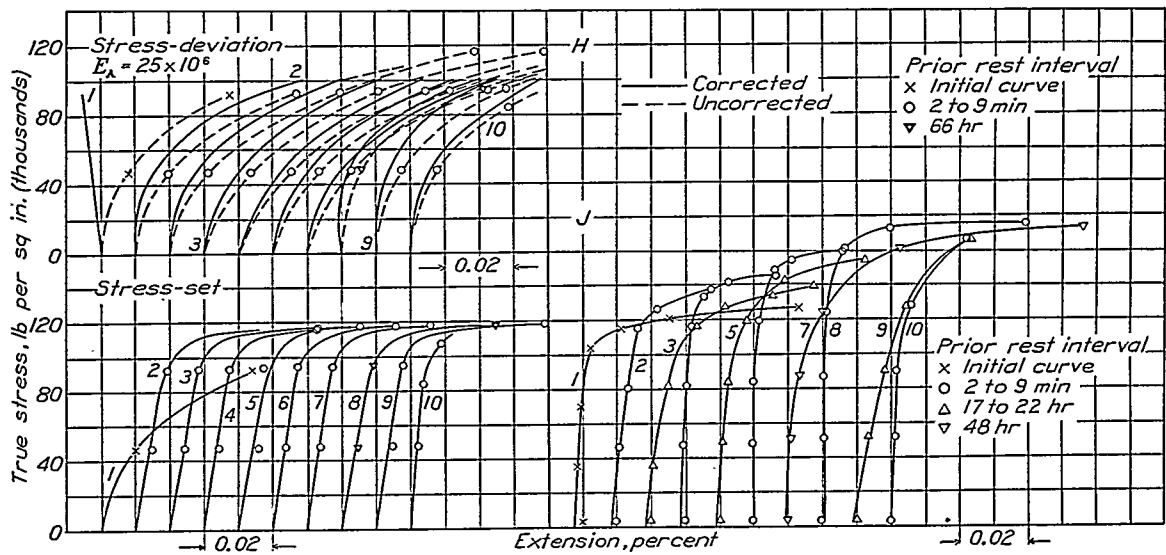
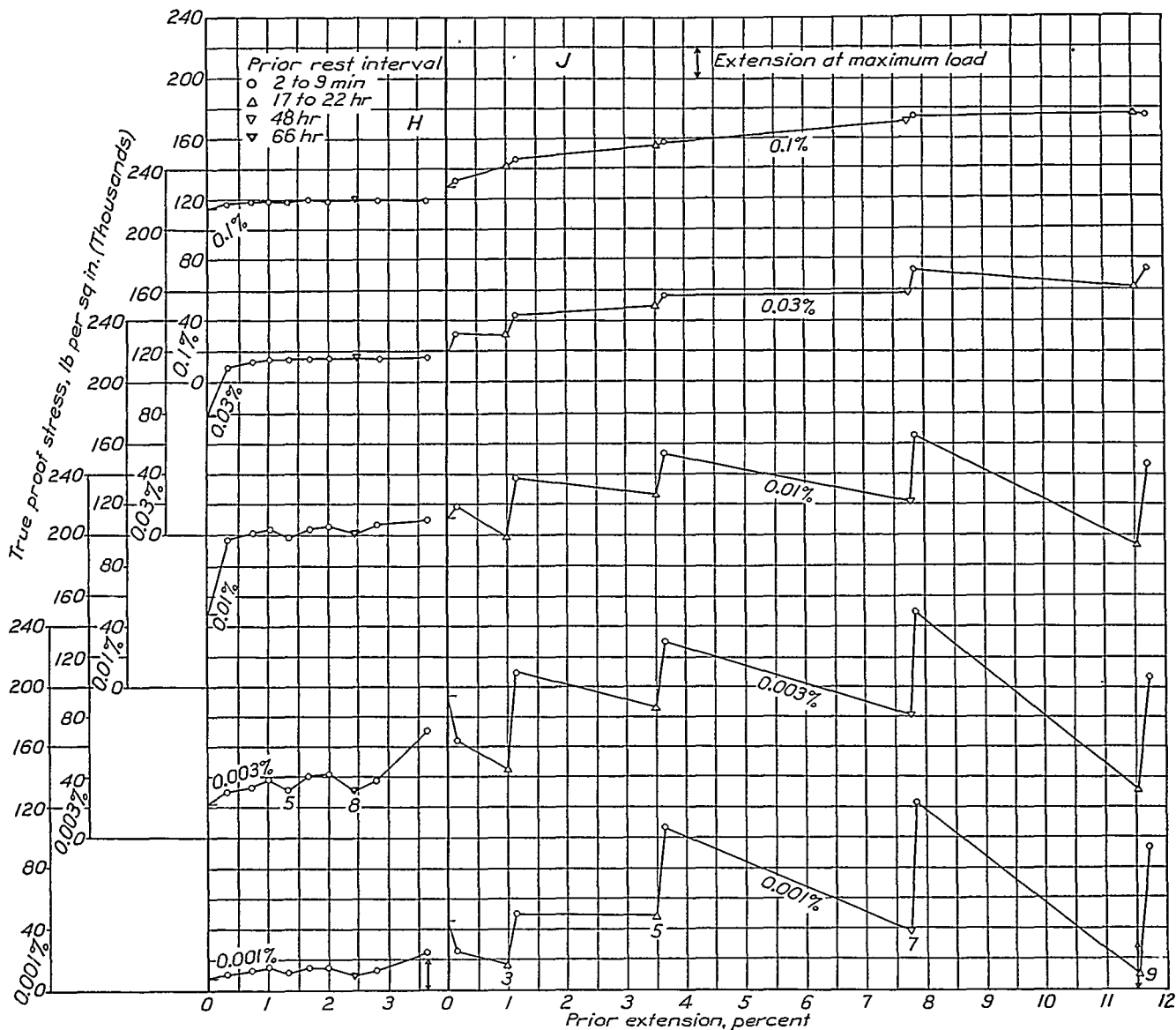


FIGURE 16.—Influence of prior plastic extension on the modulus of elasticity and on its stress coefficient for Inconel L-17.5; cold-drawn; annealed at 1,750° F.



Aluminum-monel metal H; quenched and cold-drawn.  
Aluminum-monel metal J; quenched, cold-drawn, and tempered.

FIGURE 17.—Influence of prior plastic extension on stress-deviation and stress-set curves for aluminum-monel metal.



Aluminum-monel metal H; quenched and cold-drawn.  
 Aluminum-monel metal J; quenched, cold-drawn, and tempered.

FIGURE 18.—Influence of prior plastic extension on proof stresses for aluminum-monel metal.

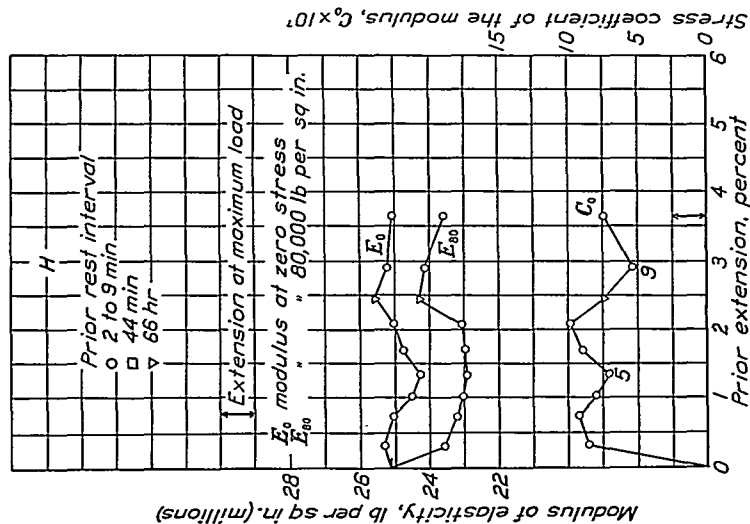
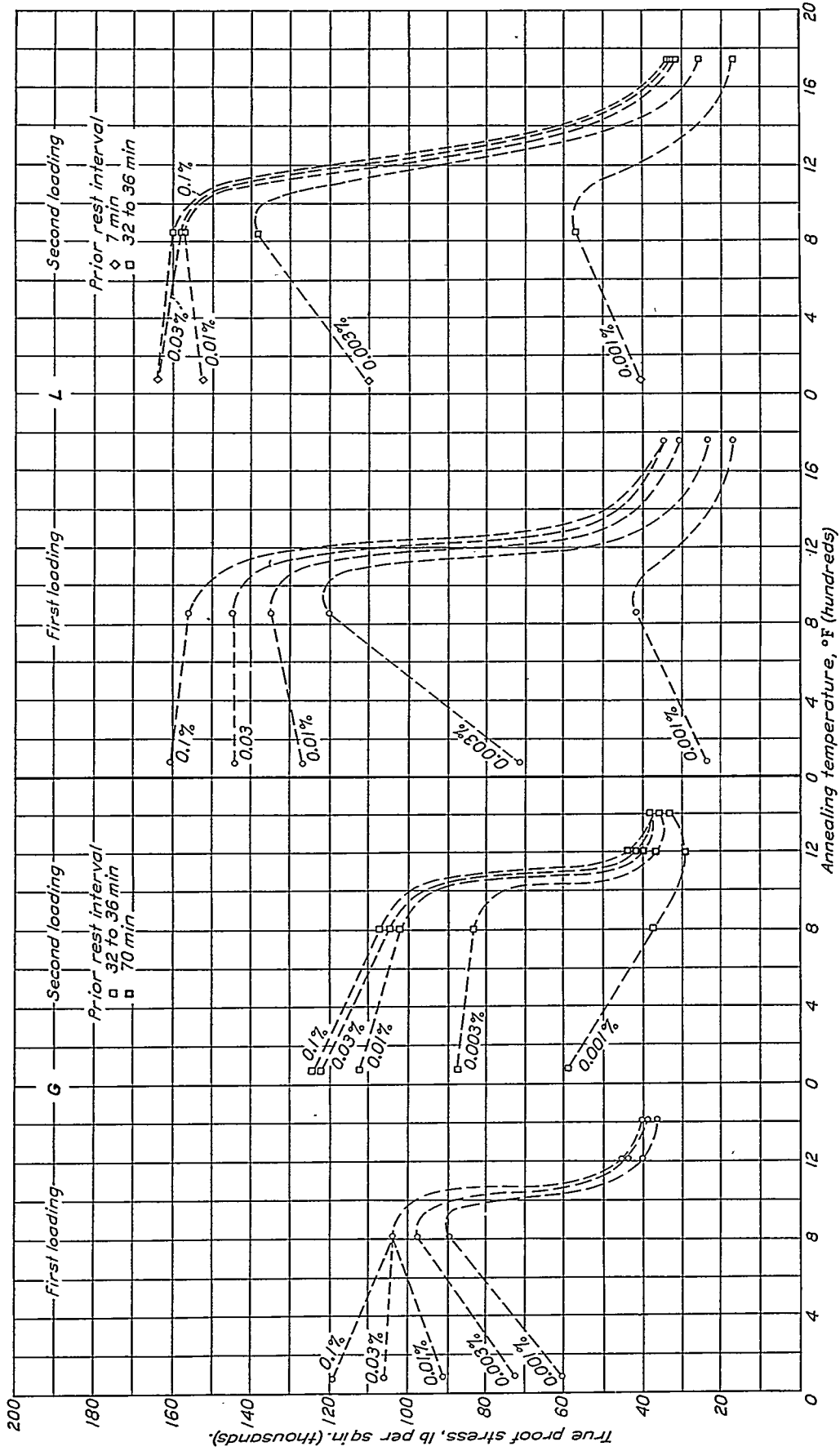


FIGURE 19.—Influence of prior plastic extension on the modulus of elasticity and on its stress coefficient for aluminum-monel metal H; quenched and cold-drawn.



Monel metal G; annealing time at 800° F, 5 hr.; at 1,200° and 1,400° F, 2 hr.  
 Inconel L; annealing time 2 to 2½ hr.

Figure 20.—Influence of annealing temperature on proof stresses for monel metal and Inconel; cold-drawn; annealed at indicated temperatures.

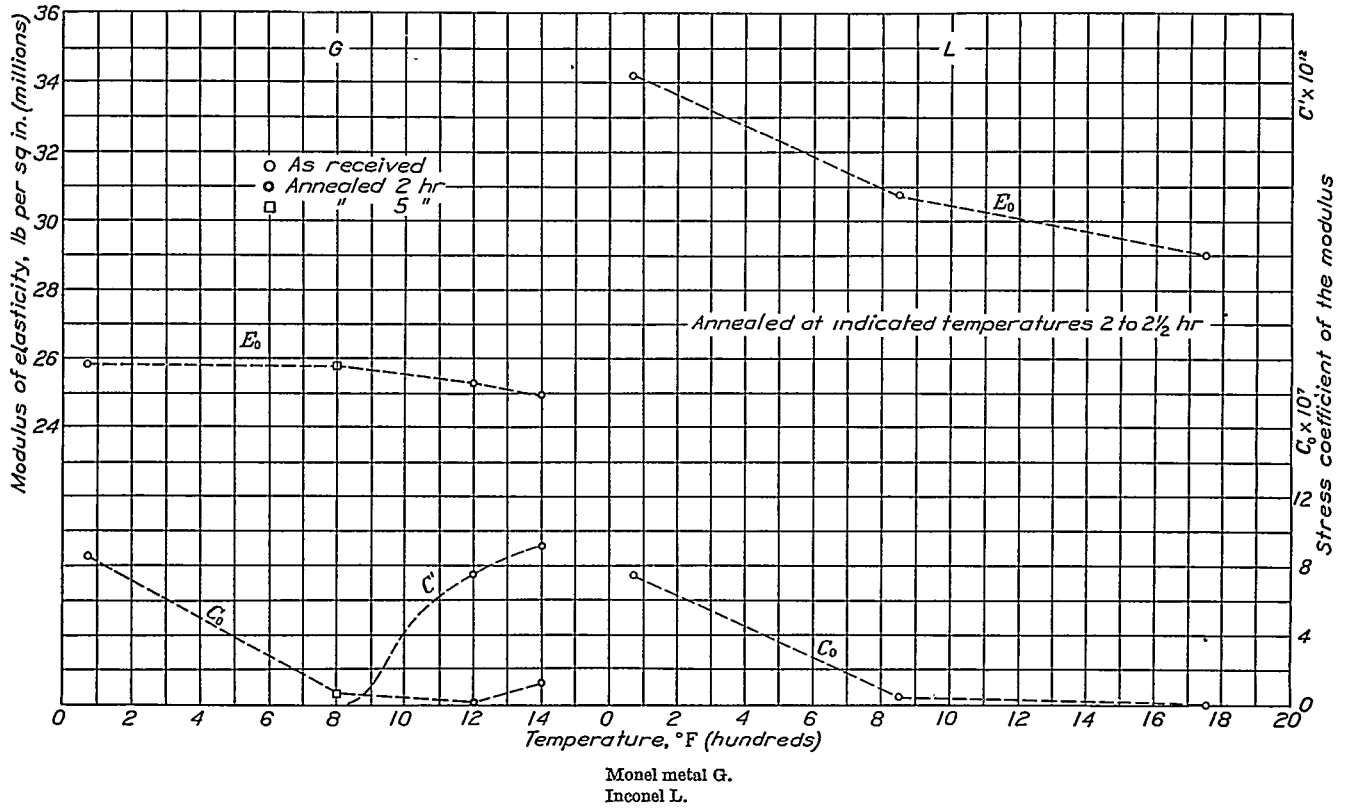


FIGURE 21.—Influence of annealing temperature on the modulus of elasticity and on its stress coefficient for monel metal and Inconel; cold-drawn; annealed at indicated temperatures.

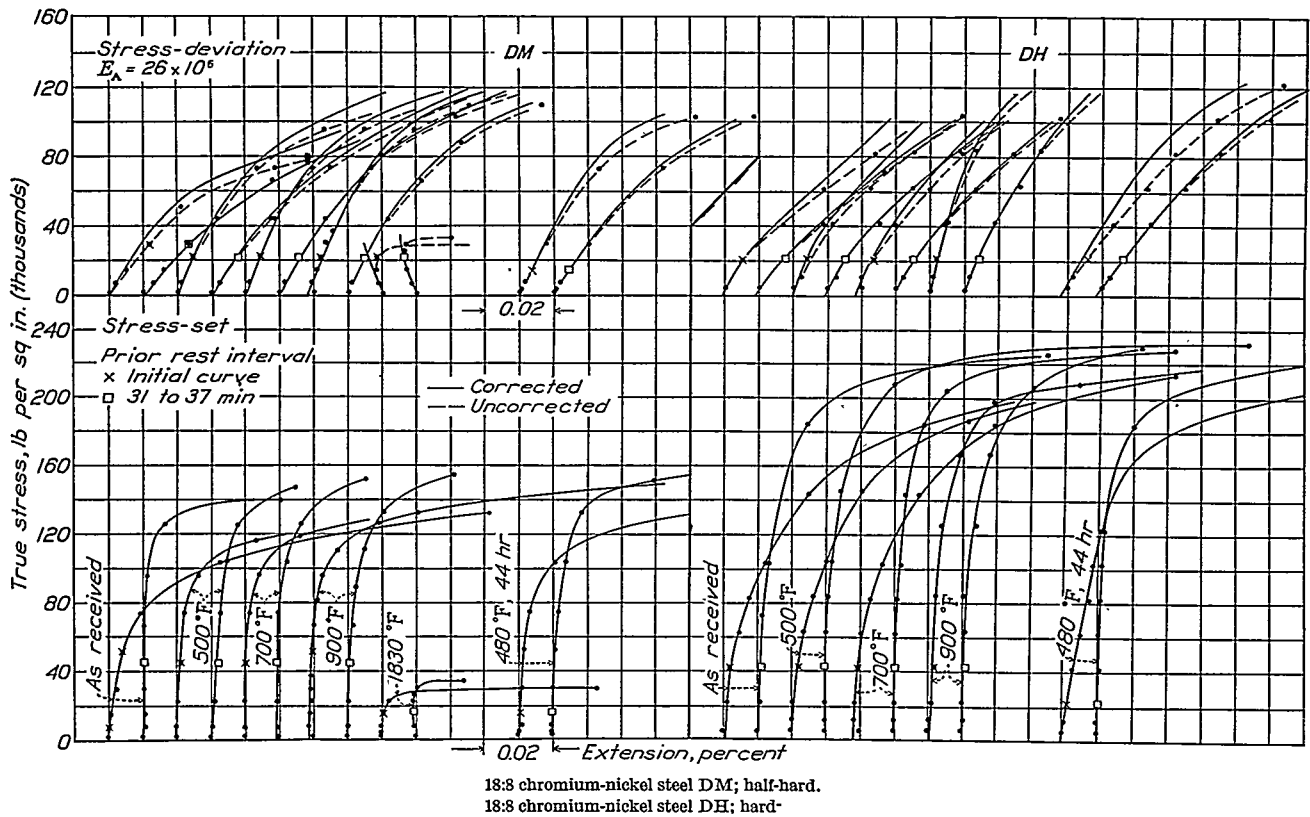
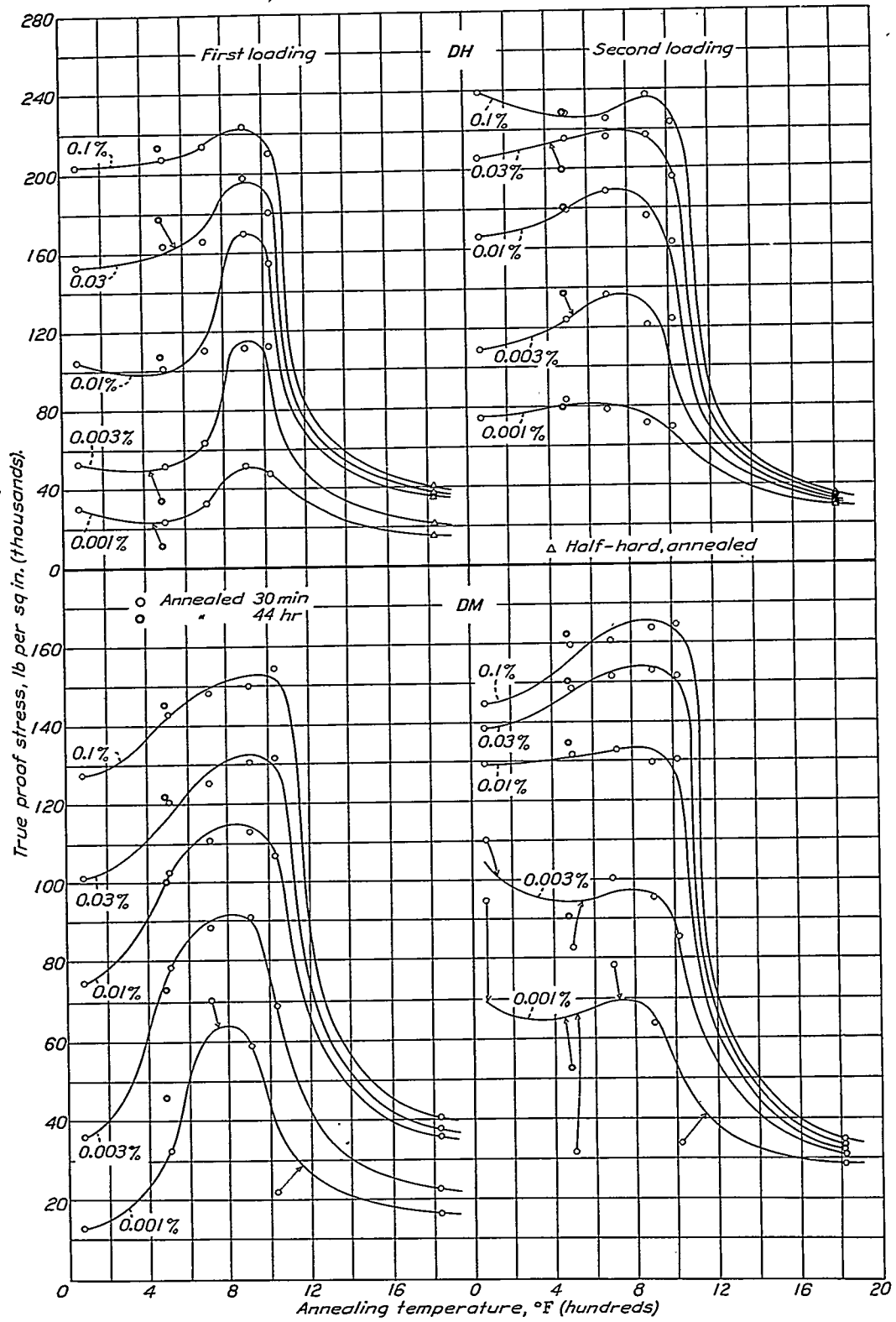


FIGURE 22.—Influence of annealing temperature on stress-deviation and stress-set curves for 18:8 chromium-nickel steel; cold-drawn; annealed at indicated temperatures.



18:8 chromium-nickel steel DH; hard.  
 18:8 chromium-nickel steel DM; half-hard.

FIGURE 23.—Influence of annealing temperature on proof stresses for 18:8 chromium-nickel steel; cold-drawn; annealed at indicated temperatures. The rest interval between first and second loading ranges from 31 to 37 minutes.

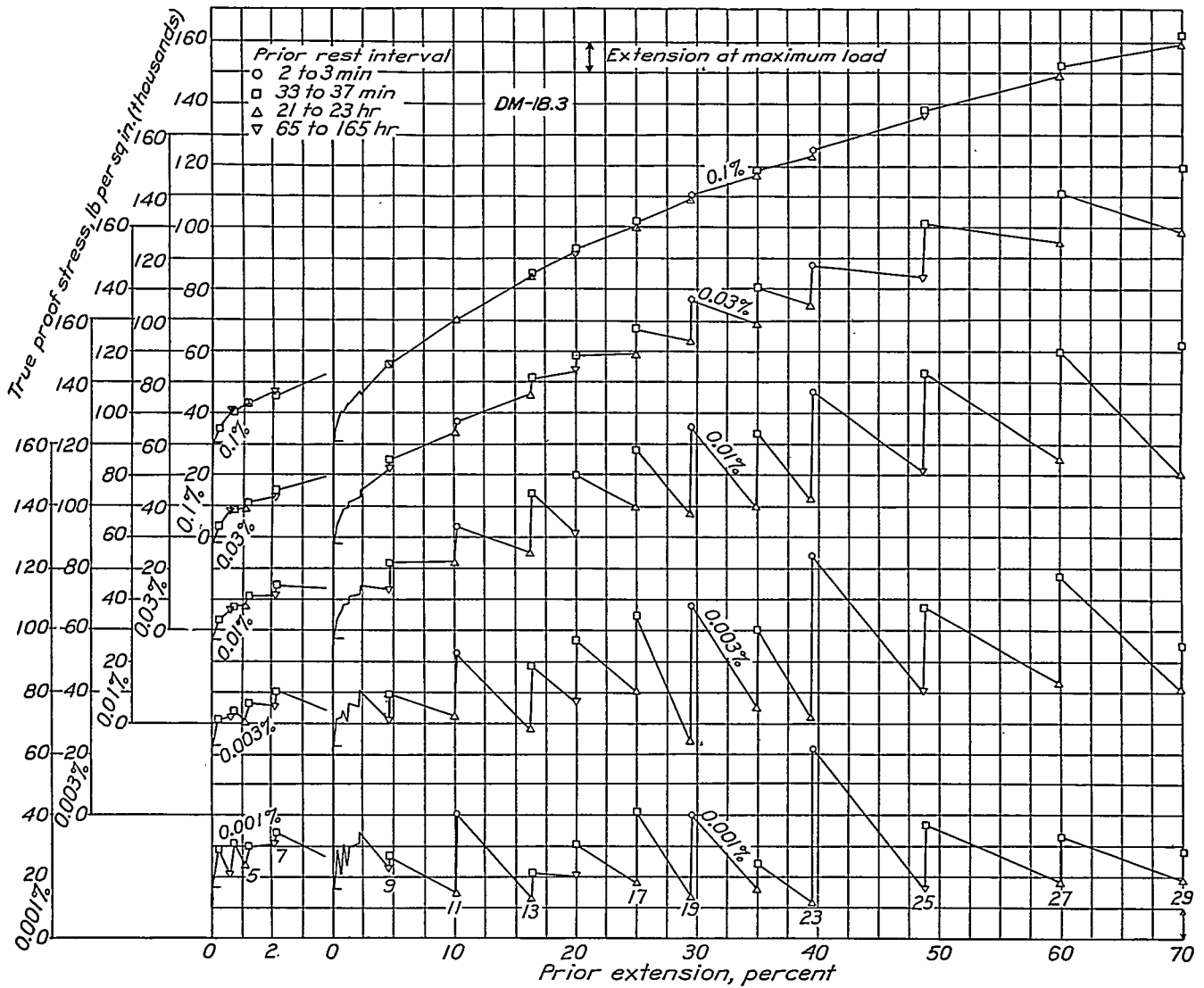
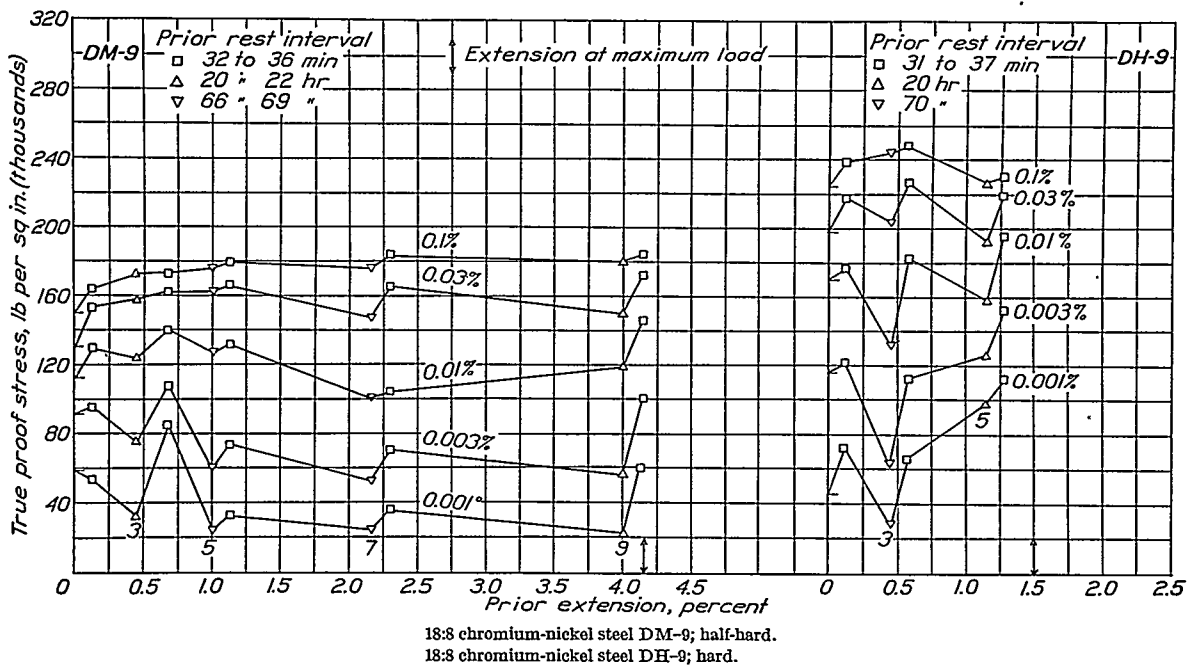


FIGURE 24.—Influence of prior plastic extension on proof stresses for 18:8 chromium-nickel steel DM-18.3; cold-drawn; annealed at 1,830° F.



18:8 chromium-nickel steel DM-9; half-hard.  
18:8 chromium-nickel steel DH-9; hard.

FIGURE 25.—Influence of prior plastic extension on proof stresses for 18:8 chromium-nickel steel; cold-drawn; annealed at 900° F. for relief of internal stress.

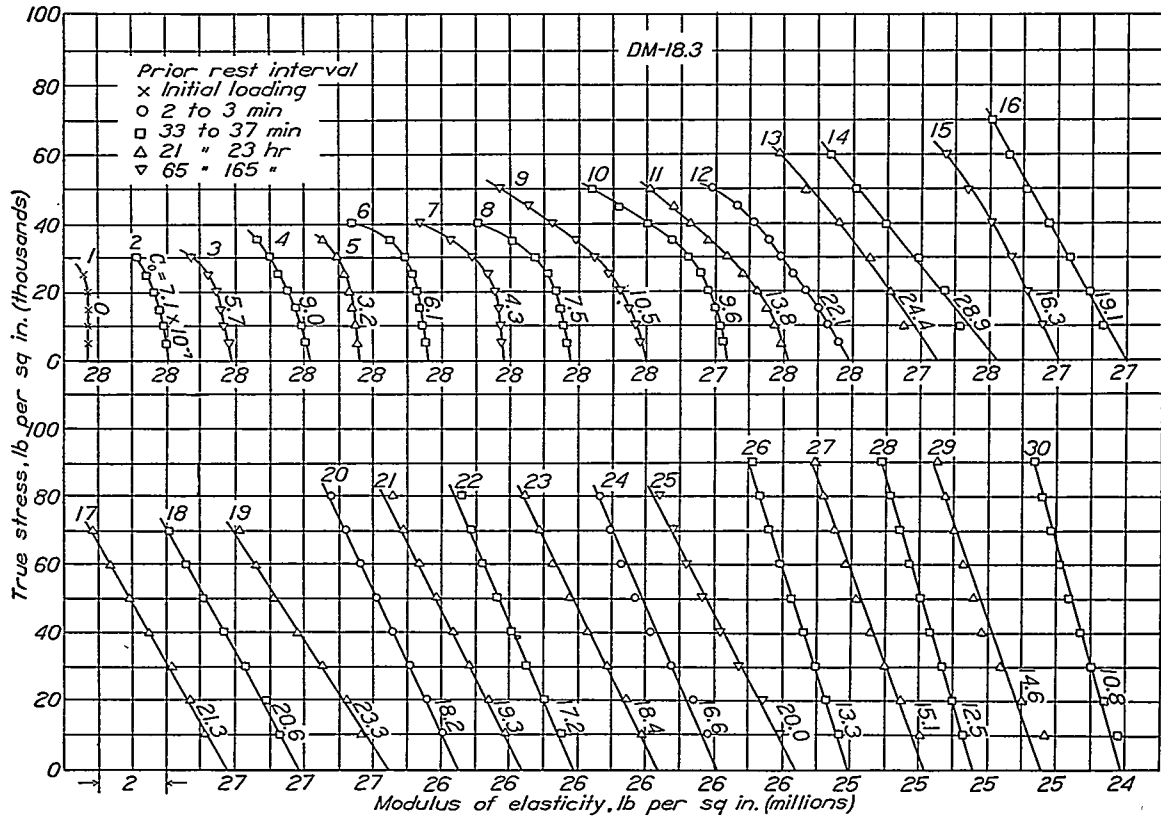


FIGURE 26.—Influence of prior plastic extension on the stress-modulus line for 18:8 chromium-nickel steel DM-18.3; cold-drawn; annealed at 1,830° F.

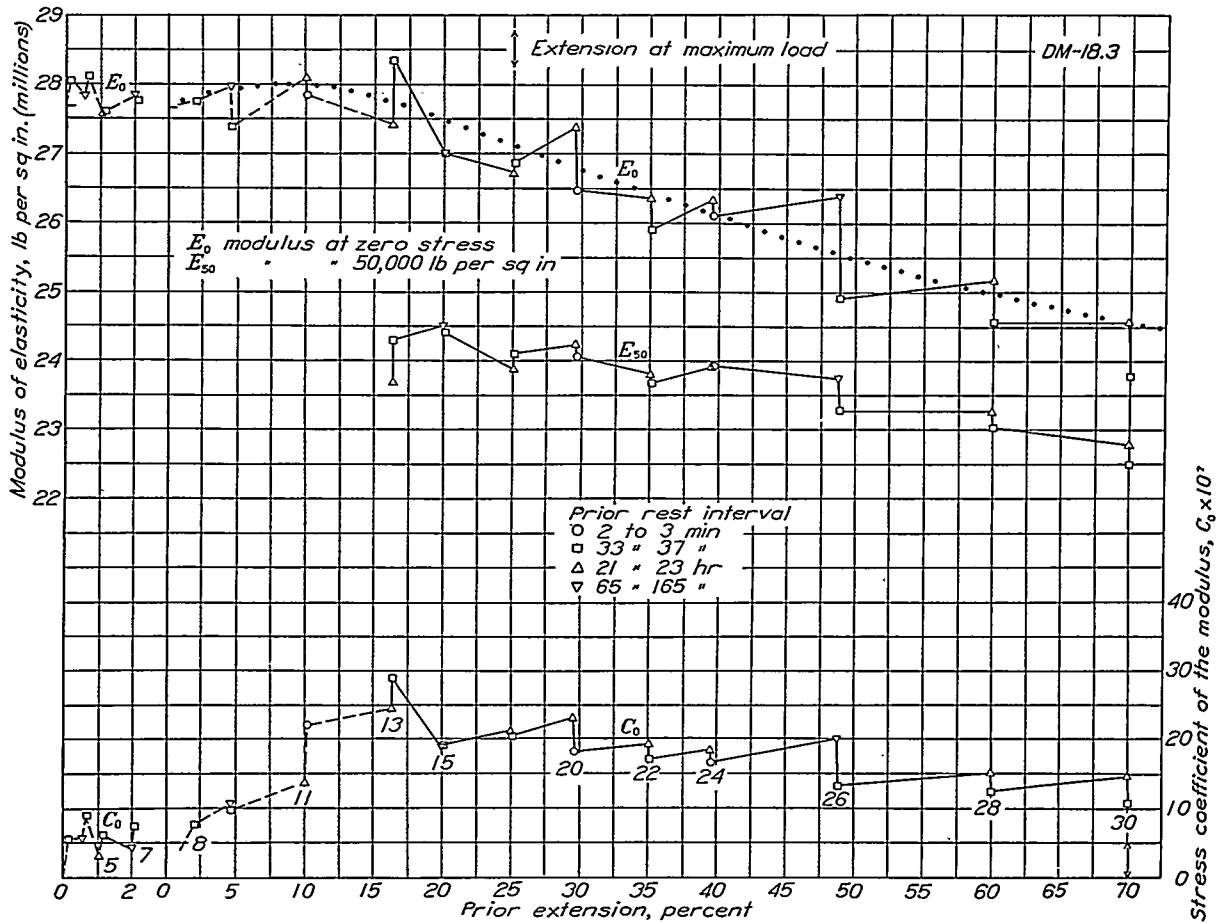


FIGURE 27.—Influence of prior plastic extension on the modulus of elasticity and on its stress coefficient for 18:8 chromium-nickel steel DM-18.3; cold-drawn; annealed at 1,830° F.

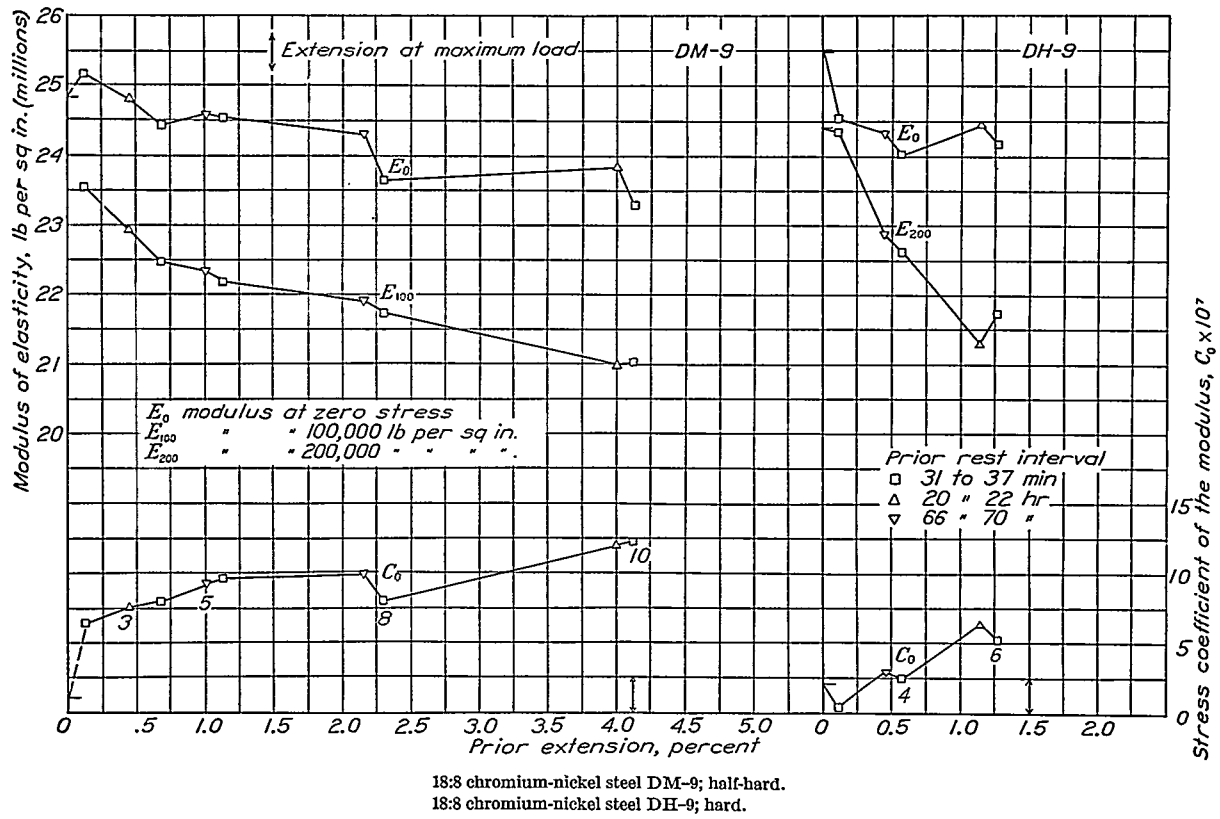


FIGURE 28.—Influence of prior plastic extension on the modulus of elasticity and on its stress coefficient for 18:8 chromium-nickel steel; cold-drawn; annealed at 900° F. for relief of internal stress.

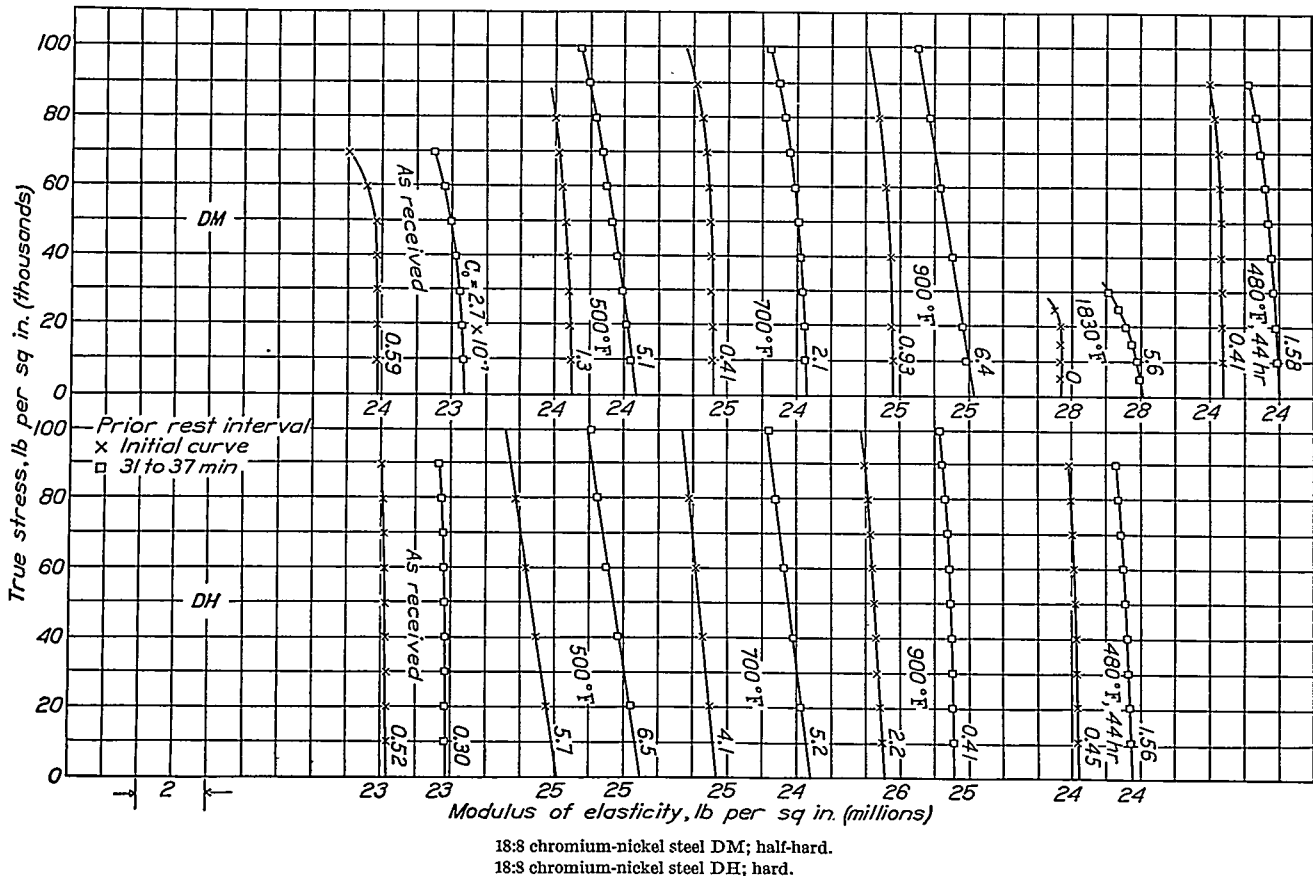


FIGURE 29.—Influence of annealing temperature on stress-modulus curves for 18:8 chromium-nickel steel; cold-drawn; annealed at indicated temperatures.  
407300°—41—25

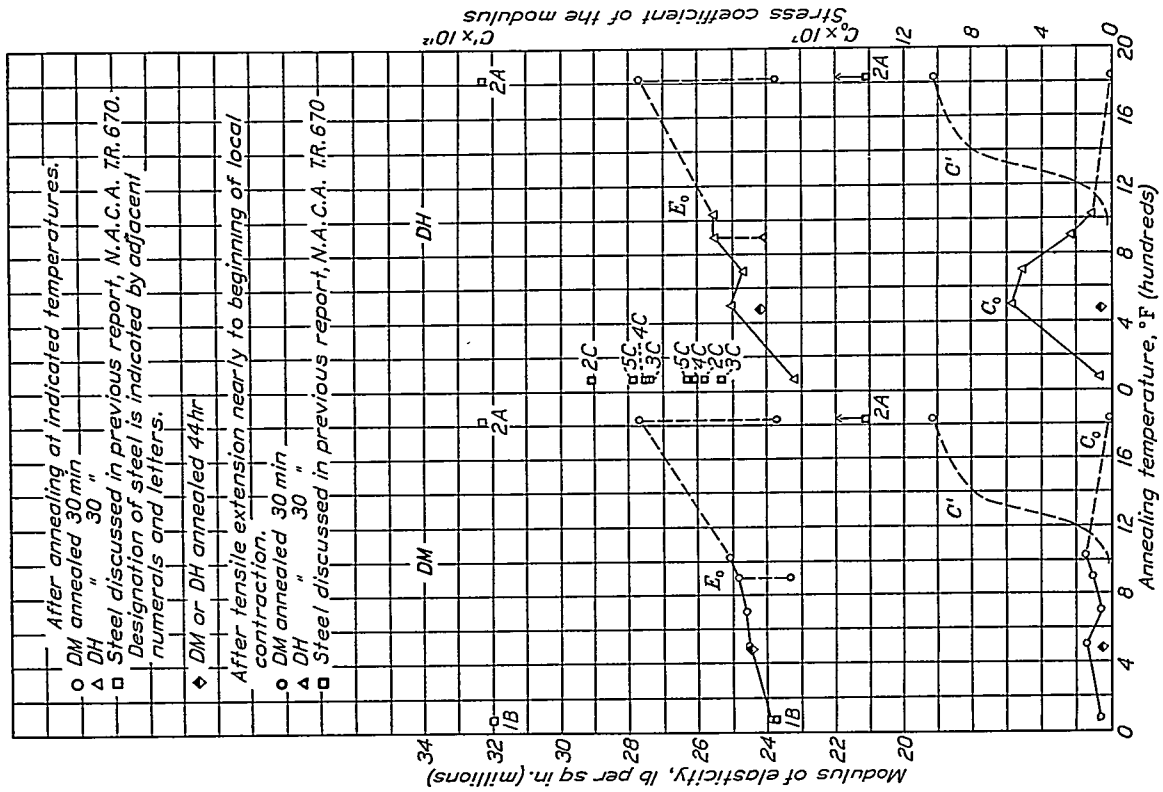


FIGURE 30.—Assembled data on the influence of plastic deformation and annealing temperature on the modulus of elasticity and on its stress coefficient for 188 chromium-nickel steel; cold-drawn. These values are each obtained from the first loading curve of a pair of curves.

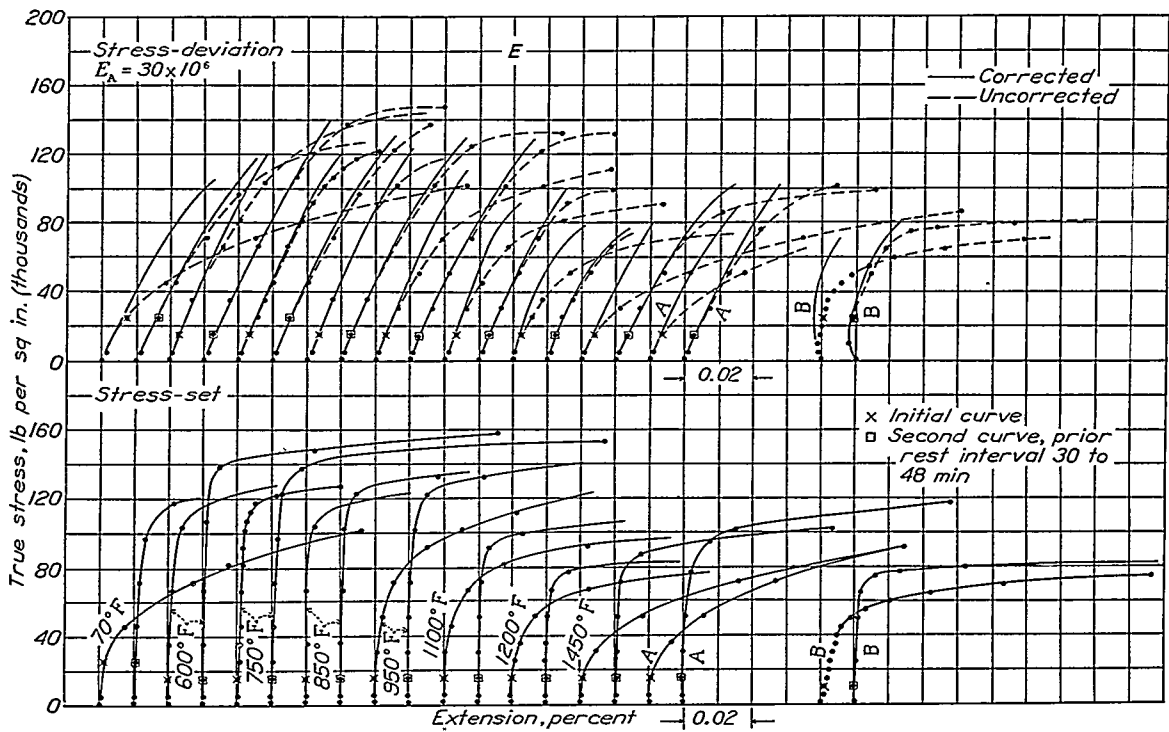


FIGURE 31.—Influence of tempering temperature on stress-deviation and stress-set curves for 13.2 chromium-nickel steel E; unless otherwise indicated, air-cooled from 1,760° F, tempered at indicated temperature, and furnace-cooled. Curves A are for steel furnace-cooled from 1,750° F; curves B, for steel furnace-cooled from 1,240° F by manufacturer.

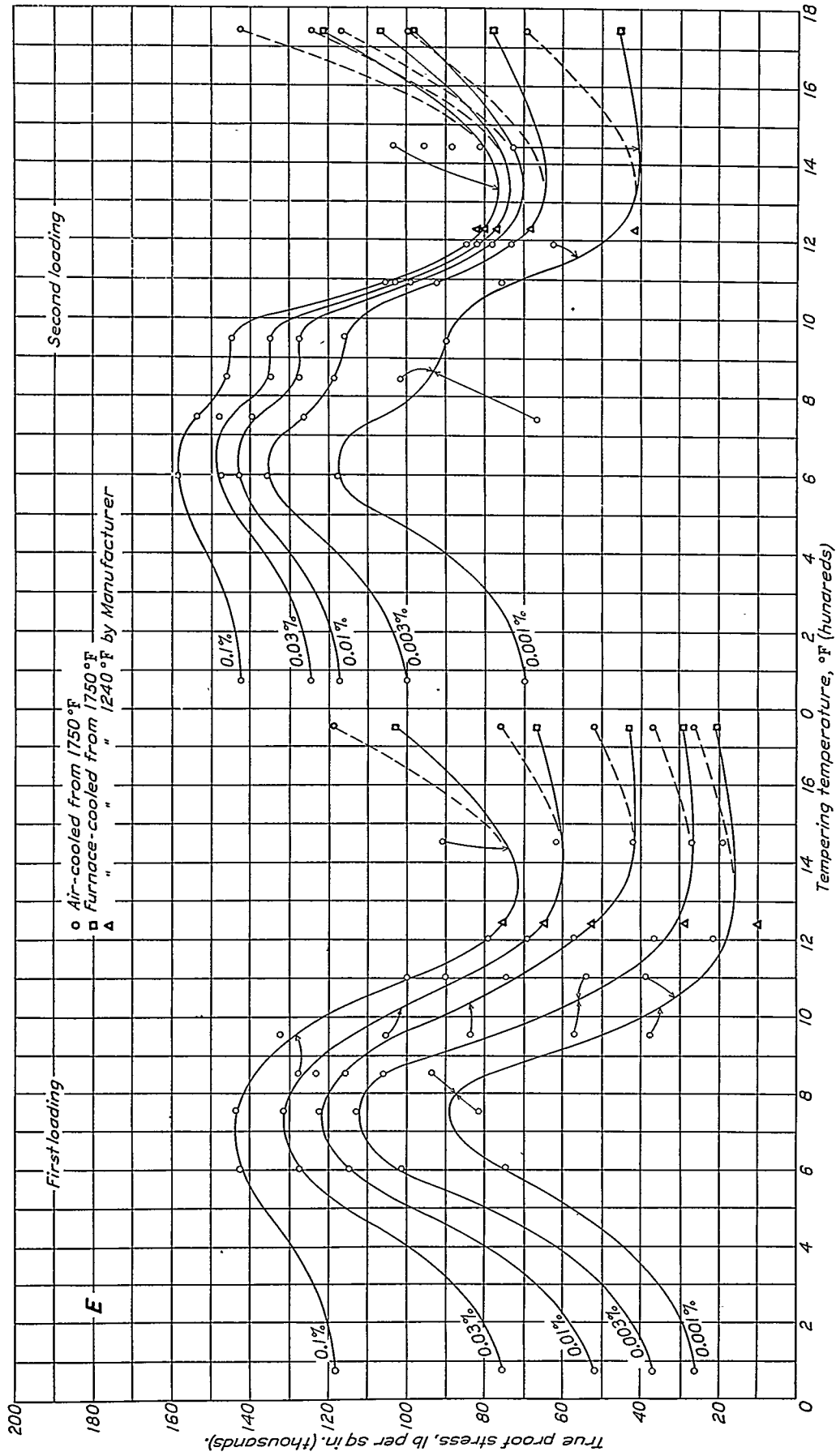


Figure 32.—Influence of tempering temperature on proof stresses for 13:2 chromium-nickel steel E; unless otherwise indicated, air-cooled from 1,750° F., tempered at indicated temperatures; and furnace-cooled; interval between first and second loading, 30 to 46 minutes.

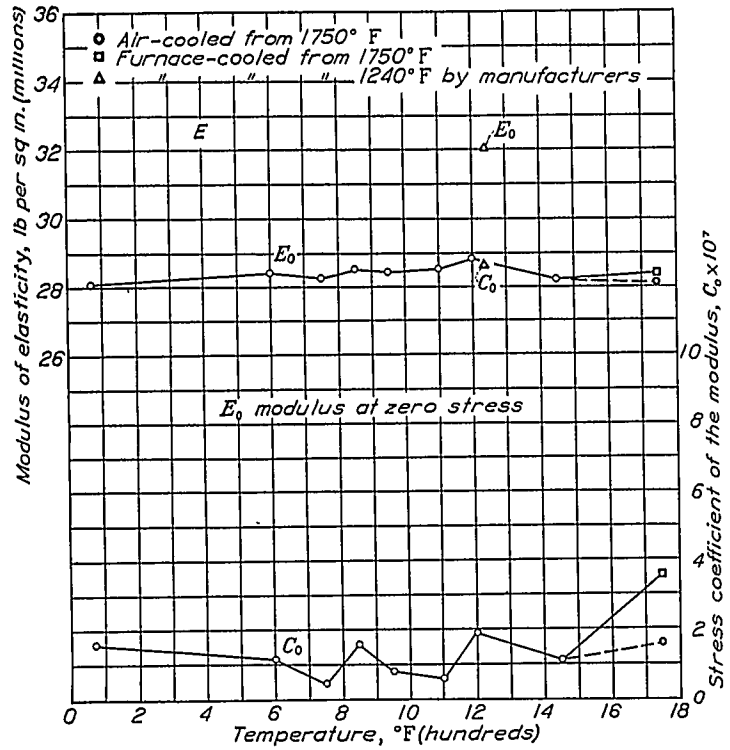


FIGURE 34.—Influence of tempering temperature on the modulus of elasticity and on its stress-coefficient for 13:2 chromium-nickel steel E; unless otherwise indicated, air-cooled from 1,750° F., tempered at indicated temperatures, and furnace-cooled. These values are obtained from the initial stress-modulus lines.  $E_0$  is the modulus at zero stress.

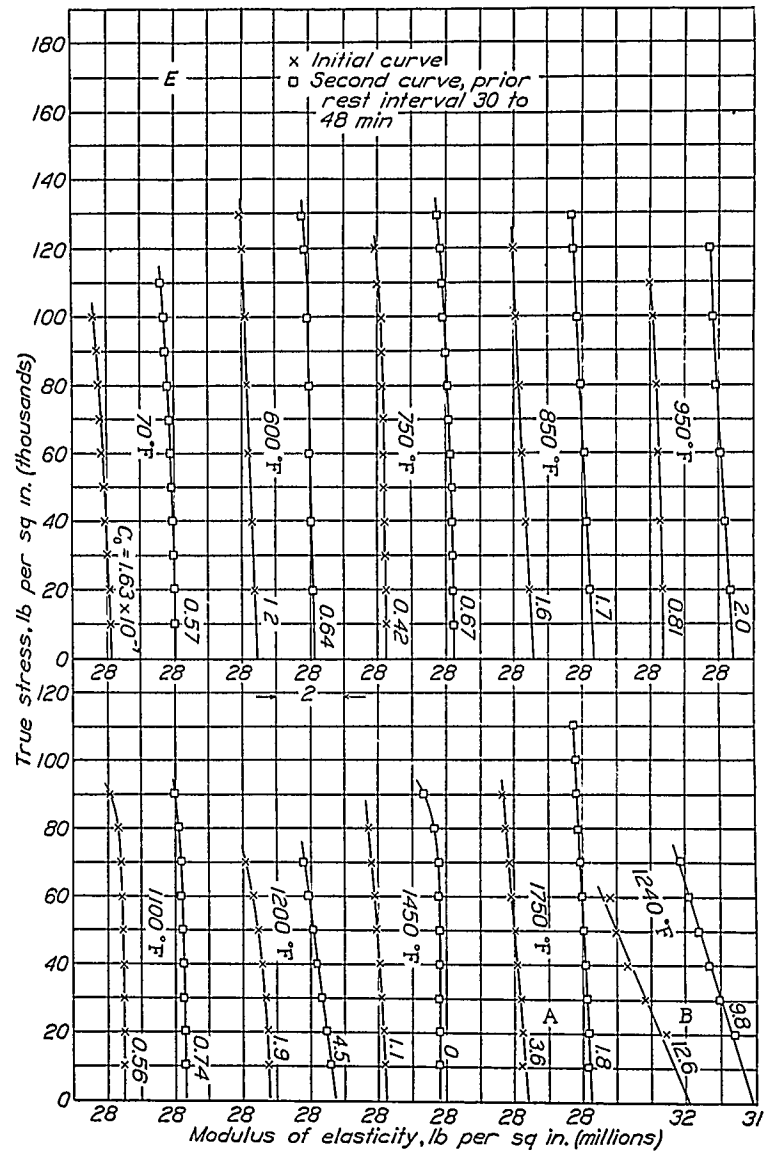


FIGURE 33.—Influence of tempering temperature on stress-modulus lines for 13:2 chromium-nickel steel E; unless otherwise indicated, air-cooled from 1,750° F, temper temperatures, and furnace-cooled. Curves A are for steel furnace-cooled from 1,750° F; curves B, for steel furnace-cooled from 1,240° F by manufacturer.

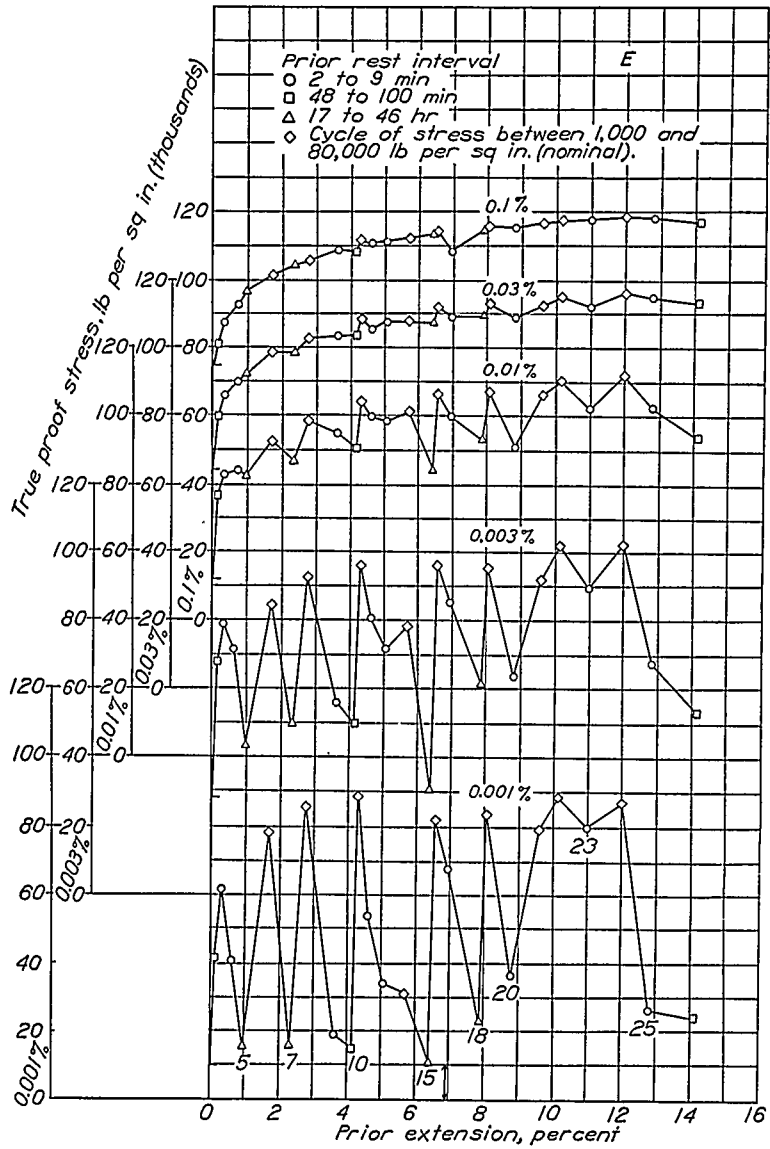


FIGURE 36.—Influence of prior plastic extension on proof stresses for 13:2 chromium-nickel steel E; as received.

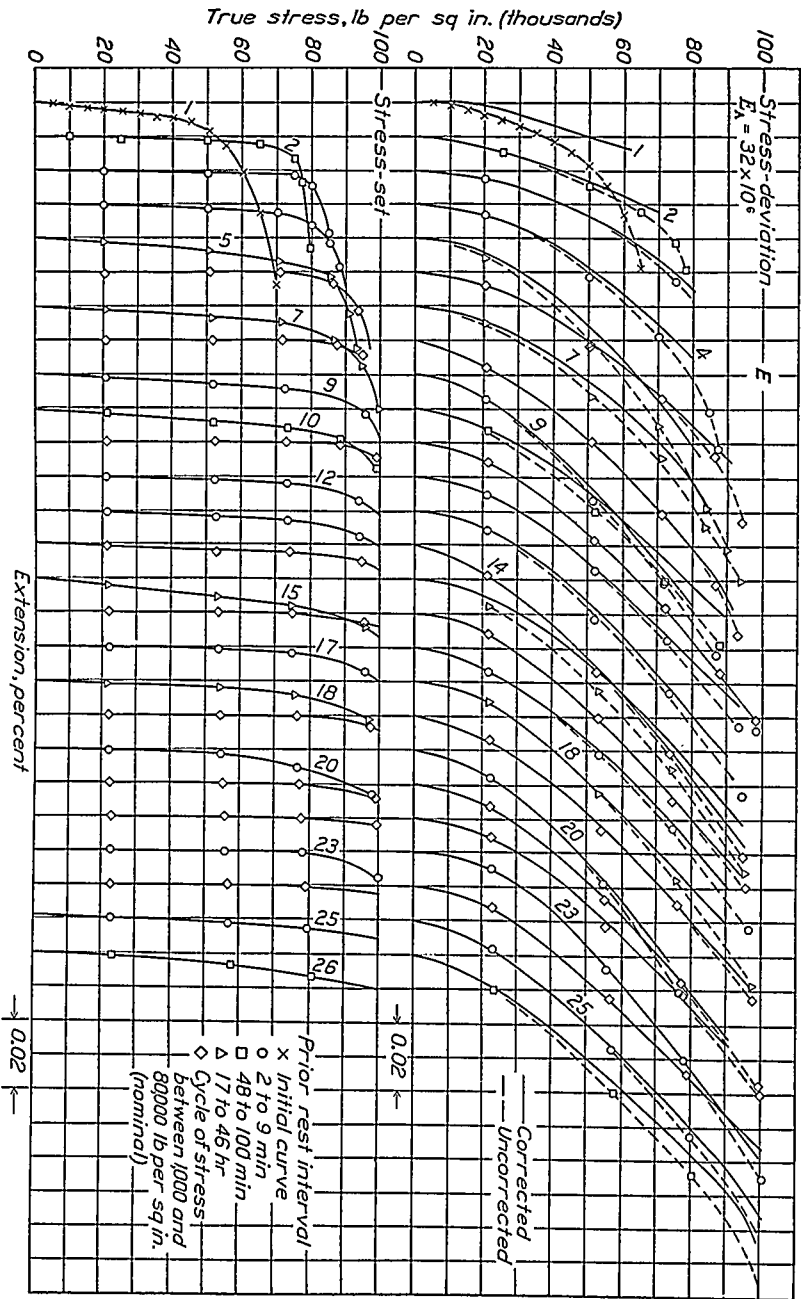


FIGURE 35.—Influence of prior plastic extension on stress-deviation and stress-set curves for 13:2 chromium-nickel steel E; as received.

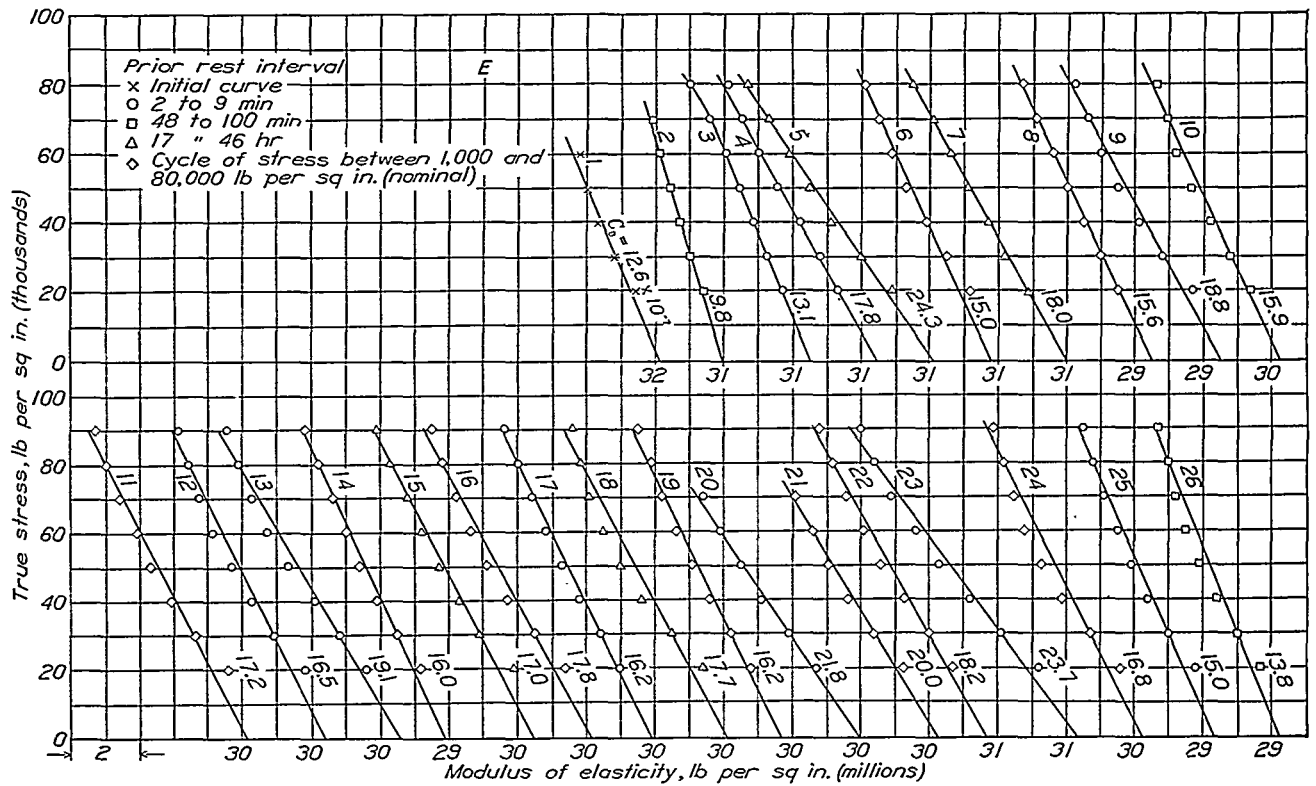


FIGURE 37.—Influence of prior plastic extension on the stress-modulus line for 13:2 chromium-nickel steel E; as received.

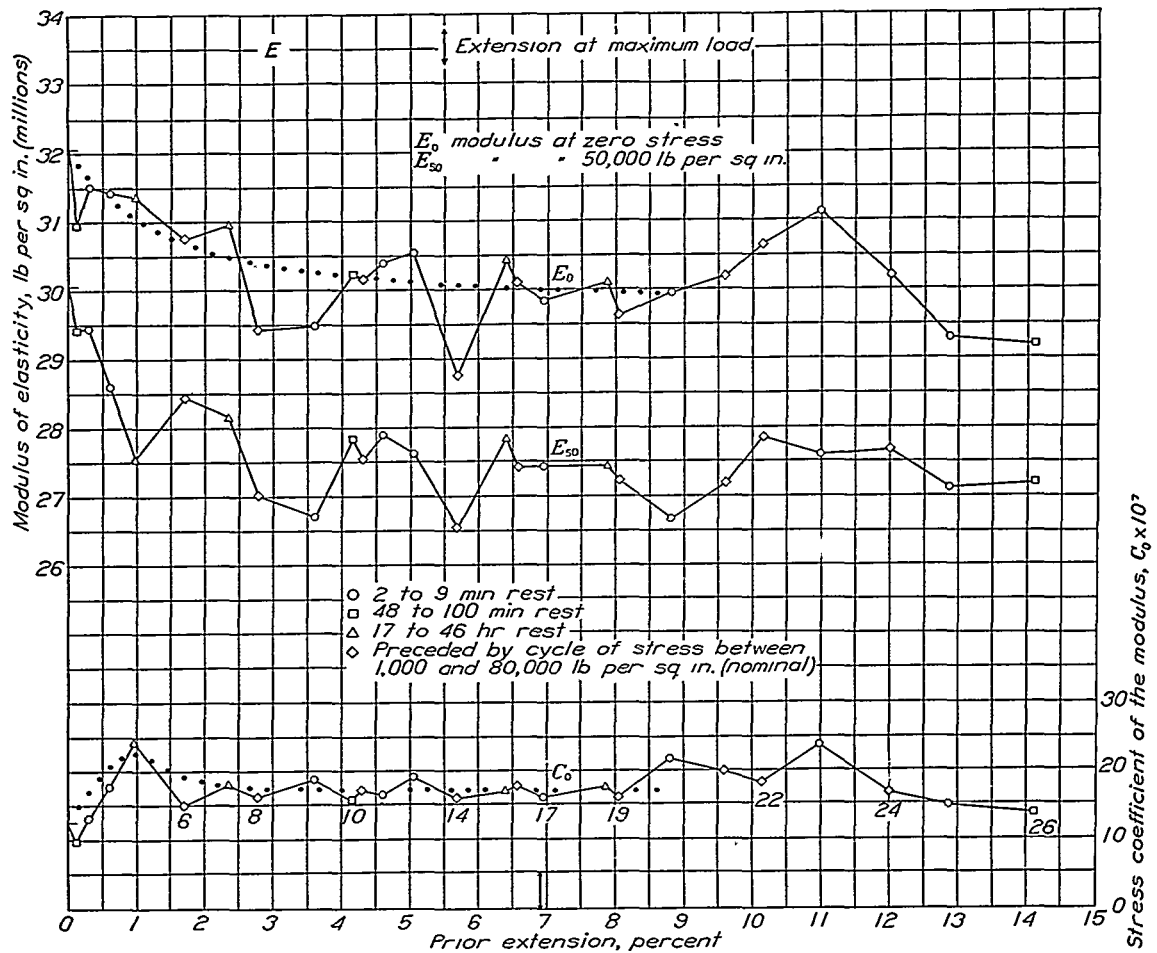


FIGURE 38.—Influence of prior plastic extension on the modulus of elasticity and on its stress coefficient for 13:2 chromium-nickel steel E; as received.

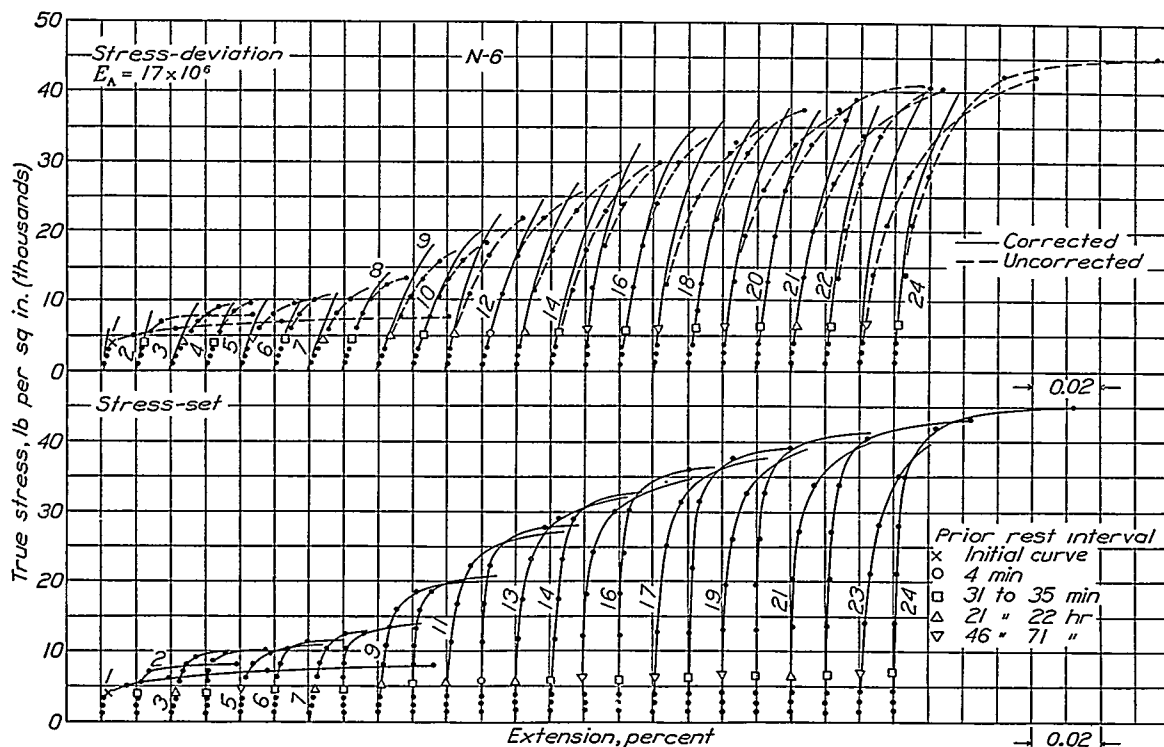
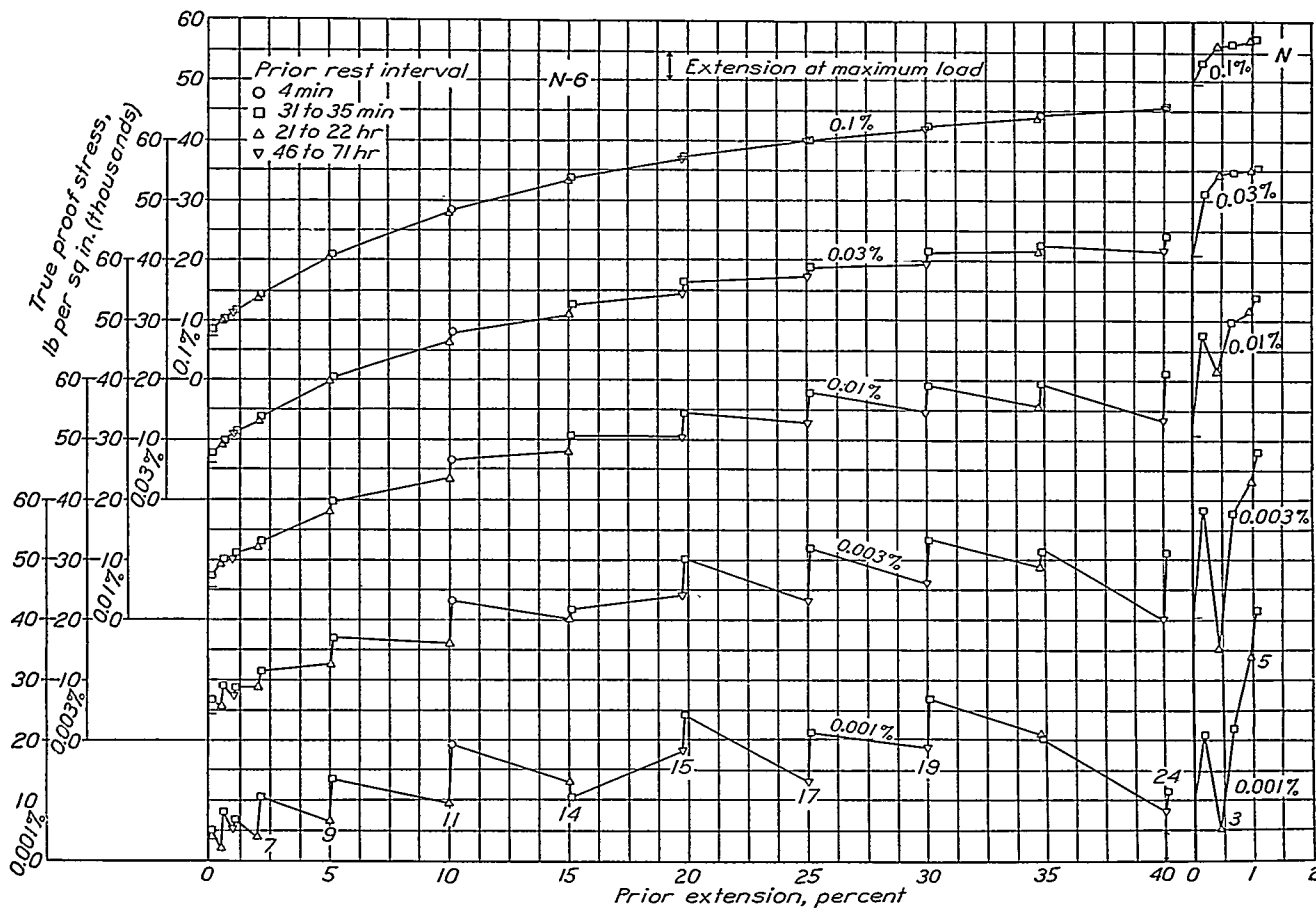
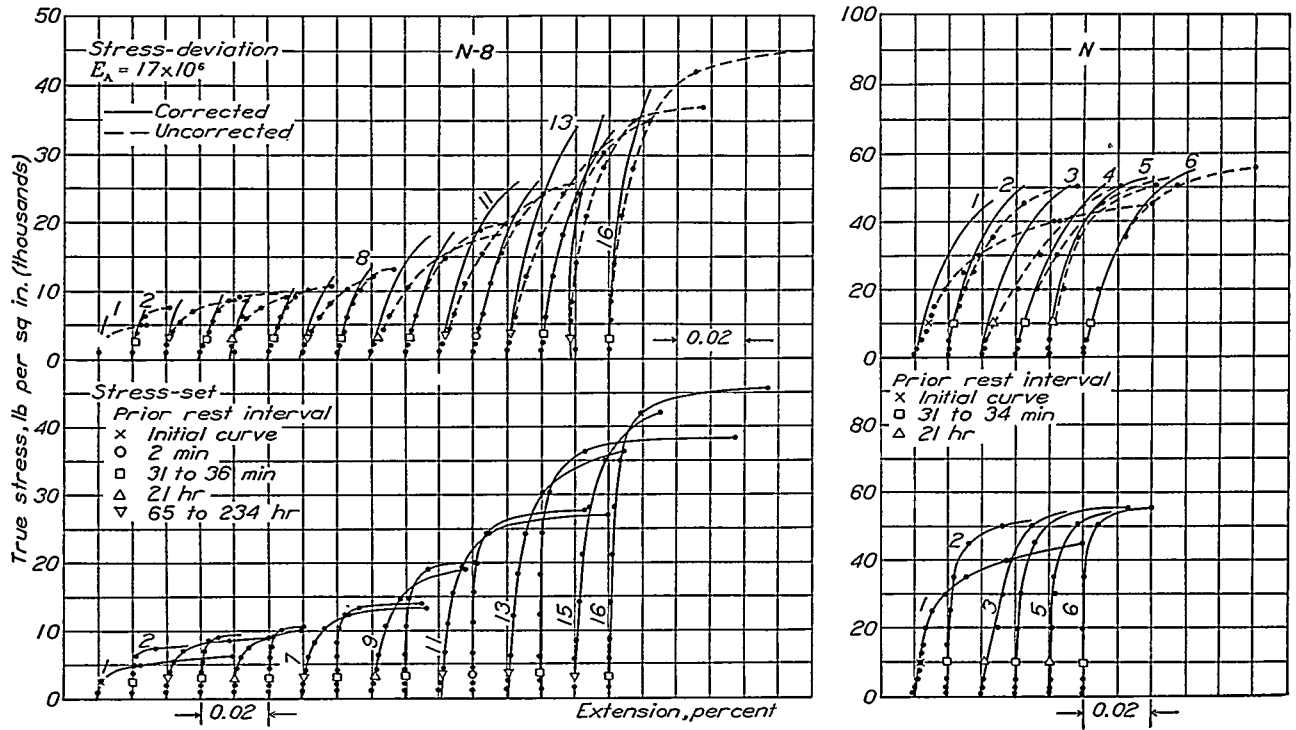


FIGURE 39.—Influence of prior plastic extension on stress-deviation and stress-set for copper N-6; cold-rolled; annealed at 600° F.



Copper N-6; cold-rolled; annealed at 600° F.  
Copper N; cold-rolled; as received.

FIGURE 40.—Influence of prior plastic extension on proof stresses for copper.



Copper N-8; cold-rolled; annealed at 800° F.  
Copper N; cold-rolled; as received.

FIGURE 41.—Influence of prior plastic extension on stress-deviation and stress-set curves for copper.

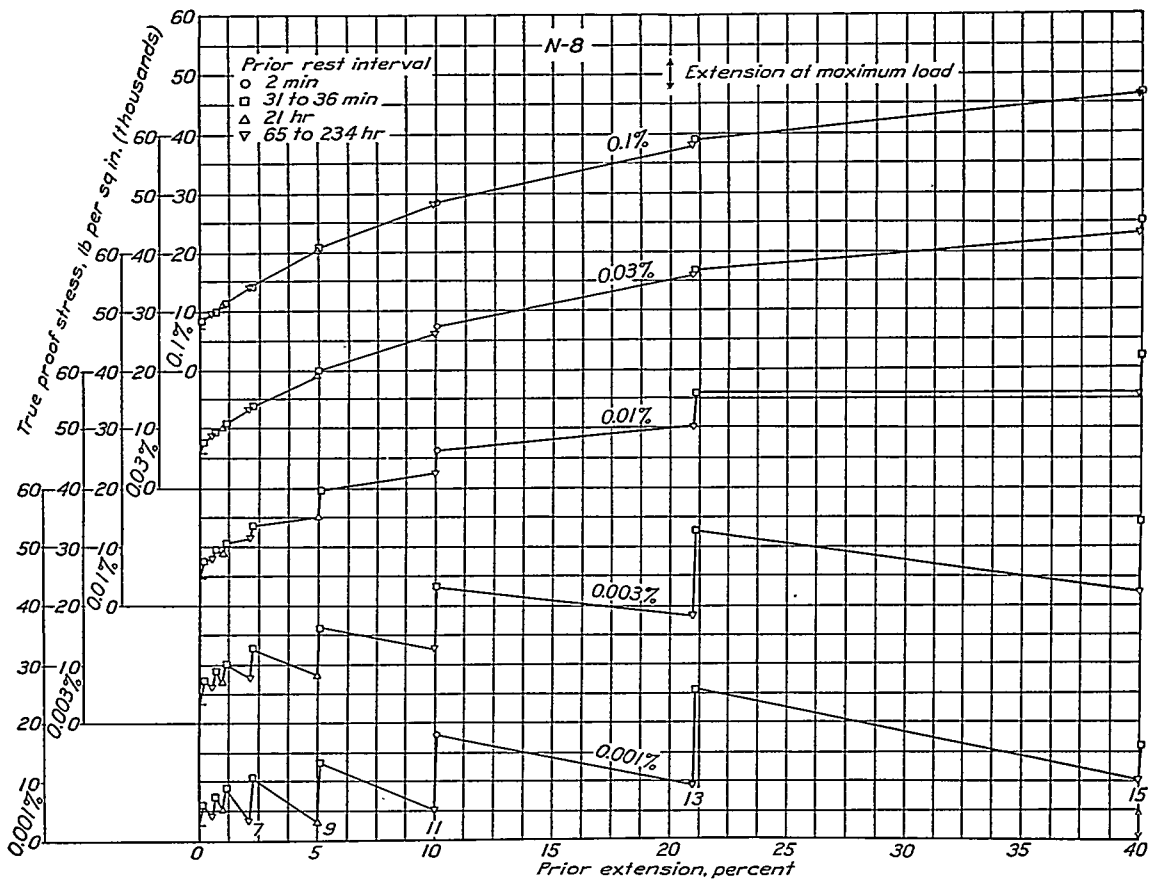


FIGURE 42.—Influence of prior plastic extension on proof stresses for copper N-8; cold-rolled; annealed at 800° F.

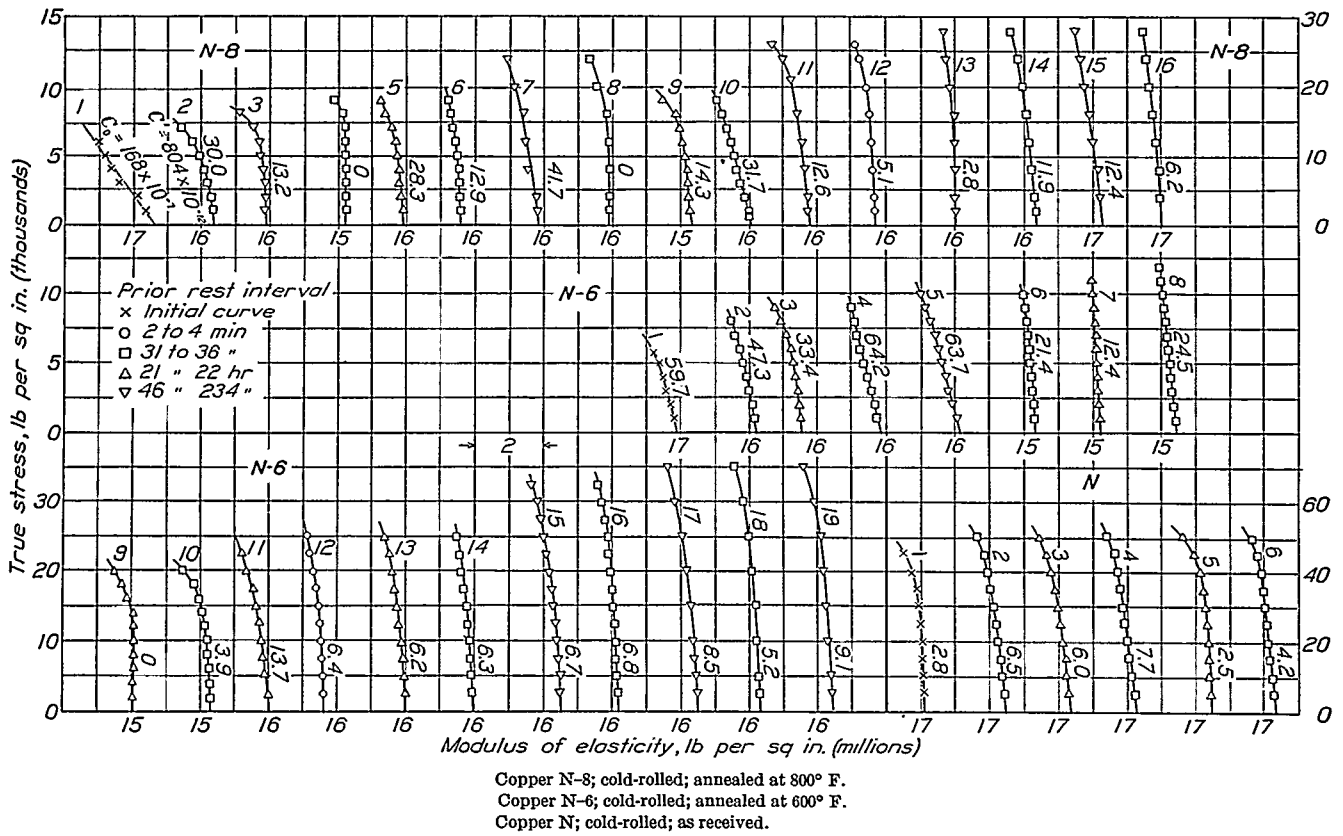


FIGURE 43.—Influence of prior plastic extension on the stress-modulus line for copper.

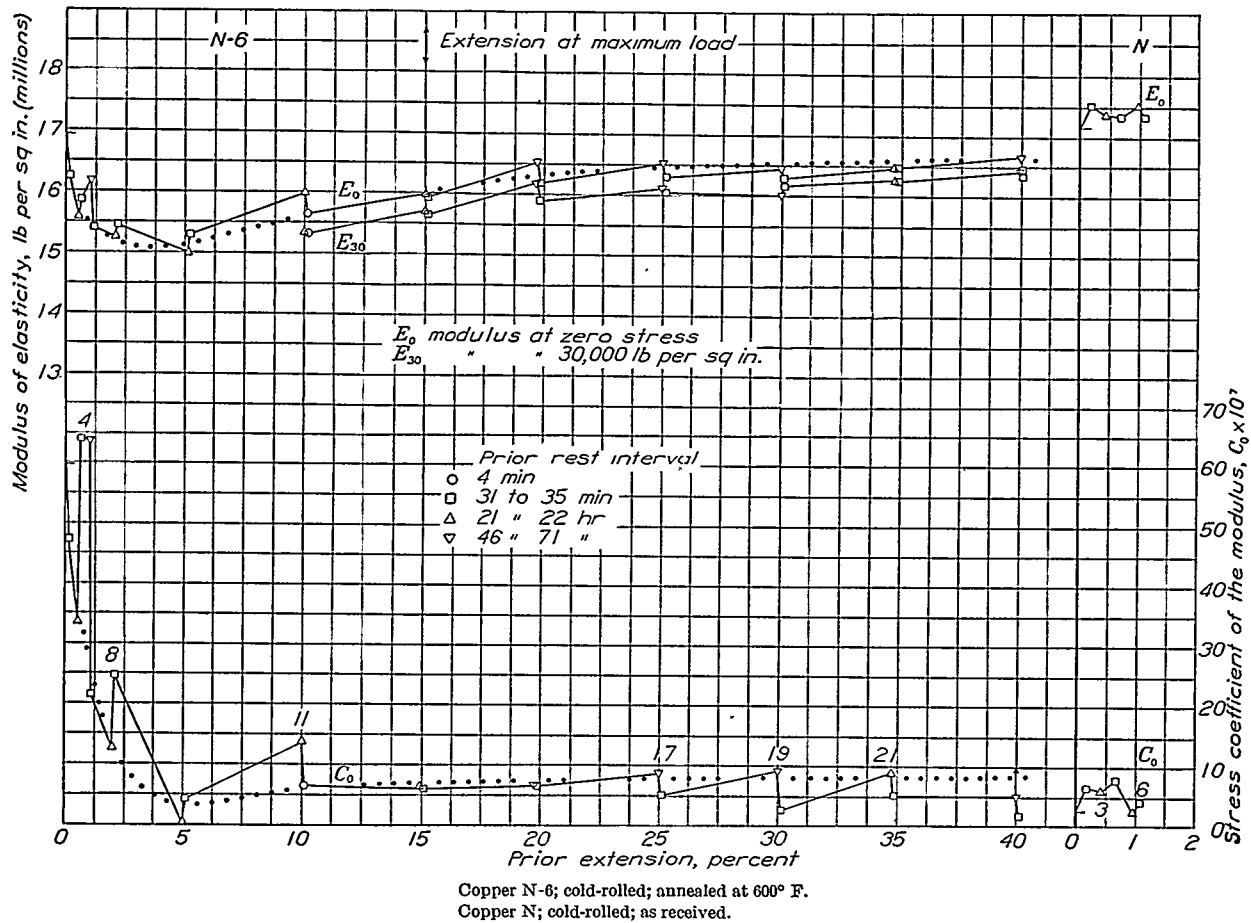


FIGURE 44.—Influence of prior plastic extension on the modulus of elasticity and on its stress coefficient for copper.

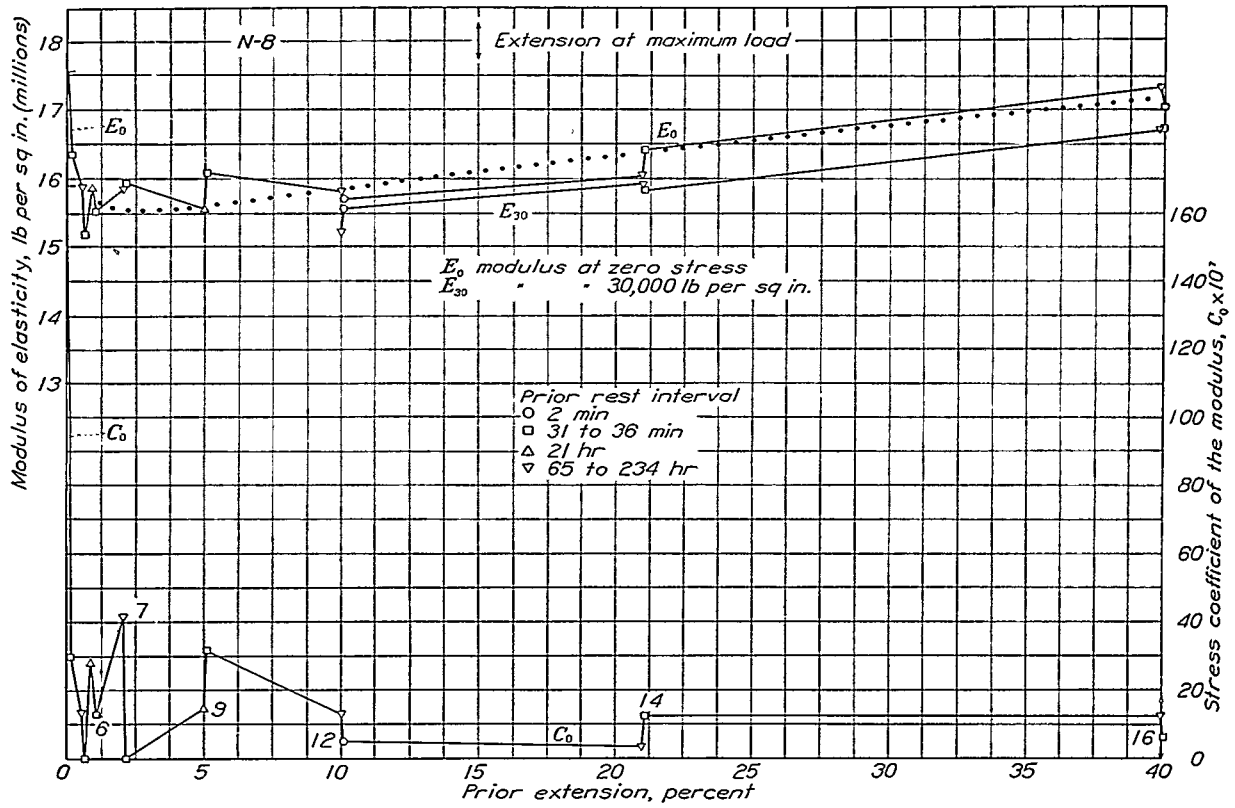
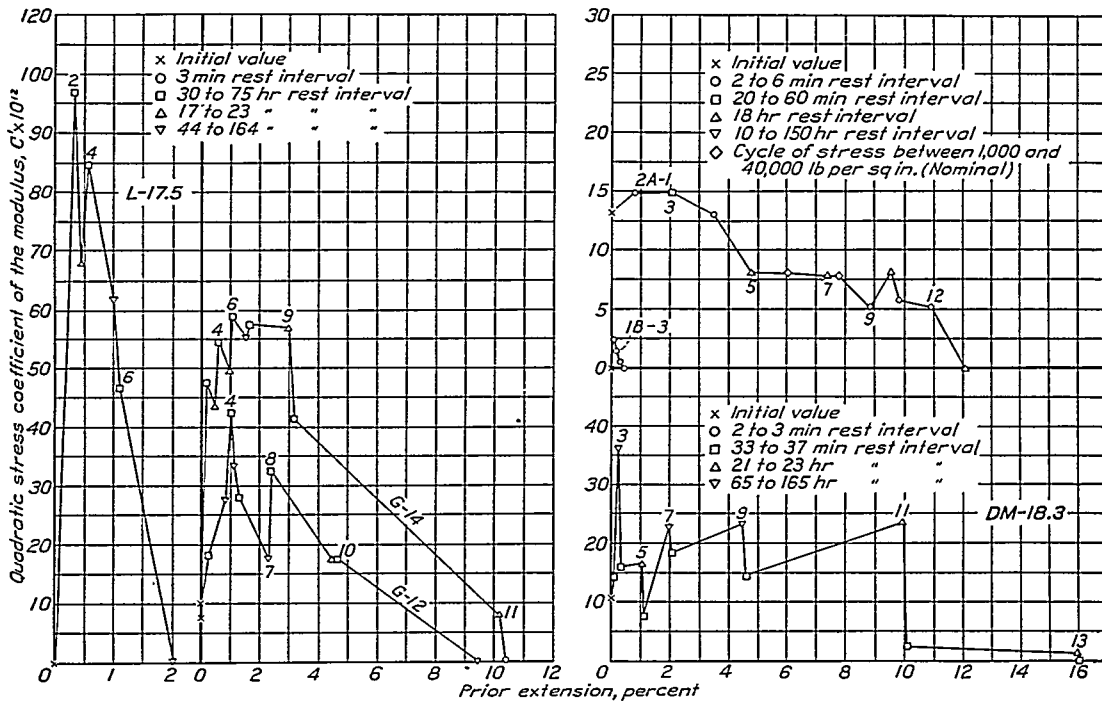
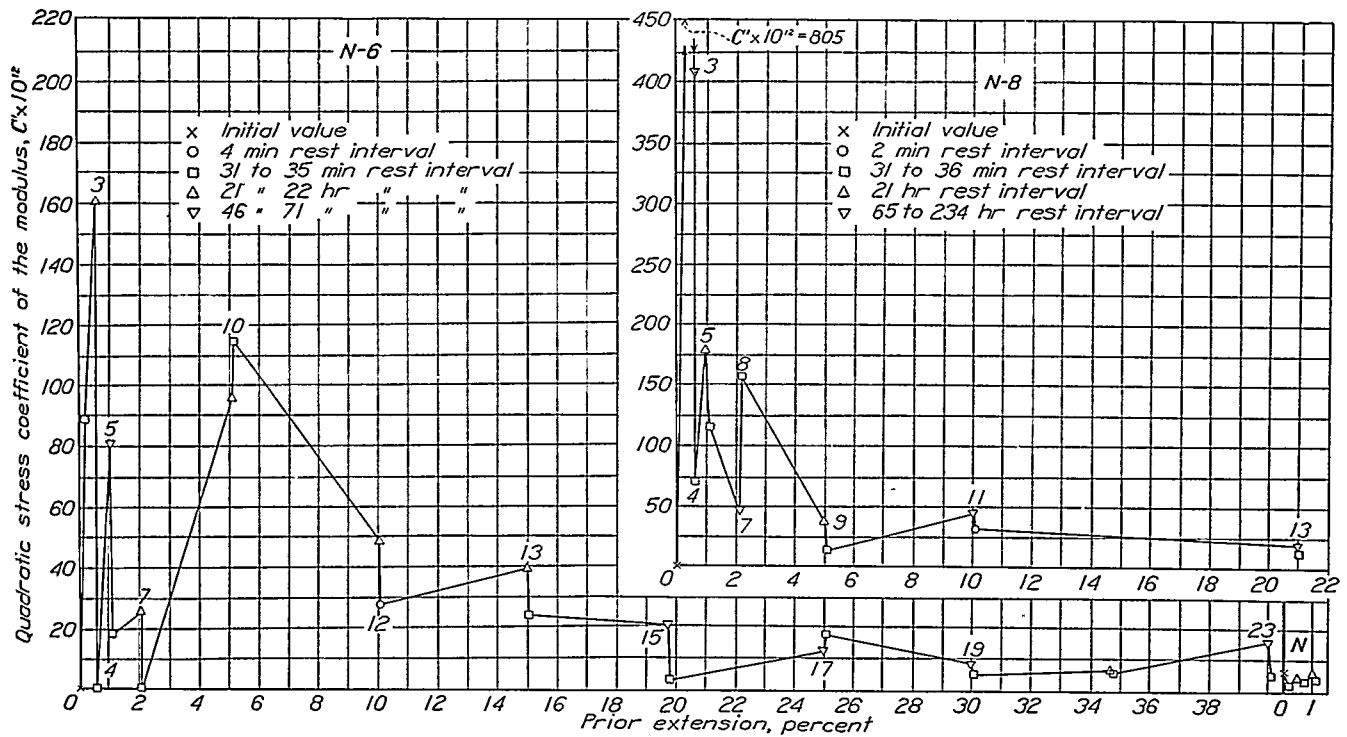


FIGURE 45.—Influence of prior plastic extension on the modulus of elasticity and on its stress coefficient for copper N-8; cold-rolled; annealed at 800° F.



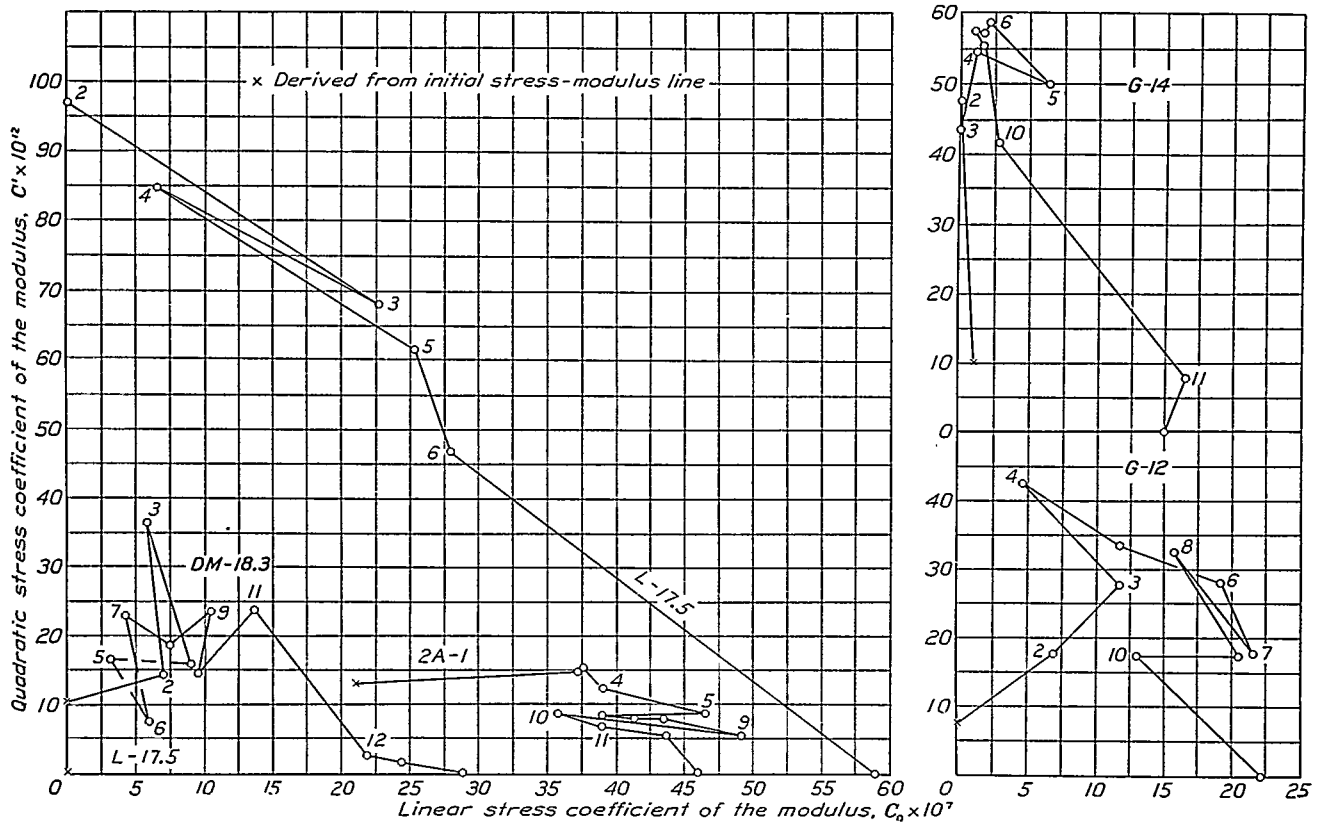
Inconel L-17.5; cold-drawn; annealed at 1,750° F.  
 Monel metal G-12, cold-drawn; annealed at 1,200° F; and monel metal G-14; cold-drawn; annealed at 1,400° F.  
 18:8 chromium-nickel steel 2A-1, annealed; and 18:8 chromium-nickel steel 1B-3, half-hard (reference 1).  
 18:8 chromium-nickel steel DM-18.3; annealed at 1,830° F.

FIGURE 46.—Variation of quadratic stress coefficient  $C'$  with prior plastic extension.



Copper N-6; cold-rolled; annealed at 600° F.  
 Copper N-8; cold-rolled; annealed at 800° F.  
 Copper N; cold-rolled; as received.

FIGURE 47.—Variation of quadratic stress coefficient  $C'$  with prior plastic extension for annealed copper.



18:8 chromium-nickel steels DM-18.3 and 2A-1 and Inconel L-17.5.  
 Monel metal G-14.  
 Monel metal G-12.

FIGURE 48.—Relation between  $C'$  and  $C_0$ . Numerals adjacent to small circles indicate serial numbers of corresponding stress-modulus lines.

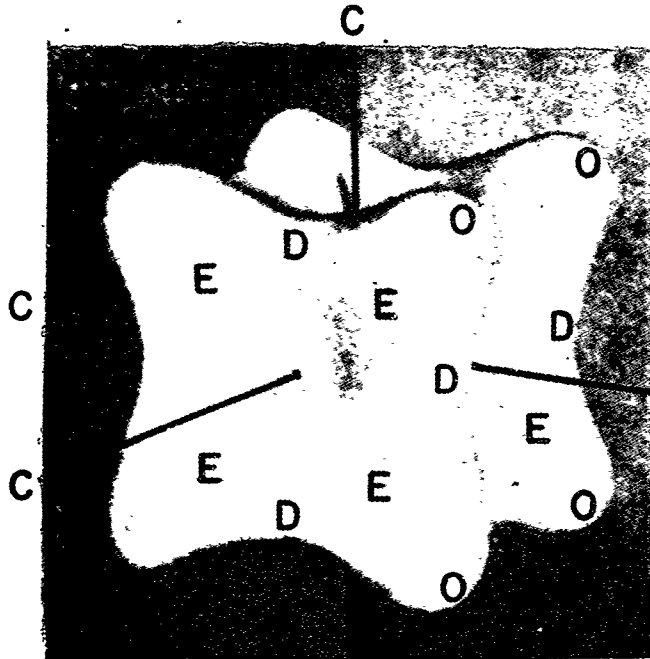


FIGURE 49.—Directional variation of the tensile modulus of elasticity of a crystal of gold.

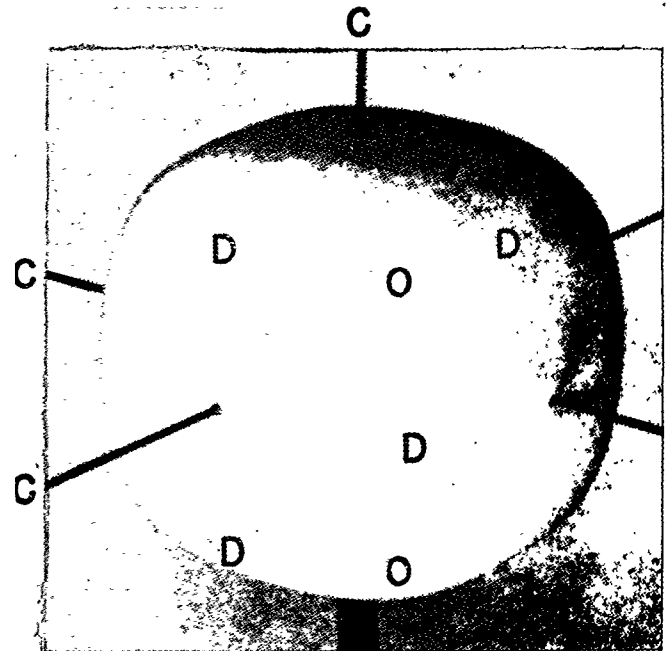


FIGURE 50.—Directional variation of the tensile modulus of elasticity of a crystal of aluminum.

Key for figures 49 to 53:

Mark	Crystallographic direction Name	Symbol
C	Cubic	(100)
O	Octahedral	(111)
D	Dodecahedral	(110)
E	Icositetrahedral	(112)

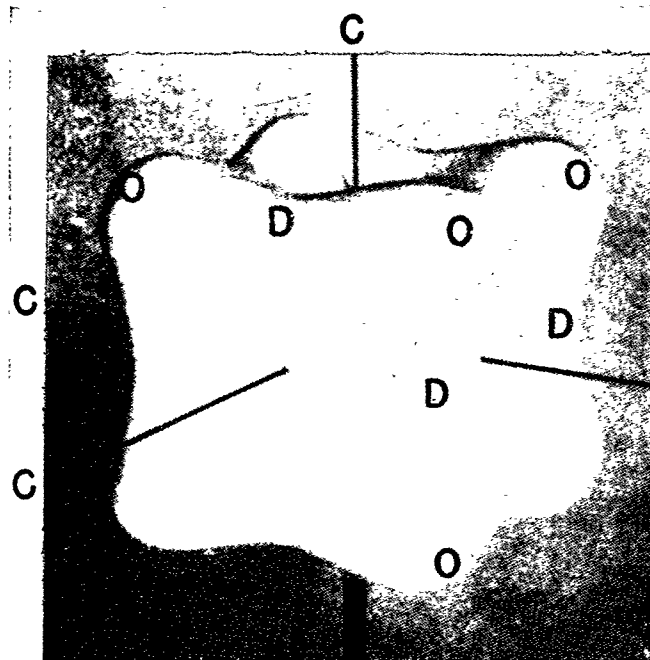


FIGURE 51.—Directional variation of the tensile modulus of elasticity of a crystal of alpha iron.

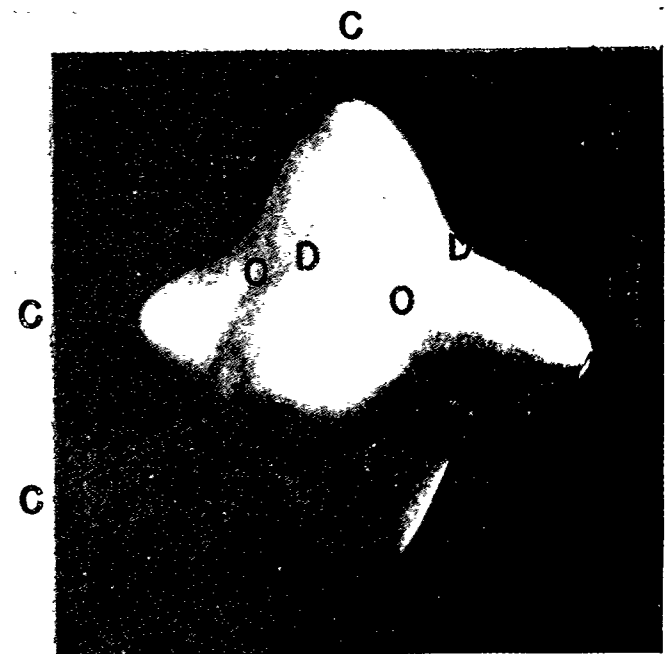


FIGURE 52.—Directional variation of the shear modulus of elasticity of a crystal of alpha iron.

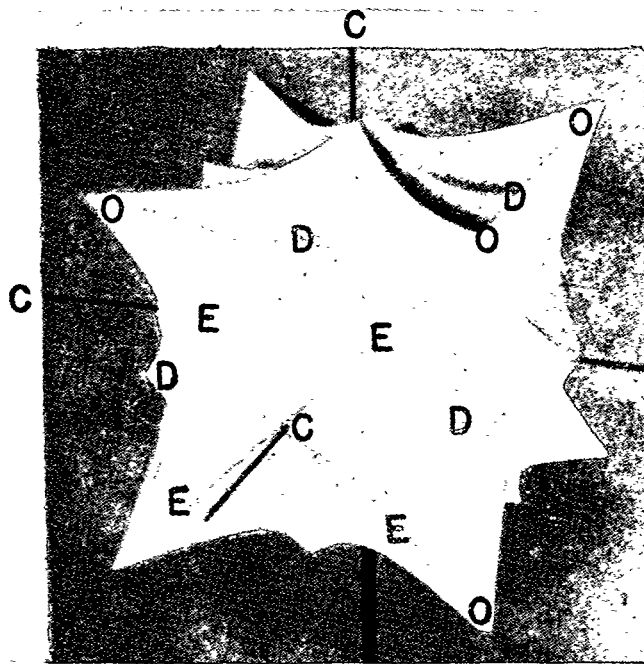


FIGURE 33.—Directional variation of the elastic limit of a face-centered cubic crystal.

TABLE I.—MECHANICAL TREATMENT AND CHEMICAL COMPOSITION OF THE SIX METALS TESTED

Material	Designation	Mechanical treatment	Chemical composition (percent)									
			C	Cr	Ni	Fe	Cu	Mn	Al	Si	P	S
18 : 8 Cr-Ni steel.....	DM	Cold-drawn (half hard).....	0.10	18.82	9.38	Diff.		0.47		0.35	0.015	
18 : 8 Cr-Ni steel.....	DH	Cold-drawn (hard).....	.10	18.82	9.38	Diff.		.47		.35	.015	
13 : 2 Cr-Ni steel.....	E	Hot-rolled.....	.09	13.3	2.06	Diff.		.48		.26		
Monel metal.....	G	Cold-drawn.....	.18		Diff.	1.24	28.46					
Aluminum-monel metal.....	H	Quenched, cold-drawn.....	.22		Diff.	1.7	28.9		2.9			0.007
Aluminum-monel metal.....	J	Quenched, cold-drawn and heat treated.....	.23		Diff.	1.4	31.7		3.6			
Inconel.....	L	Cold-drawn.....	.04	13.2	Diff.	5.3						
Oxygen-free copper.....	N	Cold-rolled.....					99.97					

TABLE II. TENSILE PROPERTIES OF MATERIALS AS RECEIVED AND AFTER HEAT TREATMENT

Material	Condition as regards heat treatment <sup>a</sup>	Bar diameter (in.) <sup>b</sup>	Nominal gage diameter (in.)	Elongation in 2 inches (percent)		Reduction of area (percent)	Tensile strength (lb./sq. in.)	Initial proof stress (lb/sq in.)					
				Maximum load	Total			0.1 percent	0.03 percent	0.01 percent	0.003 percent	0.001 percent	
Half-hard 18:8 Cr-Ni steel.....	DM.....	5/8	0.417				128,000	101,600	77,700	36,400	13,500		
	DM-5.....						143,000	120,800	110,400	83,000	33,000		
	DM-7.....						147,500	125,700	111,000	89,000	70,500		
	DM-9.....			4.2		181,000	150,300	130,700	113,200	91,500	59,000		
	DM-18.3.....			72.5	84	78.7	96,500	30,800	27,700	26,200	22,500	16,200	
Hard 18:8 Cr-Ni steel.....	DM-4.8.....	0.471	.250				145,600	122,300	100,700	73,500	46,000		
	DH.....						204,000	153,000	94,600	53,000	31,000		
	DH-5.....						207,800	163,800	92,000	52,000	24,000		
	DH-7.....						214,000	166,500	111,000	64,000	33,000		
	DH-9.....			1.5			243,000	224,000	198,600	170,000	116,000	46,000	
Annealed 13:2 Cr-Ni steel.....	DH-4.8.....	3/8	.505				214,000	178,000	108,000	35,000	12,000		
	E.....			6.9	27.5	68.6	109,310	74,900	64,000	51,700	28,000	9,500	
	E-A.....						117,900	75,100	51,300	36,300	25,500		
	E-A-6.....						141,700	127,100	114,300	100,300	74,000		
	E-A-7.5.....						143,200	131,300	122,000	112,000	81,000		
	E-A-8.5.....						127,500	122,700	115,100	105,500	92,700		
	E-A-9.5.....						132,000	104,800	83,200	56,200	37,000		
	E-A-11.....						99,300	89,500	73,600	53,000	38,000		
	E-A-12.....						78,500	68,500	56,600	35,600	20,400		
	E-A-14.5.....						90,100	61,200	41,600	26,300	18,000		
Monel metal.....	E-F.....	3/8	.505				102,000	65,800	42,200	27,700	19,700		
	G.....			2.16			125,700	119,000	106,000	90,700	72,500	60,300	
	G-8.....						104,820	104,820	104,820	104,700	97,300	89,000	
	G-12.....			34.3			94,800	45,250	45,250	45,250	43,700	40,000	
Aluminum-Monel metal.....	G-14.....	1/2	.333				92,500	40,170	40,170	40,000	38,500	36,300	
	H.....			3.7	11.5	57.4	116,960	114,300	78,600	47,000	22,000	8,500	
	Heat-treated aluminum-Monel metal.....			J.....	11.5	15.0	39.9	164,150	128,800	120,000	110,800	93,000	45,000
	Inconel.....			L.....	1/2	.333				164,900	160,430	144,000	126,600
L-8.5.....		2.3	7.5	43.9			164,900	156,000	144,500	134,700	119,800	41,000	
L-17.5.....		35.5					92,800	33,980	33,980	30,100	22,600	16,200	
Oxygen-free copper.....	N-6.....	3/8	.505				33,000	7,760	6,470	5,330	4,340	3,500	
	N-8.....			40.0			33,400	7,100	5,900	4,700	3,300	2,500	

<sup>a</sup> In the designation of the condition of the material, a letter following a dash indicates the cooling medium in a hardening or softening treatment: A, air; F, furnace. When this letter is followed by another dash and a number, the number indicates a subsequent annealing or tempering temperature (degrees Fahrenheit, in hundreds).

<sup>b</sup> As received.

TABLE III.—DETAILS OF THERMAL TREATMENT

Material	Designation	Temperature (°F)	Time held (min.)	Cooled in—	Temperature (°F)	Time held (min.)	Cooled in—
Half-hard 18:8 Cr-Ni steel	DM			As received			
	DM-5	500	30	Air			
	DM-7	700	30	Furnace			
	DM-9	900	30	do			
	DM-18.3	1,830	30	Water			
	DM-4.8	480	2,640	Air			
Hard 18:8 Cr-Ni steel	DH			As received			
	DH-5	500	30	Air			
	DH-7	700	30	Furnace			
	DH-9	900	30	do			
	DH-4.8	480	2,640	Air			
Annealed 13:2 Cr-Ni steel	E			do	1,240		Furnace.
	E-A	1,750	60	do			Furnace.
	E-A-6	1,750	60	do	600	120	Do.
	E-A-7.5	1,750	60	do	750	180	Do.
	E-A-8.5	1,750	60	do	850	150	Do.
	E-A-9.5	1,750	60	do	950	120	Do.
	E-A-11	1,750	60	do	1,100	60	Do.
	E-A-12	1,750	60	do	1,200	120	Do.
	E-A-14.5	1,750	60	do	1,450	60	Do.
	E-F	1,750	60	Furnace			
Monel metal	G			As received			
	G-8	800	300				
	G-12	1,200	120				
	G-14	1,400	120				
Aluminum-monel metal	H			As received			
	Do			do			
Inconel	L			do			
	L-8.5	850	120	Furnace			
	L-17.5	1,750	120	do			
Oxygen-free copper	N-6	600	1,320				
	N-8	800	300				

° By manufacturer.  
 † Quenched and cold-drawn followed by precipitation hardening treatment (by manufacturer).

TABLE IV.—STRESS-DEVIATION CURVES FOR ANNEALED OR TEMPERED METALS

Material	Condition	Designation	First loading			Second loading			Stress-deviation line <sup>a</sup>	
			E <sub>0</sub>	C <sub>0</sub>	C'	E <sub>0</sub>	C <sub>0</sub>	C'	First loading	Second loading
Monel metal	Annealed 1,200° F.	G-12	25.3x10 <sup>5</sup>	0	7.4x10 <sup>-12</sup>	25.4x10 <sup>5</sup>	7.1x10 <sup>-7</sup>	17.7x10 <sup>-12</sup>	Cubic	Intermediate.
	Annealed 1,400° F.	G-14	25.0	1.1x10 <sup>-7</sup>	10.0	25.0	0	47.5	Intermediate	Cubic.
Inconel	Annealed 1,750° F.	L-17.5	29.0	0	0	29.5	0	97.0	Straight	Do.
	Annealed 1,830° F.	DM-18.3	27.7	0	10.3	28.1	7.1	14.3	Cubic	Intermediate.
18:8 alloy	Annealed	2A-1	32.4	21.0	13.6	31.5	37.4	14.9	Intermediate	Do.
18:8 alloy	Tempered 1,240° F.	E	32.1	12.6	0	31.0	9.8	0	Quadratic	Quadratic.
13:2 alloy	Annealed	N-6	16.9	59.7	0	16.3	47.3	88.0	Intermediate	Intermediate.
	Annealed 600° F.	N-8	17.6	168.0	0	16.4	30.0	805.0	Quadratic	Do.

<sup>a</sup> The words "quadratic" and "cubic" refer to the type of parabola. The word "intermediate" means that the curve is intermediate between a quadratic and a cubic parabola.